TWO-STAGE AROMATICS HYDROGENATION OF BITUMEN-DERIVED LIGHT GAS OIL

A Thesis Submitted to the College of Graduate Studies and Research

In Partial Fulfillment of the Requirements for the

Degree of Master of Science

In the Department of Chemical Engineering

University of Saskatchewan

Saskatoon

By

Abena Owusu-Boakye

COPYRIGHT

ABSTRACT

In this research, two-stage hydrotreating of bitumen-derived light gas oil (LGO) from Athabasca oil sands was studied. The objective was to catalytically upgrade the LGO by reducing the aromatics content and enhancing the cetane content via inter-stage removal of hydrogen sulfide. The impact of hydrogen sulfide inhibition on aromatics hydrogenation (HDA), hydrodenitrogenation (HDN) and hydrodesulfirization (HDS) activities was investigated. Experiments for this study were carried out in a trickle-bed reactor loaded with commercial $NiMo/Al_2O_3$ and lab-prepared NiW/Al_2O_3 in the stage I and stage II reactors, respectively. Temperature was varied from 350 to 390 ^oC at the optimum LHSV and pressure conditions of 0.6 h^{-1} and 11.0 MPa, respectively. The results from two-stage process showed significant improvement in HDA, cetane rating and HDS activities compared to the single-stage process after the inter-stage removal of hydrogen sulfide. Hence, the presence of hydrogen sulfide in the reaction retarded both the HDA and HDS processes in the single-stage operation. Negligible hydrogen sulfide inhibition was however, observed in the HDN process.

Prior to the two-stage hydrotreating study, single-stage hydrotreating reactions were carried out over commercial $NiMo/Al_2O_3$ catalyst to determine the optimum operating conditions for maximizing hydrogenation of aromatics. A statistical approach via the Analysis of Variance (ANOVA) technique was used to develop regression models for predicting the conversion of aromatics, sulfur and nitrogen in the LGO feed. Experiments were performed at the following operating conditions: temperature (340-390 ^oC); pressure (6.9-12.4 MPa) and liquid hourly space velocity, LHSV (0.5-2.0 h^{-1}). Hydrogen-to-oil ratio was maintained constant at 550 ml/ml. The results showed that the

two-level interaction between temperature and pressure was the only significant interaction parameter affecting HDA while interaction between temperature and LHSV was the most important parameter affecting both HDS and HDN activities. A maximum 63 % HDA was obtained at 379 ^{o}C, 11.0 MPa and 0.6 h^{-1}. Experiments with NiW/Al_2O_3 were also performed in a single-stage reactor with LGO blend feedstock by varying temperature from 340-390 ^{o}C at the optimum pressure and space velocity of 11.0 MPa and 0.6 h^{-1}, respectively. The following order of ease of hydrogenation was observed: poly- > di- >> monoaromatics. The order of ease of hydrogenation in other LGO feedstocks (atmospheric light gas oil, ALGO; hydrocrack light gas oil, HLGO; and vacuum light gas oil, VLGO) was studied and found to follow the order: VLGO > ALHO > HLGO. Studies on mild hydrocracking (MHC) in the gas oil feedstocks showed a net increase in gasoline with a corresponding decrease in diesel with increasing temperature.

Both the single and two-stage HDA and HDS kinetics were modeled using Langmuir-Hinshelwood rate equations. These models predicted the experimental data with reasonable accuracy. The degree of conversion of the gas oil fractions in ALGO, HLGO and VLGO via mild hydrocracking was best described by a pseudo-first order kinetic model based on a parallel conversion scheme.

ACKNOWLEDGEMENT

I would like to take this opportunity to express my profound gratitude to my supervisors, Dr. Ajay Kumar Dalai and Dr. John Adjaye for their immense contributions, support and guidance throughout my master's program. Special thank you also goes to Dr. Deena Ferdous and Mr. Christian Botchwey for their assistances: they were ever ready to give me a helping hand whenever I was faced with a difficult problem. My appreciation also goes to the members of my committee: Dr. Ding-Yu Peng and Dr. Hui Wang for their directions, contributions and precious time. Technical assistances from Mr. T. B. Wellentiny, Mr. Richard Blondin and Mr. Dragan Cekvic are also highly acknowledged. Financial assistances from NSERC, the University of Saskatchewan Graduate Education Equity Scholarship and the CRC award to Dr. Dalai are gratefully acknowledged.

Above all, I would like to thank the Almighty God for His divine wisdom, strength and protection throughout my program.

DEDICATION

This work is dedicated to my parents,

Mr. and Mrs. Owusu-Boakye,

My brothers

Cyril, Joel and Kweku Owusu-Boakye

And my fiance

Kwame Koom-Dadzie

TABLE OF CONTENTS

LIST OF TABLES

LIST OF FIGURES

NOMENCLATURE

A*	Reactant
A^*_{AD}	Adsorbed reactant species A^*
b	constant parameter
C_A	Product concentration of aromatics
C_{AE}	Equilibrium concentration of aromatics
C_{AH}	Concentration of saturated products
C_{AO}	Concentration of aromatics in feed
Car	aromatics content [%]
C_D	Concentration of diesel fraction [wt %]
C_G	Concentration of gasoline fraction [wt %]
C_H	Concentration of heavy gas oil fraction
C_N	Concentration of total nitrogen [wppm]
C_s	Product concentration of sulfur species
C_{SO}	Concentration of sulfur species in feed
E_i	Activation energy [kJ/mol]
f_i	Fugacity
H	Heat of adsorption [kJ/mol]
I	Average integrated detector response
I*	Inhibitor
Iar	integral of total aromatics
Isat	integral of total saturates
K_A	Adsorption equilibrium constant for aromatics [MPa^{-1}]

k_A	Rate constant for HDA
k_{actual}	Actual rate constant [h^{-1}]
k_F	Forward rate constant
Kg	Gravimetric dilution factor
K_{H2}	Adsorption equilibrium constant for hydrogen [MPa^{-1}]
K_{H2S}	Adsorption equilibrium constant for hydrogen sulfide [MPa^{-1}]
k_{obs}	Observed rate constant [h^{-1}]
k_R	Reverse rate constant
K_s	Adsorption equilibrium constant of sulfur [MPa^{-1}]
ks	Rate constant for HDS
M	Mid-boiling point [^oC]
M*	Mass of test specimen
N	Number of experimental runs
n	Reaction order
n_{H2S}	Number of moles of hydrogen sulfide
NH_3	Ammonia
P^a	Atmospheric pressure [MPa]
P_{H2}	Partial pressure of hydrogen [MPa]
P_{H2S}	Partial pressure of hydrogen sulfide
P^o	Standard pressure [MPa]
R	Universal gas constant
r_A	Rate of aromatics hydrogenation reaction
r_{Aobs}	observed reaction rate for hydrogenation of aromatics [% h^{-1}]
r_S	Rate of hydrodesulfurization reaction

S	Slope
T	Temperature [^{o}C]
T^{a}	Actual temperature [^{o}C]
T^{o}	Standard temperature
V^{a}	Actual volume [ml]
V^{o}	Standard volume [ml]
W	Lambert W function
x	Number of design factors
X_{A}^{*}	Fraction of reactant A* adsorbed [%]
X_{TA}	Conversion of total aromatics [%]
X_{TN}	Conversion of total nitrogen [%]
X_{TS}	Conversion of total sulfur [%]
Y	y-intercept
Y_{A}	Mole fractions of aromatic compound
Y_{A}	Mole fractions of aromatic compound
Y_{AH}	Mole fractions of saturated aromatic compounds
Y_{AH}	Mole fractions of saturated aromatic compounds
y^{exp}	Experimental response
y^{p}	Model prediction response

ABBREVIATIONS

ALGO	Atmospheric light gas oil (160-393 ^{o}C)
ANOVA	Analysis of Variance
CI	Cetane index
CN	Cetane number
D	Diesel fraction (205-345 ^{o}C)
FT	Fourier Transform
G	Gasoline fraction
H	Heavy gas oil fraction
H/C	Hydrogen to carbon ratio
H_2O	Water
H_2S	Hydrogen sulfide
HC	Hydrocarbon
HDA	Aromatics hydrogenation
HDN	Hydrodenitrogenation
HDO	Hydrodeoxygenation
HDS	Hydrodesulfurization
HLGO	Hydrocrack light gas oil (163-404 ^{o}C)
HT	Hydrotreating
LGO	Light gas oil
LGOB	Light gas oil blend (191-420 ^{o}C)
LHSV	Liquid hourly space velocity [h^{-1}]
MHC	Mild hydrocracking

SFC	Supercritical fluid chromatigraphy
SSE	Sum of squares
TEM	Transmission electron microscopy
VLGO	Vacuum light gas oil (271-482 ^{o}C)

Greek letters

ρ	Density measurement (g/cc)
δ^-	Partial negative
δ^+	Partial positive

1. INTRODUCTION

The global demand for oil has increased by 150 % over the last 40 years and 20 % in the past two decades to the current 80 million barrels per day and is projected to grow by 50 % more in the next 20 years (Isaacs, 2004). This demand for oil comes at a time when there is a gradual decline in supply from relatively cheap conventional crude and discoveries are not being replaced with new ones (Laherrere, 2003). However, the world has over twice as much supply of unconventional oil as compared to conventional oil and it is estimated that there are 8-9 trillion barrels of heavy oil and bitumen in place worldwide, of which potentially 900 billion barrels of oil are commercially exploitable with today's technology (Davis, 2002).

In 2003 the total conventional light and heavy production was 1,120,000 b/d and by 2015 this is expected to decline to 600,000 b/d. The significant growth in oil sands production far exceeds the decline in conventional production. Oil sands production currently make up approximately half of Canada's total crude oil output and by 2015 it is expected to account for three quarters of all Western Canadian production (Canadian Association of Petroleum Producers, 2004-2015 crude oil forecast). Figure 1.1 shows the conventional petroleum vs. oil sands production in Western Canada alone. Oil sands production includes both raw bitumen and upgraded synthetic crude oil while the conventional portion includes light and heavy oil.

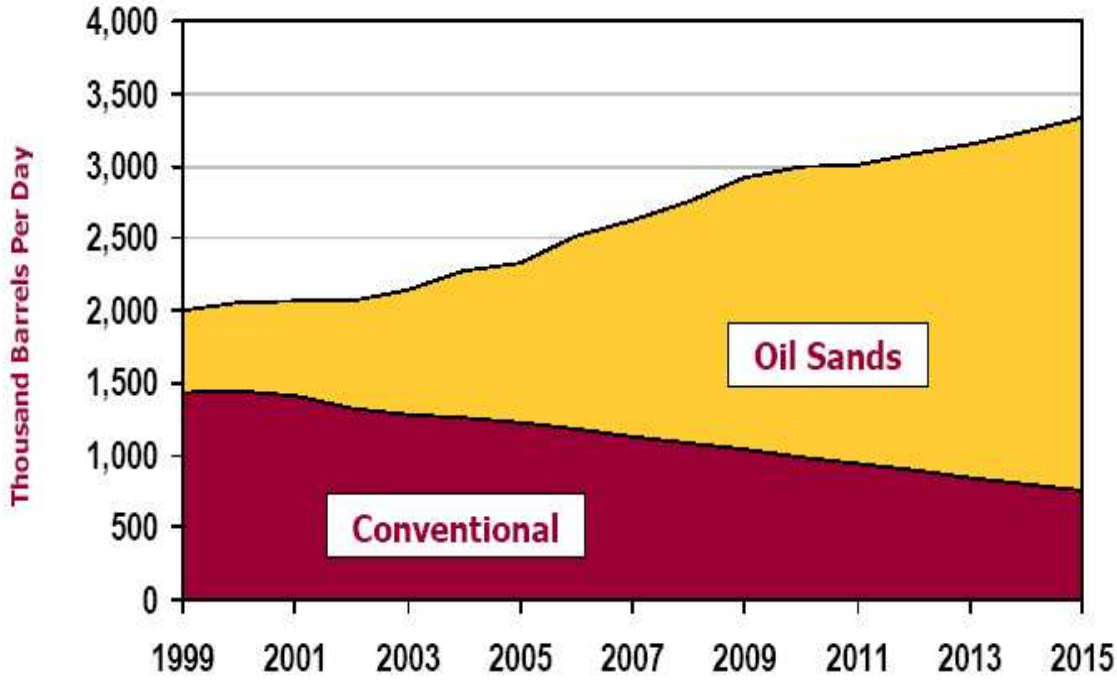

Figure 1.1: Conventional vs. Oil Sands Production in Western Canada: 1999-2015 (Canadian Association of Petroleum Producers, July 2004)

As production of upgraded oil increases, there is a strong potential for market limitation for synthetic crude oil (Isaacs, 2004). This is because of the high aromatics contents of the synthetic crude oil derived from bitumen which consequently reduces diesel cetane (Wislon and Fisher, 1985). Also, present in these distillates are high concentrations of sulfur and nitrogen compounds. At the moment, Canadian and United States refineries are not designed to mix more than 10 to 15 % into their conventional crude supply to meet end product quality specifications (Isaacs, 2004).

The heightened concern to produce high quality middle distillates has led to the enforcement of stricter fuel specifications worldwide. New diesel fuel specifications will mainly require a reduction in sulfur and aromatic content, while the cetane number will be set to a minimum value of about 53 units (Eliche-Quesada et.al., 2003). Presently, the

minimum cetane number should be at least 40 (US EPA, Diesel Fuel Quality, 1999). Reducing diesel aromatics from 30 to 10 % will reduce NO_x emissions by more than 5 %. Cetane number is a measure of the ignition property of the diesel fuel and has an inverse relationship with the constituent aromatic hydrocarbons. Aromatics, especially the polycyclics, have very low cetane numbers while paraffin hydrocarbons have relatively high ones. Thus a key factor for boosting the cetane number is to decrease the aromatic content in distillates.

Reduction of aromatics has become a key processing parameter in processing middle distillates and intensive efforts have been made in recent years to develop catalysts and processes for producing low-aromatic diesel fuel. Several attempts by researchers including Matarresse et.al., 1983; Wilson and Kriz, 1984 have been made to optimize the process variables and maximize hydrogenation using existing hydrotreating catalysts such as NiMo (W) and CoMo supported on γ-alumina. Due to the nature of the hydrogenation activity of such catalysts, high temperatures are required for hydrotreating. However, the high temperatures have a negative effect of shifting equilibrium in favor of the reverse reaction, which is undesirable. To eliminate the equilibrium effects, high pressures are usually used although it increases the cost of production and hydrogen consumption (Stanislaus and Cooper, 1996).

Catalytic hydrogenation is an essential process for reducing aromatics since after removal of sulfur and nitrogen there still remains appreciable amounts of aromatics. Presence of these aromatics does not only generate particulate emissions but also decrease the cetane number. Unlike the other hydrotreating reactions; hydrodesulfurization (HDS) and hydrodenitrogenation (HDN), hydrogenation of

aromatics (HDA) is very difficult due to the exothermic and reversible nature of the reaction. Hence, application of hydrotreating techniques including single and dual stage processes have been used by many refineries to enhance the catalytic activity for hydrogenation of aromatics to improve the fuel quality.

1.1 Research background

Product quality is often a significant issue with hydrotreated products from synthetic crude distillates (Gray, 1994). These fractions can be more aromatic than conventional crude oil distillate in the same boiling range, which may be a concern in reducing the total aromatics content of transportation fuel (Pauls and Weight, 1992). To be able to produce diesel fuel with very low aromatics contents, a thorough understanding of the effects of process variables, catalyst type and the interaction of these variables on chemistry and thermodynamic equilibria of different types of aromatic compounds present in petroleum distillates is necessary. Figure 1.2 shows the functional relationship of the most important factors affecting hydrogenation of aromatic compounds.

Generally, it is the feed properties that determine the type of hydroprocessing technology and catalysts to use for reducing the aromatics content. Real feedstock contain a complex mixture of hydrocarbons and other elements such as sulfur, nitrogen and metals which require high reaction temperatures before they can be removed. Hydrogenation of aromatics on the other hand requires moderate temperatures and high pressure conditions. Consequently, a tactful combination of the operating conditions such as temperature, pressure, and space velocity and hydrogen-to-oil ratio is required to effectively reduce diesel aromatics and remove the other objectionable elements.

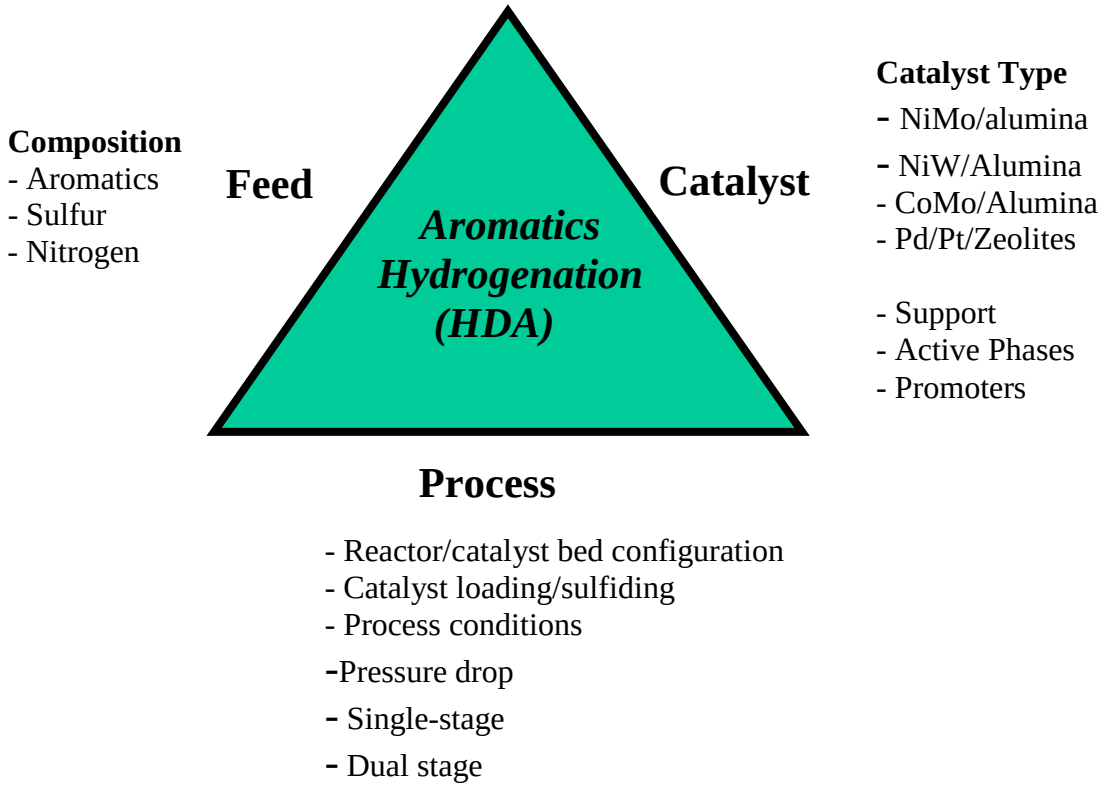

Figure 1.2: Key factors affecting aromatics hydrogenation (HDA)

Several reactions occur during hydrotreating, some of which are known to affect reactivity. One such reaction is hydrodesuphurization (HDS) which produces hydrogen sulfide as one of its by-products. Presence of the hydrogen sulfide is well known to retard hydrogenation activity of hydrotreating catalysts. (Girgis and Gates, 1991; Ishihara et.al., 2003; Kabe et.al.,. 1999; Stanislaus and Cooper, 1996). Hence, the choice of the hydrotreating catalyst plays a vital role in hydrotreating since different catalysts present various degrees of hydrogenation activities and tolerance to heteroatom poisoning and/or inhibition in aromatics hydrogenation.

The object of this project is to improve the product quality of a middle distillate fraction from Athabasca bitumen oil sands. The content of this report includes a careful review of literature, knowledge gaps and statement of purpose for hydrogenation of aromatics in petroleum distillates. Also included in the thesis are discussions on

experimental, results, conclusions and recommendations for improving the product quality of middle distillates from Athabasca oil sands.

1.2 Knowledge gaps

Although a number of studies have been conducted to maximize hydrogenation of aromatic compounds, most of the data were obtained using model compounds thus making direct application of the results to industrial processes quite a challenge. Information gathered from literature so far shows that existing data on the interaction effects of operating conditions on hydrogenation of aromatics in gas oils from Athabasca oil sands is scarce. Also, few reports have been published on single and dual stage kinetic studies of HDA over NiW catalyst supported on alumina in bitumen derived LGOs from Athabsaca oil sands. Finally, since production of hydrogen-sulfide gas from sulfur removal is known to inhibit catalytic hydrogenation activity, it is important to design the hydrotreating process so as to reduce its inhibition effect on hydrogenation. However, studies so far shows that limited information exist on the kinetics of H_2S inhibition on hydrogenation of aromatics in distillates from synthetic crude using alumina supported NiMo and NiW catalyst systems in a two-stage process.

1.3 Hypotheses

The following hypotheses have been outlined for this research.

1. Although hydrogen partial pressure has been determined to be the key processing factor affecting aromatics saturation, interactions of temperature, liquid hourly space velocity (LHSV) and pressure have superior effects on HDA compared to pressure alone.

2. Under the same hydrotreating conditions, HDA characteristics will be different for each light gas oil feedstock.
3. Clean fuels with relatively low amounts of aromatics and heteroatom can be successfully produced after a two-stage upgrading as compared to a single-stage process. Hydrogen-sulfide, produced as a by-product of the HDS process inhibits hydrogenation of aromatics as well as the HDS reactions during hydrotreating. Therefore, removing the hydrogen sulfide inter-stage, will improve HDA and HDS activities.
4. The Langmuir-Hinshelwood rate equation would truly account for the hydrogen sulfide inhibition in HDA and HDS reactions during hydrotreating.

1.4 Research objectives

The main objective of this research was to study the catalytic upgrading of light gas oil from Athabasca bitumen by reducing the aromatic contents and thereby enhancing the diesel cetane using a two-stage hydrotreating process. Within this objective, various phases of the research were defined with each phase having a set objective(s):

1. **Phase I-** Determine the impact of the interaction of temperature, pressure and liquid hourly space velocity on aromatics hydrogenation and the best combination of these factors to give maximum HDA, HDS and HDN. This study will be performed in a single-stage hydrotreater loaded with NiMo/Al_2O_3 catalyst. A statistical approach will be used to design the experiments and analyze the hydrotreating data. The intent of this approach is to develop regression models that describe HDA, HDS and HDN. Another objective of this

phase of the experiment is to determine the optimum operating conditions for maximum HDA.

2. **Phase II**- Following the optimum conditions obtained in Phase I, the hydrogenation activity of NiW/Al_2O_3 catalyst will be studied on a variety of light gas oil feedstock from Athabasca bitumen. Experiments for this study will be performed in a single-stage hydrotreater.
3. **Phase III**- In this phase, the effect of H_2S removal on the hydrogenation propensity of aromatics using NiMo in stage I and NiW in stage II in a two-stage hydrotreating process unit will be studied.
4. **Phase IV**- The H_2S inhibition kinetics on aromatics hydrogenation and hydrodesulfurization reactions using Langmuir-Hinshelwood rate equations will be developed.

2.0 LITERATURE REVIEW

This chapter presents a review on upgrading of middle and heavy gas oil. Particular emphasis is placed on the concepts of hydrogenation of aromatics and the challenges involved in hydrogenation of aromatics (HDA) in both model and industrial feed. The concepts of hydrogenation catalysts and their catalysis as well as kinetic modeling of hydrogenation of aromatics are also discussed in this chapter.

2.1 Hydrotreating

Hydrotreating is a process to catalytically stabilize petroleum products and or remove objectionable elements from products or feedstock by reacting them with hydrogen (Gary and Handwerk, 2001). It is also used to include a variety of catalytic hydrogenation processes used in fuels refining or for purification of products such as industrial solvents. In contrast to hydrocracking, hydrotreating produces very little change in volatility of chemical species (Satterfield, 1981). Hydrotreating also encompasses processes such as sulfur removal (hydrodesulfurization, HDS), nitrogen removal (hydrodenitrogenation, HDN) as well as hydrogenation of some or all unsaturated species including aromatics, present in a feedstock. The typical hydrotreating catalysts are sulfided $CoMo/Al_2O_3$ or $NiMo/Al_2O_3$. A minimum concentration of hydrogen sulfide is usually required to maintain the catalyst in the sulfided state (Ishihara et.al., 2003; Stanislaus and Cooper, 1996; Girgis and Gates, 1991).

During the process of hydrotreating the oil feed is mixed with pure hydrogen before or after it is preheated to a proper reactor inlet temperature which is usually below 427 ^{o}C to minimize cracking. The combined feed with the hydrogen-rich-gas then enters the top of the fixed-bed reactor. In the presence of a metal-sulfide catalyst, the hydrogen reacts with the oil to produce saturated hydrocarbons, hydrogen sulfide, ammonia, and free metals. The process of saturation of the aromatic rings is aromatics hydrogenation (HDA). The general reaction mechanism for hydrotreating is shown in equation 2.1.

$$\text{Feed} \xrightarrow[\text{Heat, pressure}]{\text{Catalyst, } H_2} \text{Saturated hydrocarbons} + H_2S + NH_3 + H_2O \qquad (2.1)$$

Hydrotreating, as an intermediate processing step for catalytic reforming of gas oil fraction may be carried out for the following reasons (Satterfield, 1981):

1. Prior hydrodesulfurization provides a means for control of air pollution because some of the sulfur present in a feedstock can be deposited in the form of coke on the hydrotreating catalyst which would otherwise be emitted to the air.
2. HDN removes nitrogen compounds that otherwise deactivate acidic sites on hydrotreating catalysts and also contribute to coke formation.
3. Saturation of aromatic rings is required for: cracking of heavier feedstock such as heavy gas oil. This improves the cetane number of diesel fuels and smoke point of jet fuel and reduces particulate emission from exhaust gases. Without such prior saturation, multi-ring aromatic compounds pass through catalytic cracking reactor and undergo very little or no reaction.

2.2 Hydrogenation of aromatics (HDA)

Hydrogenation of aromatic compounds (equation 2.2) is reversible and exothermic with heats of reaction typically in the range of 63-71 kJ/mole (Reid et.al., 1977 and Jaffe et.al., 1974). Under typical hydrotreating conditions, complete conversion of aromatics is not possible and as a result, the kinetics is complicated by a significant reverse reaction at high temperatures.

$$\text{Aromatics} + n\text{H}_2 \rightleftharpoons \text{Saturated Hydrocarbons} \qquad (2.2)$$

High temperatures, low space velocities and high hydrogen partial pressures are required to achieve appreciable hydrogenation of aromatics. The reactions and thermodynamic properties of aromatic hydrogenation are further discussed in sections 2.4. Typical ranges of process variables for hydrogenation of aromatics are shown in Table 2.1.

Table 2.1: Typical ranges of HDA process variables (Gray, 1994)

Process Variable	Range
Temperature	270 - 340 ^{o}C
Pressure	0.68 - 20.7 MPa
Hydrogen, per unit of feed for:	
recycle	360 m^3/m^3
consumption	36-142 m^3/m^3
space velocity (LHSV)	1.5-8.0 h^{-1}

2.3 Aromatic compounds in petroleum fractions

Aromatic compounds are a class of organic compounds containing an unsaturated ring of carbon atoms. Benzene as well as the fused ring systems of naphthalene, anthracene and their derivatives is included in the aromatic groups. Analytical techniques such the supercritical fluid chromatography (SFC), high pressure liquid chromatography (HPLC) and infra-red (IR) techniques (Chasey, 1991; Ijam et.al., 1990; Wilson et.al., 1985), have detected three main groups of aromatic compounds present in petroleum fractions. These are the mono, di and polyaromatics. The mono and diaromatics are predominantly found in middle distillates while the polyaromatics, constituting three or more fused benzene rings, are found in larger quantities in higher boiling fraction (> 350 ^{o}C). Table 2.2 shows some of the typical aromatic species present in petroleum fractions.

Table 2.2: Typical structure of some aromatic compounds in petroleum distillates

Type of aromatics	Typical structure
Monoaromatic e.g. alkyl benzene	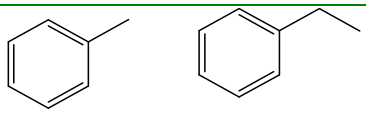
Diaromatics e.g. Naphthalene	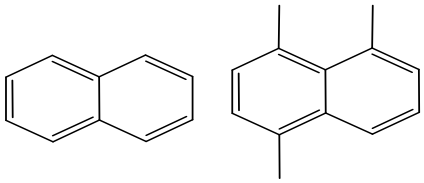
Triaromatics e.g.Anthracene	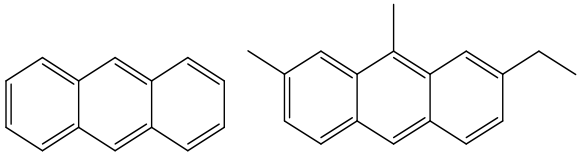

There are variations in the amount and type of aromatic species present in petroleum fractions depending on the origin and processing conditions of the feedstock. Higher concentrations of aromatics are contained in unconventional crude distillates as compared to the conventional petroleum crude distillates (Yui, 1989). Table 2.3 shows the aromatic type distribution in light gas oil fractions from two different sources; Athabasca (unconventional) and Kuwait petroleum (conventional). Petroleum feedstock also contain a moderately large concentrations of heteroatom (sulfur and nitrogen), which are distributed over the whole boiling range and generally increase in concentration in the higher boiling point fractions.

Table 2.3: Aromatic type distribution in untreated light gas oils (LGO) from different sources

	Source of LGO	
Aromatic Type	**Athabasca***	****Kuwait**
Mono	20.7	17.7
Di	12.2	11.5
Poly	3.6	4.5
Total Aromatics	36.5	33.7

*unconventional crude distillate ** Conventional crude distillate

2.4 Reaction and thermodynamic properties of HDA

In the presence of a catalyst and hydrogen gas, aromatic groups are hydrogenated to give hydroaromatic and naphthenes. The more rings in an aromatic cluster, the more thermodynamically favorable the hydrogenation reaction. Monoaromatics are the least reactive and this is due to the unusually high stability of the benzene ring arising from resonance (Gray, 1994). Poly-aromatics on the other hand, are easily hydrogenated and can undergo cycles of hydrogenation and dehydrogenation (Figure 2.1). Generally, for aromatic species containing more than one ring, hydrogenation proceeds via successive reversible steps and each successive stage requires progressively more vigorous conditions (higher temperatures and pressures and longer times) for saturation (Stanislaus and Cooper, 1996).

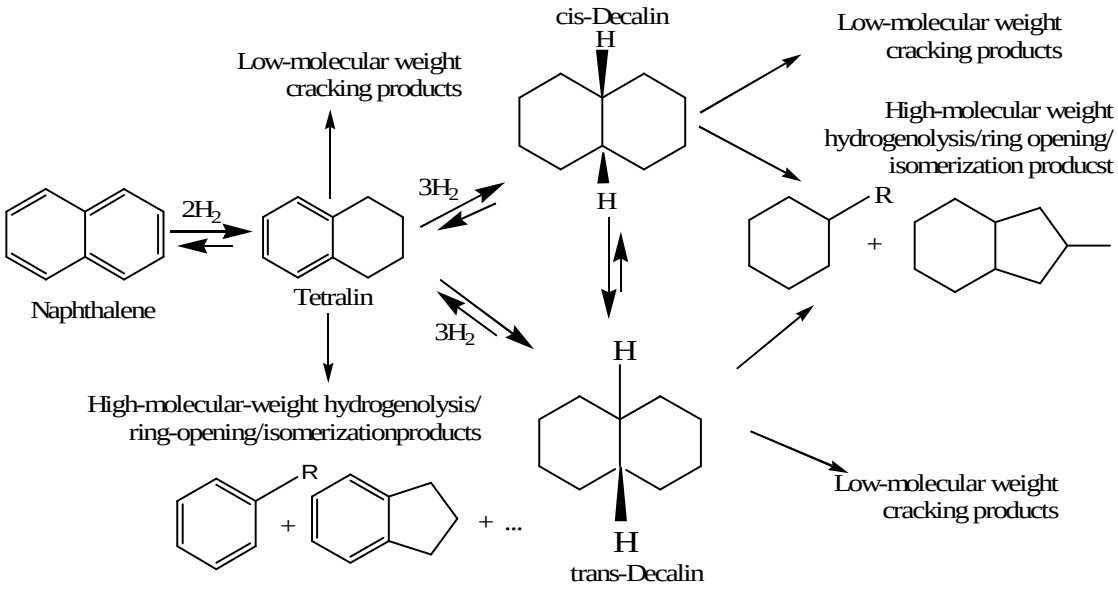

Figure 2.1: Proposed reaction pathway for hydrogenation of naphthalene at high pressure (Albertazzi et.al., 2004).

From the reversible and exothermic nature of HDA, Gully et.al., 1963 postulated that the equilibrium concentration of aromatics (based on equation 2.2) can be approximated by:

$$\frac{Y_A}{Y_A + Y_{AH}} = \frac{1}{1 + K_A \times (P_{H2})^n} \qquad (2.3)$$

where Y_A and Y_{AH} are the mole fractions of the aromatics and saturated hydrocarbon, K_A is the equilibrium constant and P_{H2} is the partial pressure of hydrogen. The equilibrium adsorption coefficient, K_A decreases with increasing temperature leading to a net increase in equilibrium aromatics concentration. Experimental data for calculation of the equilibrium constants are sparse but the few calculated equilibrium constants indicate that there is a considerable variation from one family of aromatics to another (Stanislaus and Cooper, 1996). For example in the hydrogenation of benzene homologues, the value of the equilibrium constant decreases with an increase in both the number of side chains and the number of carbon atoms in each side chain (Lepage,1987; Girgis and Gates,1991). The same is found for naphthalene (Gully et.al., 1963).

The substitution of alkyl groups leads to a very slight decrease in the heat of hydrogenation. However, for hydrogenation of hydrocarbons on sulfide catalysts including NiW and NiMo on alumina support, a complete reverse order of reactivity is observed. In other words, addition of an alkyl group to the aromatic ring favors the reactivity of these molecules for hydrogenation. This is due to the influence of the π electron delocalization through resonance on hydrogenation and hydrogenolysis. Thus hydrogenation is favored by highly electron-donating substituents and it is easier when the aromatic rings to be hydrogenated are less aromatic (Moreau et.al., 1990).

2.5 Reactions of sulfur and nitrogen species

Hydrogenation of the aromatics may involve removal of heteroatom such as sulfur (HDS) and nitrogen (HDN) species. Sulfur species in petroleum may exist in two forms: (1) as thiophene and its derivatives in Figure 2.2, which can be resistant to further processing and (2) as sulfides which are more easily removed.

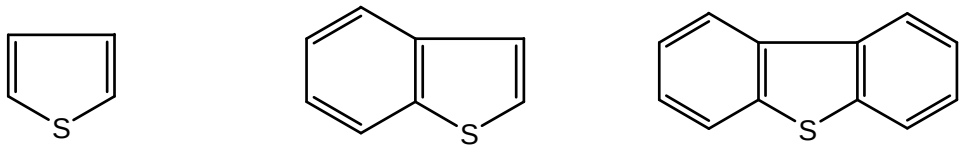

Thiophene Benzothiophene Dibenzothiophene

Figure 2.2: Some organosulfur compounds in petroleum (Gray, 1994)

Studies (Gray, 1994) show that the higher order ring compounds are more reactive than expected and this has been attributed to two main trends: electronic effects on adsorption of the reactant onto the catalyst and subsequent reaction, and steric hindrance of substituents. The least reactive sulfur species are the thiophenes. Removal of sulfur in the presence of a catalyst and hydrogen produces hydrogen sulfide gas (H_2S) as a by-product which can inhibit hydrogenation of aromatic compounds. The two main pathways by which HDS of thiophenic compounds occur are shown in Figure 2.3. They are: (1) an initial step of ring hydrogenation followed by sulfur extraction (steps 1 & 2 and steps 1& 4) or (2) direct sulfur extraction-hydrogenolysis (steps 3, 6 and 7). Depending on the reaction conditions and the type of catalyst used, either pathway can be favored. Studies by Girgis and Gates, 1991 have shown that hydrotreating with $NiMo/Al_2O_3$ at high hydrogen partial pressures will favor the hydrogenation step.

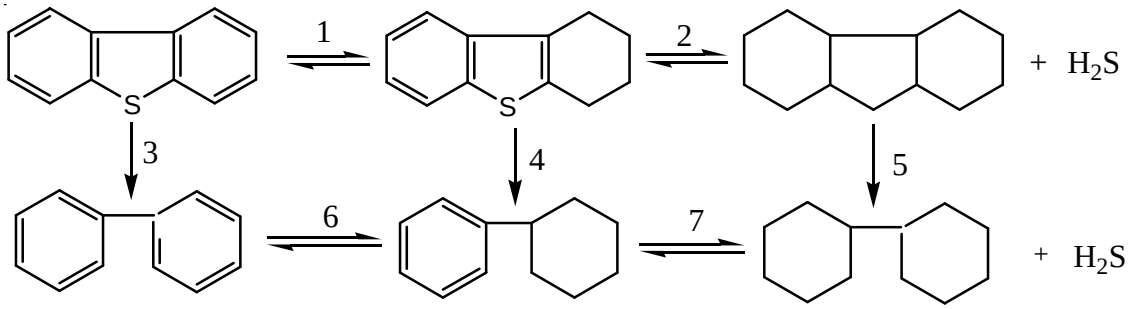

Figure 2.3: Reaction pathways in the HDS of dibenzothiophenes (Whitehurst et.al., 1998)

HDN has a direct relationship with hydrogenation of aromatic compounds. This is because nitrogen is mainly present as heterocyclic aromatic compounds. Two forms of the heterocyclic nitrogen compounds are found: the non-basic derivatives of pyrole and indole and the basic derivatives of pyridine (Figure 2.4) (Girgis and Gates, 1991; Ho, 1988).

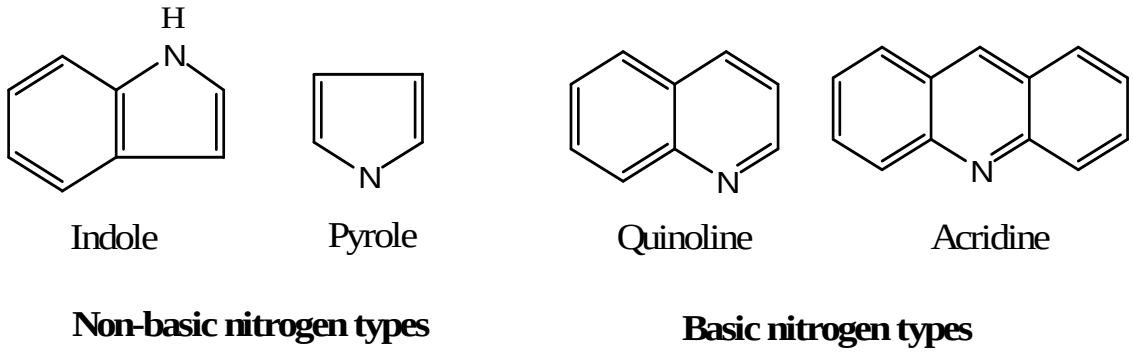

Figure 2.4: Some nitrogen compounds present in petroleum distillates (Gray, 1994)

Higher-ring nitrogen species such as acridine and quinoline have also been identified in gas oils (Schmitter et.al., 1984). The type of nitrogen present is determined by the species' structure. Basic nitrogen species contain a six-ringed structure while the non-basic compounds contain at least one five-ringed member. Unlike HDS reactions, HDN of heterocyclic compounds follow only the hydrogenation pathway before nitrogen extraction (hydrogenolysis) (Girgis and Gates, 1991). This is partly because the C=N bond is very strong compared to the C-H bond (Katzer and Sivasubramanian, 1979; Kabe et.al., 1999). The hydrogenation step thus reduces the large energy of the C-N bond in the ring thereby enhancing the ease of C-N bond cleavage. This suggests that HDN is also limited by equilibrium effects. Figure 2.5 illustrates the HDN reaction pathway in pyridine.

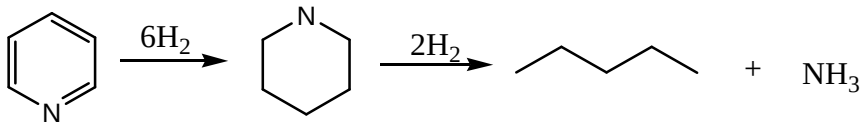

Figure 2.5: Hydrodenitrogenation (HDN) of Pyridine

High hydrogen partial pressures are usually used in the industry to force equilibrium towards the products thus, making HDN irreversible. Generally, the hydrogenation step in HDS is not considered to be critical (Girgis and Gates, 1991; Mascot, 1982; Variant, 1983) whereas this may pose as a difficult step for HDN (Girgis and Gates, 1991; Ho, 1988; Perot, 1991).

2.6 Hydrogen sulfide (H_2S) inhibition studies

Hydrogen sulfide, which is produced as a by-product of sulfur removal, has been reported to significantly inhibit hydrogenation of aromatic compounds (van Gestal et.al., 1992; Girgis and Gates, 1991; Massoth et.al., 1982). However, modeling of the inhibition is complicated since H_2S adsorption can modify the catalyst surface leading to interconversion of catalytic sites and thereby enhancing the hydrogenation activity by increasing the density of Bronsted acid sites. Some of the studies in an attempt to model the inhibition are outlined below.

Ishihara et.al., 2003 investigated phenanthrene (PHE) hydrogenation reaction inhibition over $NiMo/Al_2O_3$ induced by the presence of dibenzothiophene (DBT) molecule in a conventional fixed-bed reactor. Results from their study showed that PHE hydrogenation in the presence of DBT slightly increased when the DBT concentration decreased. Furthermore, the progressive reintroduction of DBT in the feed after a reaction performed in the absence of DBT led to a significant decrease in the PHE hydrogenation activity as well as DBT conversion. Both the PHE and DBT conversions exhibited values lower than the initial ones when DBT was reintroduced in the feed. Their results show that although the presence of sulfur in a feed is essential to preserve good catalytic performance, some hydrogenation catalytic sites can be permanently poisoned, thus reducing the hydrogenation activity.

Mild inhibition of biphenyl hydrogenation over $CoMo/Al_2O_3$ catalyst due to hydrogen sulfide has been reported by Satterfield and Gultekin (1981). Kaszetlan et.al., 1994 studied the influence of H_2S partial pressure on the activity of a model MoS_2/γ-Al_2O_3 catalyst over a wide range of H_2S partial pressure from 0-0.3 MPa, under a total

pressure of 6 MPa, at 320-410 ^{o}C and 0.5-0.7 h^{-1}. Moderate inhibiting effects of H_2S on aromatics hydrogenation were observed on the hydrogenation activity for H_2S partial pressure up to 0.06 MPa. For partial pressures higher than 0.06 MPa, no apparent inhibiting effect of H_2S on the hydrogenation activity was detected. Ancheyta-Juarez et.al., 1999 also studied the effects of hydrogen sulfide on the hydrotreating of middle distillates over Co-Mo/Al_2O_3 catalyst. Using an isothermal fixed-bed reactor, they discovered that the inhibiting effect of hydrogen sulfide in hydrogenation of aromatics decreased with increasing temperatures. This is in agreement with other literature (Gestal et.al., 1992 and Leglise et.al., 1994).

In summary, hydrogen sulfide can modify the catalyst surface (e.g. by increasing the density of Bronsted acid sites), especially at high concentrations, which occur at elevated reaction temperatures. Furthermore, hydrogen sulfide is required to maintain the catalyst in the form of sulfides, rather than oxides. However, excess amounts of the hydrogen sulfide can lower the rate of hydrogenation and the inhibiting effect of H_2S on the hydrogenation activity varies with the absolute level of H_2S in the reactor, and the reaction conditions.

2.7 Cetane rating of diesel

The ignition properties of diesel fuels are expressed in terms of cetane number (CN) or cetane index (CI) (analogous to gasoline octane number). Cetane number is the performance rating of a diesel fuel, corresponding to the percentage of cetane ($C_{16}H_{34}$) in a cetane-methylnaphthalene mixture with the same ignition performance. A higher cetane number indicates greater fuel efficiency. The current minimum cetane index

specification is 40 (US EPA, Diesel Fuel Quality, 1999). The cetane index on the other hand is an estimate of the cetane number.

The cetane number (CN) is measured using a standard diesel test engine according to ASTM D613 test method and is a function of both the chemical and physical characteristics of the fuel. Influence of the chemical properties includes the molecular structures of its constituent hydrocarbons (Wong and Steere, 1982; Gulder et.al., 1985). For example, a high proportion of normal (unbranched) paraffins (C_nH_{2n+2}) in the fuel, especially those with long molecular chains, generally improves the CN. However, cycloparaffins and aromatics with their stable structures are more difficult to break down and ignite, thus reducing the CN.

Since measurement of CN by engine testing requires special equipment as well as being time consuming and costly, they are estimated using mathematical correlations. The number derived is called the cetane index and is a function of the physical properties of the fuel such as the boiling point, aniline point, gravity and density of the sample (Gary and Handwerk, 2001). The aniline point is the minimum temperature for complete miscibility of equal volumes of aniline and the test sample under the ASTM D611 method. A product of high aniline point will be low in aromatics and naphthenes and, therefore, high in paraffins. One of the correlations (cetane index) for estimating the cetane number is the ASTM D976 (equation 2.4). Use of this correlation has a number of limitations; it can only be applied to fuels containing no additives for boosting CN, they are also applicable to pure hydrocarbons and synthetic fuels although substantial inaccuracies may occur when used for estimating CI of crude oils, residuals or products having a volatility of below (260 ^{o}C) (500 ^{o}F) end points.

$$CI = 454.74 - 1641.416 \times \rho + 774.74\rho^2 - 0.554 \times M + 97.803(\log M)^2 \qquad (2.4)$$

where M, is the mid boiling temperature (^oC), and ρ, is density measured at 15 ^oC.

Apart from the cetane index measuring the performance rating of diesel engines, carbon monoxide, hydrocarbon and aldehyde emissions depend on the cetane number of the fuel (Martin et.al., 1997). Table 2.4 shows some hydrocarbons contained in petroleum fuel and their related ignition qualities.

Table 2.4: Hydrocarbons and related ignition quality (cetane number)

Hydrocarbon	**Empirical Formula**	**Cetane number CN**	**Boiling point ^oC**
Paraffins			
3-Methylpentane	C_6H_{14}	30	63.2
n-Heptane	C_7H_{16}	57	98.4
n-Dodecane	$C_{12}H_{26}$	80	216.2
Cyclohexanes			
Cyclohexane	C_6H_{12}	13	80.8
Methylcyclohexane	C_7H_{14}	20	100.3
Bicyclohexylhexane	$C_{12}H_{22}$	53	238.5
Benzene and Alkylbenzenes			
Benzene	C_6H_6	0	80.1
Toluene	C_6H_8	-5	110.7
n-Amylbenzene	$C_{11}H_{16}$	18	204-5
Naphthalenes			
α-Methylnaphthalene	$C_{11}H_{10}$	0	244.8
α-n-Butylnaphthalene	$C_{14}H_{16}$	7	282.5
4–Methyl-4-(β)–naphthylheptane	$C_{18}H_{24}$	10	136-8

2.8 Effects of process variables on aromatics hydrogenation

The principal operating variables for aromatic hydrogenation are temperature, hydrogen partial pressure and space velocity. A lot of studies have been performed to determine the impact of these process variables on aromatics hydrogenation (HDA) and Table 2.5 provides a summary of some of these studies. For further information on these studies, the reader is referred to the accompanying references.

For HDS and HDN reactions which occur simultaneously during aromatics hydrogenation, studies show that increasing temperature and hydrogen pressure will also increase sulfur and nitrogen removal as well as hydrogen consumption (Gary and Handwerk, 2001). Whitehurst et.al., 1998 have reported that high hydrogen partial pressure in HDS processes will lead to a corresponding low hydrogen sulfide partial pressure, thus reducing the H_2S inhibition effects during hydrogenation. Although increasing temperature improves HDS and HDN activity, excessive temperatures can cause severe side reactions such as cracking and reforming of saturated components (Gray, 1994). It can also induce rapid catalyst aging as a result of sintering and coking (Speight, 2000; Gray, 1994).

Table 2.5: Network studies on the impact of operating variables on aromatics hydrogenation (HDA)

Impact of process Variables on HDA	Reactants	Operating Conditions	Results	References
Pressure	Coal-derived Asphaltenes	390,420 450 ^{o}C 3 & 10 MPa	Higher conversions occurred at higher temperatures. Under high H_2 pressure for all temperatures carbon aromaticity and number of aromatic ring/structural unit in unreacted asphaltene were lower than those under lower H_2 partial pressure.	Yoshimoto et.al., 1984
Temperature	Coal-derived middle distillates	$NiMo/Al_2O_3$ 300-400 ^{o}C 4-12 MPa	Above 350 ^{o}C, rate of hydrogenation and thermodynamic limitation controlled the hydrogenation conversion of aromatics. At partial pressures of H_2 around 12 MPa, thermodynamic limitation of HDA was effectively released up to the temperatures of 400 ^{o}C	Machida et.al., 1998 Wilson et.al., 1985 Stanislaus and Cooper, 1996
Temperature	Australian coal	300-500 ^{o}C	Hydrogenation of aromatics passes through a maximum at 450 ^{o}C. Asphaltenes formed at 500 ^{o}C consist of dehydrogenated species produced at lower temperatures. Below 400 ^{o}C a small but significant number of carbon atoms are present in alkyl chains.	Charlesworth, 1980
	Coker LGO	Fixed bed reactor, 330-390 ^{o}C, 12.4 MPa ,0.5 h^{-1} $NiOMoO_3/Al_2O_3$	At 350 ^{o}C, 0.5 h^{-1}, 12.4 MPa, the coker LGO can be hydrotreated to meet the diesel products specifications. The cetane index and aromatics saturation are both affected by thermodynamic equilibrium at temperatures higher than 370 ^{o}C	Anabtawi,1993 Wilson et.al., 1985 Ancheyta-Juarez et.al.,1999

Table 2.5: Network studies on the impact of operating variables on aromatics hydrogenation (continued)

Impact of process Variables on HDA	Reactants	Operating Conditions	Results	Reference
Temperature Pressure LHSV	Tar (Turow brown coal)	$CoMo/Al_2O_3$ $NiMo/Al_2O_3$ 340-400 ^oC 4.0-14 MPa 0.5-2.0 h^{-1}	Hydrogenation of aromatics is markedly dependent on temperature and pressure	Sliwka et.al., 1995
	Diesel oil	Continuous flow, trickle bed reactor 280-370 ^oC 2.0-6.0 MPa 1.5-6 h^{-1}	In general product density and aromatics decreased as temperature or pressure increased or space velocity decreased. The decrease of aromatics is rapid up to about 340 ^oC. Beyond this point, the decrease is very slow. The effect of pressure is stronger up to 5 MPa. After this value, the effect is almost negligible.	Lappas et.al., 1999. Ancheyta-Juarez et.al.,1999
	Heavy distillates from Woadoan coal	CoMo and NiMo, fixed bed reactor; 350-390 ^oC 50-150 kg/cm^2 G 0.5-2 h^{-1}	Lower LHSV and higher H_2 pressure are much more effective in hydrogenation than the higher reaction temperature up to 390 ^oC. H_2 pressure was most effective to hydrogenate aromatic rings.	Sato,1997

2.9 Challenges of aromatics hydrogenation (HDA)

Existing middle distillate hydrotreating using conventional catalysts such as sulfided CoMo, NiMo and NiW supported on alumina has been adapted for reduction of aromatic compounds in diesel. However, studies (Stanislaus and Cooper, 1996; Yui, 1989; Wilson and Fisher 1985) have shown that complete hydrogenation of aromatics is not possible due to the thermodynamic equilibrium limitations under typical hydrotreating conditions. Conventional hydrotreating catalysts designed to reduce sulfur and nitrogen levels would lower the diesel aromatics only marginally (Cooper and Donnis, 1996). Thus the composition and properties of distillate products is highly influenced by the type of catalyst used. Ali et.al. (1997) performed experiments to study dearomatization, cetane improvement and deep desulfurization of diesel feedstock in a single-stage reactor. Using three catalysts; $CoMo/Al_2O_3$, $NiMo/Al_2O_3$, NiW/Al_2O_3, to study the hydrogenation activity at reactor temperatures of 325 and 350 ^oC, hydrogen pressure of 7.5 MPa and LHSV of 2 h^{-1} , these workers observed divergent effects of aromatics content and molecular weight on the cetane index of light cycle oil. Their results also showed that it was impossible to obtain a diesel product that met stringent specifications by using one type of catalyst in a single-stage reactor even under severe operating conditions.

Hydrogenation of aromatics in real feed is inhibited by organic sulfur and nitrogen compound present in the feed as well as H_2S and NH_3 produced by HDS and HDN reactions, respectively. These compounds are strongly adsorbed on the hydrogenation centers of the hydrotreating catalysts compared to the other centers that catalyze the essentially hydrogenolysis reaction (Kasztelan and Guillaume, 1994; Girgis and Gates, 1991). This condition provides a competitive environment for adsorption of

nitrogen, sulfur and aromatics compounds in the feed toward the hydrogenation sites. Preference for adsorption depends largely on the values of adsorption strengths of the different compounds (Chmielowiec, 1986 and Perot et.al., 1988). The extent of H_2S inhibition on aromatic hydrogenation also depends on the catalyst system under investigation.

With the increasingly stringent regulations on diesel oil, a lot of attention has been given to reducing the aromatic contents of distillate fuels. As hydrogenation is exothermic, hydrogenation of aromatics is favored at low temperatures but conventional hydrotreating catalysts are only active at high temperatures (Song, 2003). There is therefore the need to consider hydrogenation at low temperatures (e.g. <300 ^{o}C). One of the best catalysts for low temperature hydrotreating includes noble catalysts. However, these groups of catalysts have very low resistance to sulfur compounds.

These inhibiting effects together with equilibrium limitations (under normal operating range of hydrotreating) make aromatics reduction in industrial feeds (e.g. diesel) more difficult than the other hydrotreating reactions.

2.10 Single–stage hydrogenation of aromatic compounds

Conventional hydrotreating technology (single-stage) is adapted for saturation of aromatics and it has been recognized that aromatic hydrogenation is more difficult than sulfur removal under the conditions that are usually used for hydrotreating (Stanislaus and Cooper, 1996). The existing middle distillate hydrotreaters utilizing the single-stage process and designed to reduce sulfur and nitrogen levels would lower diesel aromatics only marginally (Asim and Yoes, 1987; McCulloch et.al., 1987).

Similarly, high severities of hydrotreating (high temperature) will introduce thermodynamic equilibrium limitation into the hydrogenation reaction and reduce the cetane index of diesel fuel (Lee and de Wind, 1992). To significantly increase the cetane index, single-stage hydrotreating at high pressures with specially designed catalysts for hydrogenation, is recommended. However, the specially developed hydrogenation catalysts such as the supported noble metal catalysts have very low resistance to sulfur and nitrogen poisoning, which means such catalysts can not be used for feedstock containing high levels of sulfur and nitrogen.

It is also observed that reduction of total aromatics is much more difficult than reduction of polyaromatics because saturation of monoaromatics to naphthenes is much more difficult than saturation of polyaromatics to monoaromatics. Processing feed blends containing cracked materials, to meet the 10 vol % total aromatics specification, will require even more severe conditions making the single-stage approach less economically attractive.

2.11 Two-stage hydrogenation of aromatic compounds

For the existing moderate pressure diesel hydrotreater (single-stage process) using base-metal catalyst (NiMo or CoMo), reduction in total aromatics content is very limited, due to the relatively low hydrogenation activity of the base metal catalyst. Addition of a second stage reactor with a high activity noble metal catalyst can produce diesel fuel with low aromatics contents. Especially in the case of noble catalysts, a separate second stage reactor is usually necessary since nitrogen and sulfur- containing compounds must be removed in the first stage reactor, as they are temporary poisons to the catalysts.

Studies conducted on two-stage hydrotreating include the work by Mahey et.al., 1992. They used a two-stage hydroprocessing technique to reduce the pronounced effects of nitrogen-containing species inhibition during hydrocracking of synthetic crude gas oils. Hydrocracking was performed using NiW catalyst supported on silica-alumina. Higher gas oil conversions were achieved and the middle distillate product quality was remarkably improved as the diesel fuel cetane number increased by 13 %. Diesel tests also indicated that the particulate emissions in exhaust gases were lowered by 20 %.

Chmielowiec (1986) has also demonstrated that product yields can be remarkably enhanced in a two-stage approach where unconventional crude gas oil is denitrogenated and then hydrocracked. The two-stage hydroprocessing technique has also found application in the upgrading of coal-derived liquids where oxygenated compounds showed on hydrocracking catalysts an inhibiting effect similar to that of nitrogen compounds (Nishijima et.al.,1987).

Nishijima et.al., 1996 also compared two-stage hydrogenation in coprocessing oil and light cycle oil (LCO) using both NiMo and NiW on alumina support. The latter catalyst was used for the second stage upgrading, because sulfur was largely removed in the first stage hydrogenation over $NiMo/Al_2O_3$ catalyst. From their study, a large improvement in the cetane index (from 36 in the feed to 53 at the end of the second stage) was observed in the coprocessing oil whereas the cetane improvement in the (LCO) remained modest (from 30 in the feed to 43 at the end of the second stage).

Generally, the two-stage process has been found to be superior to the single-stage technology. Especially for feedstock containing a high concentration of polyaromatics, single-stage hydrotreating will not be efficient for deep hydrogenation. With the two-stage hydrogenation technique, improved diesel cetane index property can be achieved

and fuel quality is also enhanced as sulfur and nitrogen levels are reduced to relatively low levels in compliance with the stringent legislature on diesel fuels quality. This technology is being applied in industries world wide (Naber and Stork, 1991; Peries et.al., 1981; Suchanek, 1990).

2.12 Hydrogenation catalysts

The choice of hydrogenation catalyst is highly dependent on the sulfur and nitrogen contents in the petroleum feedstock. When hydrotreating is carried out on feedstock containing appreciable amounts of sulfur and nitrogen compounds, sulfided NiMo, NiW or CoMo on γ-Al_2O_3 catalysts are generally used, whereas supported noble metal catalysts such as platinum or palladium are used for sulfur and nitrogen-free feedstock. Noble metal catalysts on Y-zeolite supports have increasingly been used for hydrogenation in light and middle distillates (Suchanek, 1990; Peries et.al., 1991). Among the Co (Ni)-promoted group VI (Mo or W) metal sulfides on γ-Al_2O_3, NiW are widely used to reduce aromatics, sulfur and nitrogen in petroleum feedstock via hydrotreating. The ranking order for hydrogenation in this group of catalyst is found to be NiW > NiMo > CoMo (Frank and LePage, 1981).

Most hydrogenation catalysts are used in the reduced and sulfided form prior to introduction of hydrocarbon feedstock. These catalysts have been described as consisting of specific stoichiometric combinations of Ni or Co with Mo or W. They exist as a sulfides containing one Ni or Co atom in combination with two Mo or W atoms, chemically anchored to the surface of the solid support (generally alumina or silica alumina) (Whitehurst et.al., 1998). Sulfiding is done by introducing hydrogen sulfide or

a low-boiling sulfur- containing compound (liquid feed) onto the catalyst in the presence of hydrogen. Commonly used sulfur compounds are carbon disulfide, dimethylsulfide, hydrogen sulfide gas and butanethiol. Sulfiding temperatures are within the range of 180-350 ^{o}C at pressures greater than 1.0 MPa (Speight, 2000). For real feed operations, the commonly used temperatures are 193 and 343 ^{o}C at 9.0 MPa.

2.12.1 Nature of sulfide catalytic sites

The location and promotional effects of Co and Ni catalysts have been explained by several different structural models, such as the monolayer model (Schuit and Gates, 1973; Massoth, 1975), intercalation model (Voorhoeve, 1971; Farragher and Cossee, 1973), contact synergy model (Delmon1979), Co-Mo-S phase model (Topsoe et.al., 1981, 1986 and1984) and catalytically active Co site model (Duchet et.al., 1983). The sulfided forms of Co(Ni)-Mo(W) catalysts may be represented as Co_9S_8 ,MoS_2 andWS_2.

In the contact synergy model proposed by Delmon (1979 and 1990), it is assumed that MoS_2 and Co_9S_8 exist as separate crystallites in contact with each other. The role of the promoter (Co_9S_8) is to activate and provide hydrogen atoms to MoS_2. The excess hydrogen atoms would then create reduced centers on the MoS_2 surface, which would in effect be the active sites on the catalysts surface.

In the case of the Co-Mo-S (Ni-Mo-S) phase model proposed by Topsoe and co-workers they explained that the promoter atoms (Co or Ni) are located at the edges of MoS_2-like structures in the plane of Mo cations. Candia et.al., 1984 and Topsoe et.al., 1986 reported that the relative amount of Co atoms present as Co-Mo-S phase has a linear correlation with HDS activity. The catalytically active sites for hydrotreating are viewed as sulfur or anionic vacancies. Some kinetic studies using model compounds

have reported the existence of two distinct types of catalytic sites, one responsible for hydrogenation and the other responsible for hydrogenolysis of heteroatom (Matarresse et.al., 1983; Massoth and Maralidhar, 1982; Zdrazil, 1988). These two sites have been used to explain inhibition reactions of hydrogen sulfide during aromatic hydrogenation.

2.12.2 Interaction between hydrogenation and hydrogenolysis catalytic sites

Several workers (Yang and Satterfield, 1983, Gultekin and Satterfield, 1984 and Girgis and Gates, 1991) have observed inhibition of hydrogenation by H_2S during hydrotreating. Different inhibition effects of H_2S on hydrogenation and hydrodeoxygenation (HDO) of phenols have also been observed by Gevert et.al., 1987. However, in the presence of aromatic compounds, no inhibiting effect of H_2S was observed on HDS of thiophene (Moreau et.al., 1990) and HDN of 2, 4-dimethyl pyridine (Ho, et.al., 1984). To explain this result using the two catalytic centers, Geneste and co-workers (1980 and 1990) conducted a thorough study into hydrogenation of aromatic compounds and hydrogenolysis of S, N and O-containing model compounds. They observed that hydrogenation was mainly affected by the aromatic properties of the molecules and not hydrogenolysis of S, N and O-containing model compounds. However, hydrogenolysis was found to be dependent on the nature of the heteroatom. Hence, hydrogenation and hydrogenolysis reactions could proceed by different adsorption mechanisms; hydrogenation through horizontal π-adsorption and hydrogenolysis through vertical adsorption by the heteroatom. Following this observation, the workers proposed a dual-site mechanism (Figure 2.6) involving either Mo or W atom at different oxidation levels. The higher oxidation state was assigned to

hydrogenation and the lower oxidation state was responsible for hydrogenolysis. These authors then concluded that Mo or W with three sulfur vacancies (higher oxidation) at the corners are primarily responsible for hydrogenation through π-adsorption and hydrogenolysis site could be an edge site with two sulfur vacancies.

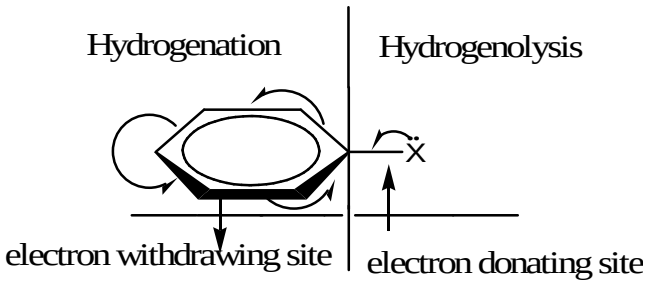

Figure 2.6: Dual-site mechanism proposed for hydroprocessing of C_2H_5X over sulfided NiMo HR 346 catalysts at 340 ^oC and 7 MPa H_2 (Moreau et.al., 1990)

Contrary to the above conclusion, Topsoe, 1989 argued that for a given catalyst, HDS, HDN and HDA can occur on the same sites. Accordingly, all the hydrotreating reactions can be visualized as taking place in vacancies in a mixed surface-sulfide-hydride and nitride phase. Simulating the HDS, HDN and HDA reactions over a series of sulfided Ni(Co)-Mo hydrotreating catalysts, Topsoe suggested that the major effect of the Co and Ni promoter atoms is to lower the equilibrium constant for adsorption of sulfur and nitrogen species.

Another group of researchers have also suggested that hydrogenolysis centers are derived from the hydrogenation sites on the catalyst surface when H_2S is adsorbed (Figure 2.7). Hence, only one type of sulfur or anion vacancy present on sulfided catalyst is required. As a result, distribution of type I (promoted sites) and type II (sites with H_2S adsorbed) sites would depend on the sulfidation state of the catalyst and the

partial pressure of H_2S. Consequently, the effect of H_2S on the rate of the hydrotreating reactions is expected to depend on the H_2S partial pressure during reaction (Vivier et.al., 1991; Topsoe et.al., 1990).

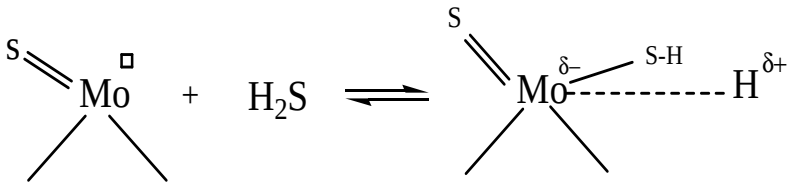

Figure 2.7: Transformation of hydrogenation sites into hydrogenolysis sites

An illustration of the Type I and Type II sites (crystallites) and 4,6-dimethyldibenzonthiophene (4,6-DMDBT) molecules in their approximate sizes is shown in Figure 2.8 (Whitehurst et.al., 1998). The Type I sites are made up of single-layered crystals with a thickness of about 6 Å. They are found either lying flat or standing perpendicular to the support surface (Bouwens et.al., 1994). Those found flat on the support surface are usually limited geometrically, that is, interaction between the reactant and the catalyst is not in the plane of the MoS_2. Thus, access to the active sites of the catalyst is still limited to approach from only one side (Chianelli, 1984; Daage and Chianelli, 1994). The reacting molecule can not approach the catalyst perpendicular since the molecule is much wider that the Type I layer thickness. Type I crystallites found perpendicular to the support are most likely to occur in crystals bonded to the alumina surface by Al-O-Mo or Al-S-Mo bonds (Whitehurst et.al., 1998). They allow a higher probability site access with higher activity.

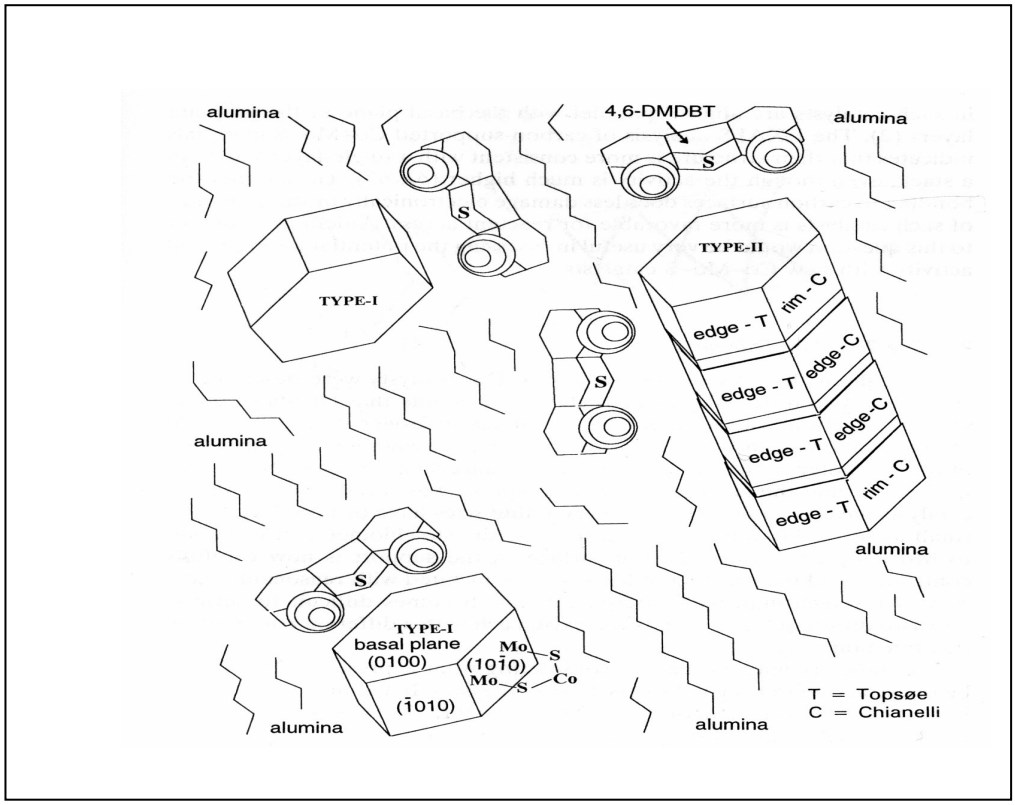

Figure 2.8: Geometric considerations in the HDS of dialkyldibenzothiophenes

Unlike the Type I sites, the Type II crystallites (shown in Figure 2.8) occur as stacks of small crystallites with a height to diameter ratio of approximately 1.5-3 (Bouwens et.al., 1994). They are much more accessible to the reactant and it is noted that about 75 % of all the edge sites can be approached by 4, 6 DMDBT molecule in a perpendicular alignment with the alumina surface. Hence, for either geometric or electronic reasons, the Type I sites are expected to have lower activity than the Type II sites.

In summary, hydrogenation of aromatics is strongly inhibited by both nitrogen species and H_2S. These compounds are strongly adsorbed on the hydrogenation centers than on the other centers that catalyze the hydrogenolysis reaction. Consequently, there

is competition between different nitrogen, sulfur and aromatic compounds present in the feed toward adsorption on hydrogenation sites. Preference for adsorption in such a competitive environment is strongly dependent on the adsorption strengths of the different compounds (Stanislaus and Cooper, 1996).

2.13 Kinetics of aromatics hydrogenation (HDA)

Several types of model aromatic compounds have been used in the study of HDA kinetics. Literature information on HDA kinetics in industrial feedstock such as petroleum and synthetic middle distillates are relatively scarce, as a result of the complexity of the reactions. Other studies (Ali, 1998; Girgis and Gates, 1991; Van Gestal et.al.,. 1992; Kasztelan et.al., 1994) have also been conducted to investigate the inhibition effects of sulfur and nitrogen removal on aromatic hydrogenation. Two main models used to kinetically model HDA are the power law and Langmuir-Hinshelwood rate equations (Girgis and Gates, 1991; Sapre and Gates, 1979). The latter accounts for inhibition reactions while the former is used to represent the overall rate law for the individual hydrogenation of the various aromatic groups.

2.13.1 Power-law kinetic modeling

The equilibrium reaction in equation 2.5 can be used as a basis for developing a kinetic model for hydrogenation of aromatics in middle distillates.

$$A + nH_2 \underset{k_r}{\overset{k_f}{\rightleftharpoons}} AH \qquad (2.5)$$

where A is the aromatic species, AH is the saturated hydrocarbon and k_f , k_r are the rate constants for the forward and reverse reactions respectively. By assuming that the forward reaction is pseudo-first order (since hydrogenation is carried out in large

hydrogen excess at constant partial pressure) and the reverse reaction is first order in saturates (Wilson and Kriz 1984), the rate expression is given by:

$$-r_A = \frac{dC_A}{dt} = k_f C_A - k_r C_{AH} \tag{2.6}$$

where r_A is the reaction rate, C_A and C_{AH} are the concentrations of the aromatic and hydrogenated hydrocarbons, respectively.

The equilibrium constant can be applied to the reactants and products when the reaction goes to completion:

$$K_A = \frac{f_A}{f_{AH} P_{H2}^n} \approx \frac{[A]}{[AH] P_{H2}^n} = \frac{k_f}{k_r P_{H2}^n} \tag{2.7}$$

where K_A is the equilibrium constant, f_i is the fugacity of either the aromatics or saturated aromatics and P_{H2} is the partial pressure of hydrogen. Manipulation and substitution of equation 2.7 into equation 2.6, the final rate expression can be written as:

$$-r_A = -\frac{dC_A}{dt} = k_f C_A - \frac{k_f}{K_A P_{H2}^n} C_{AH} \tag{2.8}$$

This model can also be used to analyze the kinetics of aromatics conversion in a tubular reactor over NiW/γ-Al_2O_3 at 340-440 ^oC and 5.0-17.0 MPa hydrogen pressure (Gray, 1994).

Wilson et.al., 1984 developed a similar model for kinetics of hydrogenation of aromatics in middle distillates by assuming reversible pseudo-first order reaction and reaction in excess hydrogen gas. On integration of equation 2.6, the following expression was derived:

$$\ln \frac{C_A - C_{AE}}{C_{AO} - C_{AE}} = -kt \tag{2.9}$$

Where C_{AO} is the initial aromatics concentration, C_{AE} is the equilibrium aromatic concentration, k is the hydrogenation rate constant, and t is the space time.

Studies by these authors on the aromatic reduction of middle-distillate fractions of Alberta synthetic crude shows that the reaction is kinetically controlled i.e. $k_f / k_r >> 1$ with the rate expression:

$$\ln \frac{C_A}{C_{AO}} = -kt \tag{2.10}$$

Other kinetic models based on a simple first-order reversible kinetics have been developed. Yui and Sanford (1984) proposed the following rate equation for aromatics hydrogenation in middle distillates:

$$-\frac{dC_A}{dt} = k_f P_{H2}^n C_A^m - k_r (1 - C_A) \tag{2.11}$$

Where k_f and k_r are the forward and reverse rate constants, respectively, P_{H2} is the hydrogen partial pressure, C_A is the concentration of aromatics, n is the reaction order with respect to hydrogen partial pressure, and m is the reaction order with respect to the aromatics contents.

Substituting 1/LHSV for t, the final integrated rate equation for equation 2.11 is:

$$\ln \frac{C_A - C_{AE}}{C_{AO} - C_{AE}} = -\frac{1}{C_{AE}} \left(\frac{k}{LHSV} \right) \tag{2.12}$$

Most of the kinetic studies on model aromatic compounds reported in literature deal mainly with the reaction pathways and reactivities, rather than quantitative kinetic models. The very few studies on kinetic modeling have proposed an overall first order reaction with respect to the aromatic reactant, neglecting the effect of hydrogen partial pressure and the thermodynamic equilibrium. For example, Sapre and Gates,1981

reported a pseudo-first order reaction rate for benzene hydrogenation over presulfided $CoMo/Al_2O_3$ catalyst at 325 ^oC and 7.1 MPa. A similar study by Lipannas et.al., 1991 on the kinetics of fluorenes on NiW/Al_2O_3 catalyst, found the reaction to be first order in the aromatic hydrocarbon as well.

2.13.2 Langmuir- Hinshelwood (L-H) modeling

Most of the kinetic studies using LH inhibition rate equations have been based on sulfur and nitrogen model compounds with the following general reaction steps;

1. Adsorption of the reactant (A*) on the active site of the catalyst with an adsorption factor K_{A*}.
2. Reaction of A* on the surface of the catalyst with other reactants adsorbed on other sites or in the bulk solution to form products
3. Desorption of the products from the active sites into the bulk solution.

In the presence of other species (I), such as H_2S which is usually taken as an inhibitor in competition with aromatics for the same adsorption sites, the concentration of the adsorbed aromatics reactant [A^*_{AD}] is markedly reduced. The rate of conversion of the reactant (X_{A*}) is thus dependent on the fraction of adsorbed sites covered by the reactant instead of the actual concentration of the reactant. The observed rate is given by:

$$r_{A_{obs}} = k_{obs}[A^*] = k_{actual} X_{A^*} \tag{2.13}$$

and

$$X_{A^*} = \frac{K_{A^*}[A^*]}{(1 + K_{A^*}[A^*] + K_I[I^*] + ...)} \tag{2.14}$$

with the degree of inhibition expressed as:

$$\frac{1}{(1 + K_{A^*}[A^*] + K_I[I^*] + ...)} \tag{2.15}$$

Although the Langmuir-hinshelwood model can represent hydrogenation kinetics better than the power law model, in general, simple power law models have been used by most researchers to represent hydrogenation kinetics since the use of Langmuir-Hinshelwood type of rate equation is complicated and there are too many coefficients that are difficult to determine.

3.0 EXPERIMENTAL

3.1 Scope

This chapter contains a discussion on statistical design of experiments, the experimental plan and procedure including operation of the fixed bed reactor and apparatus used to obtain data in this work. A discussion of the feed and product analysis is also included in this chapter.

3.2 Statistical design of experiments

Statistical design of experiments was used to design the experimental program for Phase I of the research. A response surface methodology (RSM) using the central composite inscribed design (CCI) was adopted. RSM consists of a group of statistical and mathematical techniques for empirical model building and exploitation that relate an output or a response to a number of predictors or input variable that affect it (Box et. al., 1987). Some of the attractive features of using the RSM approach are that conclusions can be drawn from the initial stage of investigation and are also very effective for determining the optimal reaction conditions for a given process (Yoon et. al., 1999).

The central composite inscribed (CCI) design was applied with three design factors or inputs; temperature (T), pressure (P), and liquid hourly space velocity (LHSV). This design consists of an embedded factorial and fractional factorial design characterized by central (0), axial (-1, +1) and star (*) points. The star points represent the extreme values of each process variable. The coded and actual levels of the design factors used in this statistical study are shown in Table 3.1 and Table 3.2 shows the design matrix of the experimental program.

Table 3.1: Actual and coded levels of the design parameters

Temperature (^oC):	340	350	365	380	390
Pressure (MPa)	6.9	8.2	9.6	11.0	12.4
LHSV (h^{-1})	0.5	0.8	1.25	1.7	2.0
Codes	-*	-1	0	+1	+*

Table 3.2: Design matrix of experimental program for statistical study

	Variables			**Measured Response: Conversion**		
Experimental Run #	**Temperature (T) ^oC**	**Pressure (P) MPa**	**LHSV h^{-1}**	**X_{TA} %**	**X_S %**	**X_{TN} %**
1	365	6.89	1.25			
2	390	9.65	1.25			
3	340	9.65	1.25			
4	365	9.65	1.25			
5	365	12.41	1.25			
6	350	8.27	1.70			
7	380	8.27	1.70			
8	350	11.03	1.70			
9	380	11.03	1.70			
10	365	9.65	2.00			
11	350	8.27	0.80			
12	380	8.27	0.80			
13	350	11.03	0.80			
14	380	11.03	0.80			
15	365	9.65	0.50			
16	365	9.65	1.25			
17	365	9.65	1.25			
18	365	9.65	1.25			
19	365	9.65	1.25			
20	365	9.65	1.25			

X_{TA} – conversion of total aromatics: X_S- conversion of total sulfur: X_{TN} – conversion of total nitrogen

The total number of runs (N) required by this design is 20, calculated from;

$$N = 2^x + 2x + 6 = 20 \text{ trials} \quad (3.1)$$

where 6 is the number of replicates at the center levels and x is the number of design factors or input variables under investigation. In comparison to the other factorial designs, the number of trials needed for a full second order factorial design would be:

$$N = 3^k + 6 = 33 \text{ trial} \quad (3.2)$$

A decrease in the total number of trials with the CCI design is significant and the benefit is more pronounced in the case of 6 factors, where the total number of trials would be 80 and 733 for the central composite and the full second order factorials, respectively (Rigas et.al., 2000).

The Design Expert software version 6.0 was used to design the experiments and process the data.

3.2.1 Test for significance of regression models

Analysis of Variance (ANOVA) technique was used to test for the adequacy of the regression models of HDA, HDS and HDN. This is a test based on the variance ratios to determine the significant differences among the means of several groups of responses and their normal distribution. The statistical F-test was used to determine the significance of effects on the regression models (Yoon et.al., 1999). For any regression equation to be statistically significant, the probability value (p-value) of the F-values should be less than 0.05 (User Manual, Design Expert 6.0, 2003).

Other statistical properties such as the R^2 coefficient and lack of fit test were used to check for the goodness of fit of the regression models (Rigas et.al., 2000).

Information obtained from the R^2 coefficient (which varied from 0-1) determined the percentage variability of the optimization parameters (conversions) explained by the model while the lack of fit test was used to validate the selected model. Probability values, (p-value), of the 'lack of fit test' greater than 0.1 were desired.

3.3 Experimental plan

3.3.1 Phase I: Single-stage HDA with sulfided $NiMo/Al_2O_3$ catalyst

Studies (Wilson et.al., 1985; Yui et. al., 1981; Gary et. al., 2001) show that temperature, H_2 partial pressure, space velocity and hydrogen-to-oil ratio are the main processing parameters affecting hydrogenation of aromatics. Gary and Handwerk, 2001 reported that among the process factors of hydrotreating, hydrogen partial pressure is the most important factor affecting HDA. However, most of the existing data in literature (Wilson et.al., 1985; Yui et. al., 1981; Gary et. al., 2001; Gray, 1994) leading to the above observations were obtained using the classical one-variable approach to design the experiments. However, this method of experimental design ignores the interaction effects of the operating variables on hydrogenation of aromatics and may be inadequate in determining the optimum conditions for maximizing the response.

The purpose of this part of the thesis was to determine the significant interaction process variables and the optimum operating conditions of aromatics hydrogenation, sulfur and nitrogen removal using a statistical technique. Experiments were done using a blend of LGO feedstock and a commercial $NiMo/Al_2O_3$ catalyst in a single-stage hydrotreater. The response surface methodology via the central composite inscribed design (CCI) was used to design the experiments and the hydrotreating data were analyzed by the ANOVA technique.

3.3.2 Phase II: Single-stage HDA over sulfided NiW/Al_2O_3 catalyst

One of the factors affecting hydrogenation of aromatics is the type of hydrotreating catalyst used. The common hydrotreating catalysts used in industries are NiMo, CoMo and NiW on alumina supports. Among these hydrotreating catalysts, the latter is known to be the most effective for hydrogenation of aromatics followed by NiMo and CoMo. NiMo is efficient for nitrogen removal but can also be used for some degree of hydrogenation since majority of nitrogen species found in petroleum are found attached to aromatics structures.

The purpose of this study was to investigate the activity of NiW/ γ-Al_2O_3 for hydrogenation of aromatic compounds in a variety of light gas oil feedstock; vacuum, atmospheric, hydrocrack and a blend (VLGO, ALGO, HLGO and LGO blend, respectively). The effects of temperature on the liquid product distribution and mild hydrocracking (MHC) in the LGO feedstock were also studied. All the experiments in were performed by varying temperature from 340-390 ^oC at the optimum pressure and LHSV conditions obtained in Phase I.

A lab-prepared NiW/Al_2O_3 was used for hydrotreating the feedstock. The catalyst was prepared by incipient wetness impregnation method (Ferdous et.al., 2004). By this approach, a solution containing 3.0 wt % of Ni in nickel nitrate [$Ni(NO_3)_2.6H_2O$], 15 wt % of tungsten in ammonium metatungstate and 2.5 wt % of phosphorus in phosphoric acid (H_3PO_4) in water was impregnated onto the alumina support at room temperature. The support (γ-Al_2O_3, Sud Chemicals India, Ltd., New Delhi) was initially dried at 120 ^{o} C overnight. Following impregnation, the catalyst was dried at 120 ^oC for 12 h and then calcined at 500 ^oC for another 4 hours. The catalyst

was characterized for its BET surface area and transmission electron microscopy (TEM) measurements (see Appendix B).

3.3.3 Phase III – Two-stage hydrotreating of LGO Blend

From literature (Stanislaus et.al., 1994; Landau et.al., 1996; Mahay et.al. 1991) the two-stage hydrotreating process has proven to be more efficient for maximum hydrogenation of aromatics. Since HDA is deemed more complex than HDS and HDN, reactions in the stage I reactor are usually targeted at heteroatom removal while the reactions in the stage II reactor are purposely used for hydrogenation of aromatics (Nishijima et.al., 1996; Stanislaus and Cooper, 1996).Removal of the heteroatom, specifically sulfur species in the stage I reactor, is to reduce the overall inhibition of hydrogen sulfide on HDA.

The focus of this part of the research was to investigate the effect of hydrogen sulfide removal on the degree of hydrogenation of aromatic compounds in LGO feed from Athabasca bitumen in a two-stage hydrotreater using two catalyst systems; $NiMo/Al_2O_3$ (stage I) and NiW/Al_2O_3 (stage II). The effect of residence time on hydrogenation of aromatics in each stage of hydrotreating was also studied in terms of the distribution of the liquid hourly space velocity between the stage I and stage II reactions.

Results from the two-stage process were then compared to those obtained from a single-stage process where hydrotreating was carried out over commercial $NiMo/Al_2O_3$ catalyst. The experiments were performed by varying temperature from 350-390 ^oC at a constant pressure of 11.0 MPa and LHSV ratios of 1:1.5; 1:1 and 1.5:1.

3.3.4 Phase IV-Kinetic modeling

Kinetic modeling of the single and two-stage experiments was done using the Langmuir-Hinshelwood rate equations. Data for the kinetic studies were obtained from the experimental results from Phases I-III. The main objective of this phase of the research was to develop mathematical models describing inhibition of HAD by H2S during hydrotreating. Further studies were also conducted on mild hydrocracking (MHC) during upgrading of the different bitumen-derived LGO feedstock. Kinetics parameters controlling MHC were determined from power law kinetic models.

3.4 Experimental procedure

3.4.1 Catalyst loading

The reactor (internal diameter =10 mm and length = 285 mm) was sealed at the bottom with a Swagelok 60 micron stainless steel filter and then packed with glass beads, silicon carbide and catalyst material from bottom to top. The extrudate catalyst (1.2-2.0 mm) was first dried at 200 ^{o}C for three hours in an oven before being loaded into the reactor. A complete catalyst loading was made up of three main parts; separate sections of various sizes of silicon carbide; catalyst bed and glass beads. Figure 3.1 shows the schematic representation of the catalyst loading in the reactor. Above and below the catalyst bed are layers of glass beads followed by a 25, 10 and 10 mm of 16, 46 and 60 mesh silicon carbide (SiC), respectively. The catalyst bed is maintained at 10 cm high by diluting the catalyst pellets with 90-mesh size SiC. The purpose of the diluents as well as the SiC layers is to provide complete catalyst wetting, reduce radial dispersion and reduce the bed porosity; thus minimizing any diffusion effects and providing plug flow conditions for isothermal reactions (Bej et.al., 2001).

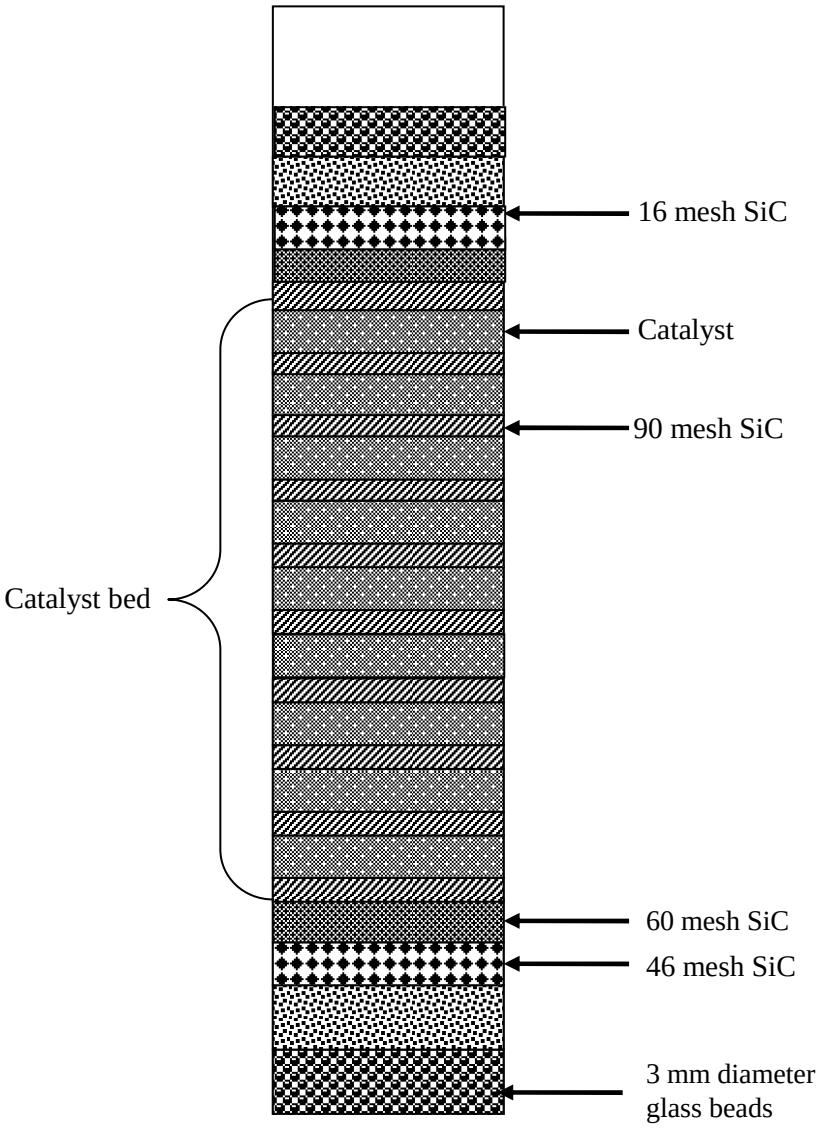

Figure 3.1: Schematic diagram of catalyst loading in the reactor

3.4.2 Catalyst sulfiding

Prior to hydrotreating, the metal-oxide catalyst was transformed to the sulfide state with a solution of butanethiol in straight-run gas oil. The essence of sulfiding was to decrease the initial high activity of the catalyst and maintain uniform catalyst activity across the catalyst surface (Yui, 1994; Nagai et.al., 1988).

Maintaining the operating pressure at 9.0 MPa, helium was allowed to flow through the system at 50 ml/min as the reactor temperature was steadily increased to 100 ^{o}C. At this temperature, 100 ml of a 2.9 vol % butanethiol solution was pumped into the catalyst bed at a very high rate to wet the catalyst. The flow rate was then reduced to maintain an LHSV of 1.0 h^{-1}. Hydrogen gas was then introduced at a rate corresponding to the hydrogen-to-oil ratio and the helium flow turned off (see Appendix A for a discussion on the calibration of the hydrogen mass flow meter). The reactor temperature was then increased to 193 ^{o}C. At this condition, sulfiding was allowed to occur for 24 hours. The temperature was then increased to 343 ^{o}C for another round of 24-hour sulfiding.

3.4.3 Catalyst activity stabilization

After sulfiding, the catalyst was stabilized at a temperature of 375 ^{o}C, LHSV of 1.0 h^{-1} and pressure of 9.0 MPa for five days by hydrotreating with heavy gas oil. The purpose of catalyst stabilization was to ensure uniform catalyst activity across the catalyst surface prior to the experimental runs (Speight, 2000). Sample products were collected after every 24 hours, stripped and analyzed for sulfur, nitrogen and aromatics contents.

3.4.4 Experimental runs

Four different light gas oil fractions from Athabasca bitumen and produced by Syncrude Canada Ltd were used for the experimental study. The feeds used were vacuum light gas oil (VLGO), hydrocrack light gas oil (HLGO), atmospheric light gas oil (ALGO) and blend of all the light gas oils (BLGO). Although the feedstock are from

the same source they have varying aromatics, sulfur and nitrogen content due to the different processing conditions used for each feedstock. Table 3.3 summarizes the properties of the feed. Commercial $NiMo/Al_2O_3$ catalyst and lab-prepared NiW/Al_2O_3 catalysts were used for hydrotreating.

Table 3.3: Properties of LGO feedstock

Feed	^{13}C-NMR [%]	Total Nitrogen [wppm]	Total Sulfur [wppm]	Cetane index CI
VLGO	23.6	634	26780	41.2
ALGO	15.0	290	15020	36.3
LGO Blend	17.1	461	17420	36.1
HLGO	24.0	1773	7149	43.2

Schematic diagram of the experimental set-up is shown in Figure 3.2. During hydrotreating, the oil feed was mixed with hydrogen rich gas which entered the top of the fixed bed reactor in a downward flow pattern. In the presence of the metal sulfide catalyst, the hydrogen reacted with the oil to produce hydrogen sulfide, ammonia, saturated hydrocarbons and free metals. The reaction temperature was provided by a twin-furnace system attached to the reactor and monitored by a temperature controller (See Appendix A for reactor temperature calibration). The reactor effluent was then stripped off any ammonia in the scrubber after which it was stored in a high pressure separator to separate the liquid products from gases. Hydrogen sulfide in the exit gas was absorbed in a sodium hydroxide solution and the excess hydrogen vented to the atmosphere. From the high pressure separator, sample products were collected and stripped off any remaining hydrogen sulfide gas and ammonia by bubbling nitrogen gas through the sample for at least 2 hours at a slow rate.

As shown in Figure 3.2, only one reactor was used throughout the experimental work. For the two-stage process, the experiment was designed such that all the stage I experiments were completed before the stage II experiments were performed (see section 3.4.5 for discussion on the two-stage hydrotreating process).

3.4.5 Two-stage hydrotreating

The LGO blend was used as feedstock for the two-stage upgrading process. Experiments were performed at 350,365,380 and 390 ^{o}C at three different space velocities ratios between stage I and stage II of 1:1.5, 1:1 and 1.5:1. Pressure was maintained constant at 11.0 MPa. The combined reaction time for both stages was 1.67 h corresponding to the same reaction time for hydrotreating of the same feed over commercial NiMo/Al_2O_3 in a single-stage hydrotreater (Phase I). The combined reaction time is also the reciprocal of the optimum LHSV for maximizing hydrogenation as obtained in Phase I.

The same procedure for catalyst loading was used in both reactors (i.e. 5 g of NiMo/Al_2O_3 in the stage I reactor and 5 g of NiW/Al_2O_3 in stage II reactor). Hydrogen sulfide was removed in the stage I effluents by bubbling pure nitrogen gas through the collected product before being further hydrotreated in the stage II reactor. The products from both stages were tested for total sulfur, nitrogen and aromatics contents. Figure 3.3 and Figure 3.4 show the experimental plan for the two-stage hydrotreating process.

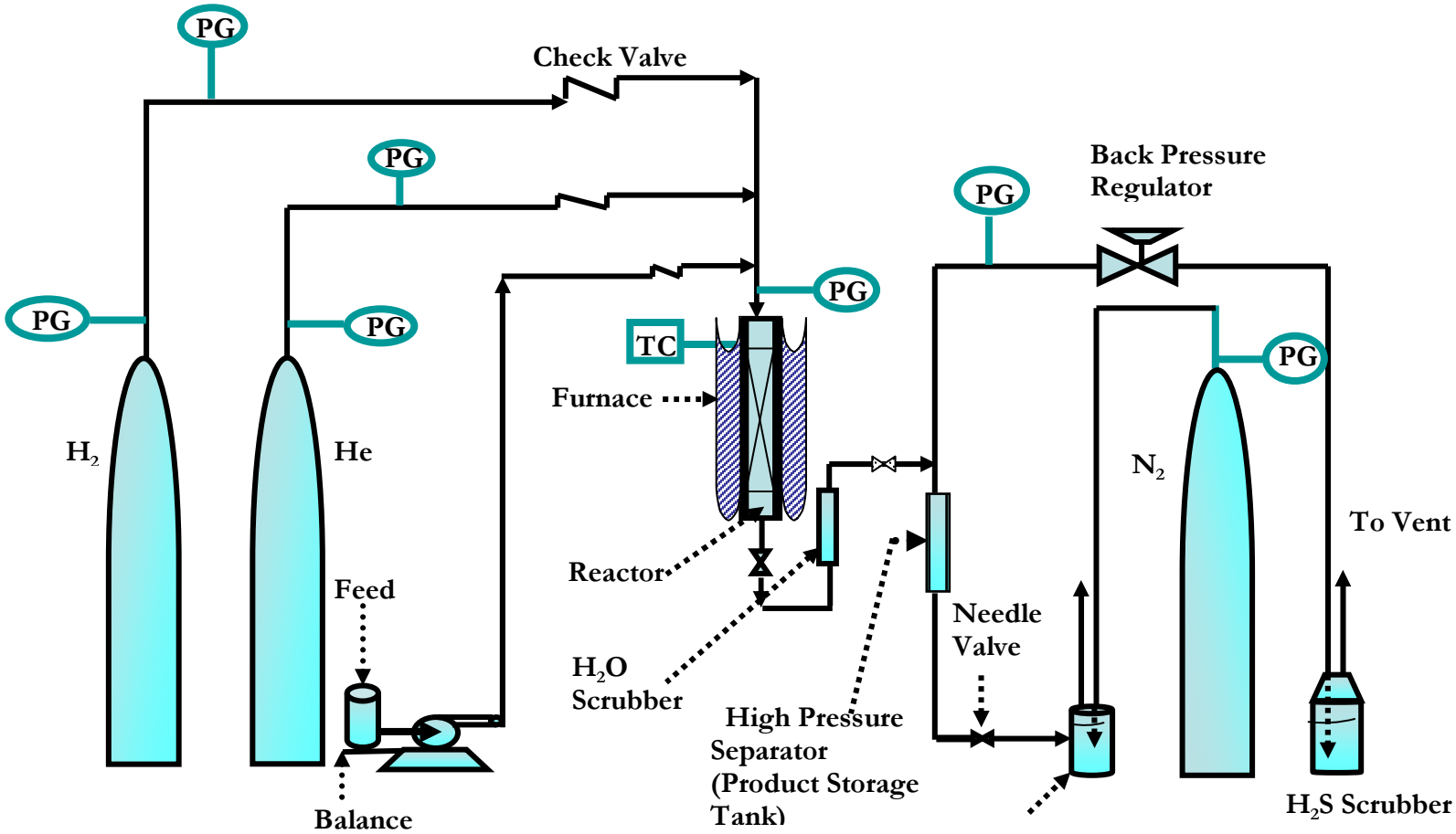

Figure 3.2: Experimental set up (PG-Pressure Gauge; TC- Temperature Controller)

3.4.6 Deactivation studies

Deactivation studies were performed at the end of each experiment to determine the extent of catalyst deactivation. This involved running the experiments at the same conditions as the catalyst stabilization step for a period of three days. Results from the deactivation tests were compared to the catalyst activity at the stabilization conditions. A few deactivation tests were also done at some selected experimental conditions to check the reproducibility of the data. The deactivation tests did not indicate significant change in the catalyst activity. A significant loss in activity would indicate that the catalyst deactivated during the experimental run.

3.5 Feed and product analysis

The feed and products were measured for aromatics, sulfur and nitrogen contents. The total aromaticity was determined using ^{13}C-NMR spectroscopy while Supercritical fluid chromatography (SFC) was used to determine the concentrations of the individual aromatics groups, namely mono, di and polyaromatics. Sulfur and nitrogen concentrations were measured by combustion/fluorescence or chemiluminescence's techniques using an Antek 9000 NS analyzer. Boiling point distribution of the feed and product samples were analyzed by GC simulated distillation using Varian model CP 3800 gas chromatography. Details of the analytical techniques are given in Appendix B. The cetane indices (CI) of the feed and sample products were calculated as a function of density and boiling point temperature using the ASTM D976 correlation.

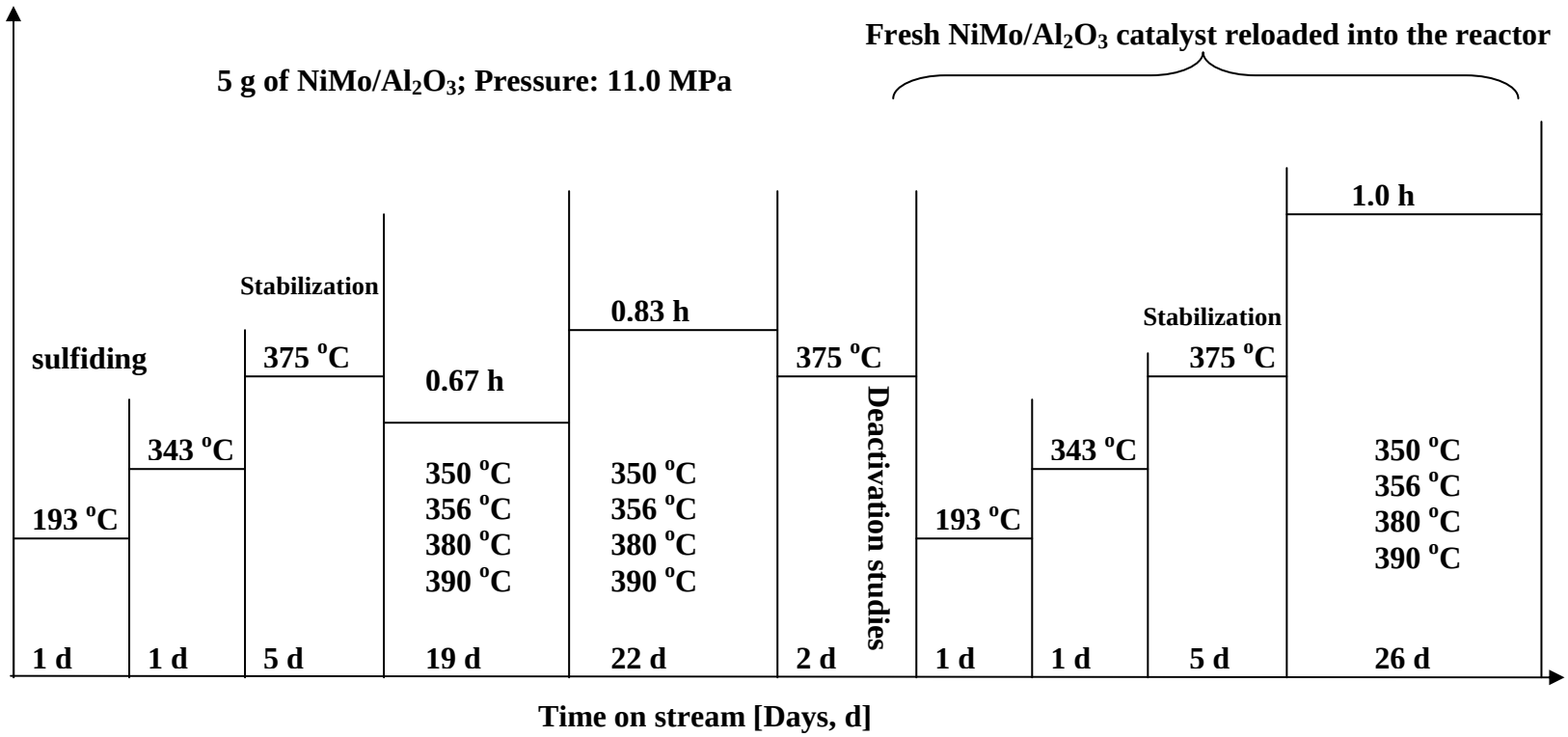

Figure 3.3: Experimental plan for stage I of the two-stage hydrotreating process

Second stage (Stage II)

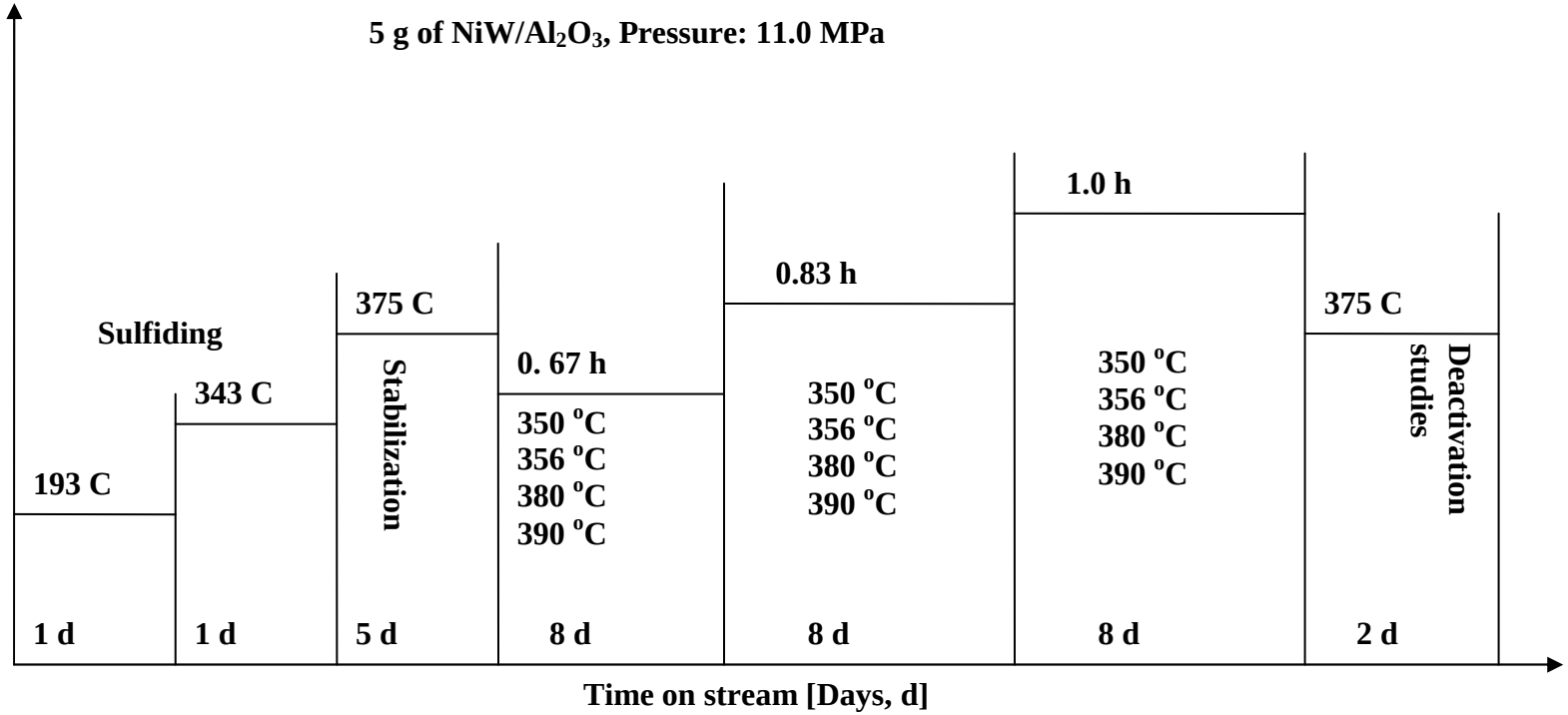

Figure 3.4: Experimental plan for stage II of the two-stage hydrotreating process

4.0 RESULTS AND DISCUSSION

This chapter describes the results obtained at the different phases of the research. Section 4.1 deals with the study of the significant interaction factors affecting HDA, HDS and HDN in a single-stage reactor with commercial NiMo catalyst. Optimization of the HDA process for maximum hydrogenation of aromatics is also discussed in this section. Studies of the hydrogenation and hydrotreating activities of lab-prepared NiW catalyst in four different light gas oil feedstocks are discussed in Section 4.2. This section also gives details on the extent of mild hydrocracking (MHC) in gas oil fractions. Section 4.3 describes the impact of hydrogen sulfide inhibition on HDA, cetane index and HDS at three liquid hourly space velocity ratios in a two-stage hydrotreating process where the commercial NiMo is used in the stage I reactor and the lab-prepared NiW in the stage II reactor. Finally, Section 4.4 describes the kinetic modeling of HDA, HDS as well as MHC.

To ensure reproducibility of the results, some of the experiments were repeated. Measurements of the concentration of aromatics, sulfur and nitrogen concentrations as well as the simulated distillation showed a maximum variation of 7 wt %, 5 wppm, 2 wppm and 4 wt %, respectively.

4.1 Single-stage HDA with $NiMo/Al_2O_3$

Statistically designed experiments based on Central Composite Inscribed Design (CCID) were conducted to investigate the significant interaction parameters controlling conversion of aromatics, sulfur and nitrogen in HDA, HDS and HDN processes, respectively. The optimum conditions for maximum hydrogenation of aromatics were also determined based on the regression model for estimating aromatics conversion. The experiments were performed by hydrotreating a blend of light gas oil from Athabasca oil sands over commercial $NiMo/Al_2O_3$. The operating conditions used were: temperature (340-390 ^oC); pressure (6.9-12.4 MPa) and LHSV (0.5-2.0 h^{-1}). Hydrogen-to-oil ratio was maintained constant at 550 ml/ml.

4.1.1 Statistical analysis

The Analysis of Variance (ANOVA) technique was used to develop response surface, interaction and contour plots as well as regression models for predicting the percent conversions of aromatics, sulfur and nitrogen in HDA, HDS and HDN processes, respectively.

The following linear regression model consisting of the main effects, interactions and quadratic terms, was used (Box et.al., 1978).

$$Y = \alpha_o + \sum_{i=1}^{3} \alpha_i X_i + \sum_{i<j}^{3} \alpha_{ij} X_i X_j + \sum \alpha_{ii} X_i^2 \qquad (4.1)$$

where Y is the estimate of the response variable and X_i's are the independent variables (temperature, pressure and LHSV) for each experimental run. The expressions α_o, α_i α_{ij} and $\alpha_{ıı}$ are the regression parameters. The main effects are represented by the X_i's, X_iX_j's account for the interaction terms, and X_i^2 terms indicate quadratic effects.

Conversion is defined as:

$$Conversion = \frac{[feed] - [products]}{[feed]} \times 100\% \quad (4.2)$$

where [feed] and [products] are the concentrations of the species in the feed and product samples, respectively.

4.1.2 Significant interacting parameters affecting HDA

The HDA model in Table 4.1 shows that the two-level interaction between temperature and pressure is the only significant interaction term influencing hydrogenation of aromatic compounds in the bitumen-derived light gas oil.

Table 4.1: Regression models for HDA, HDS and HDN

Parameter	**Model coefficients for estimating conversion**		
Model	Y_{HDA}	Y_{HDS}	Y_{HDN}
Intercept	50.10	97.80	97.60
T	15.20	2.60	4.50
P	21.80	-0.90	0.95
LHSV	-6.70	-2.50	-5.90
T^2	-26.30	-1.80	-4.60
P^2	-41.10	<0.01	-2.10
$LHSV^2$	<0.01	-2.80	-4.40
T × P*	**23.60**	<0.01	<0.01
T ×LHSV*	<0.01	**1.50**	**4.70**
LHSV × P*	<0.01	<0.01	<0.01

* Interaction terms Y_i = regression model

This means that at any constant value of LHSV, a simultaneous increase in both temperature and pressure will significantly increase conversion of the aromatics.

The three-dimensional plot in Figure 4.1a shows that conversion of aromatics passes through a maximum with increasing temperature and pressure. That is, increasing temperature accelerates the rate of reaction until the thermodynamic equilibrium limitation begins to exert a significant reverse effect on the hydrogenation reaction. The thermodynamic effect is as a result of the exothermic nature of the reversible reaction which shifts equilibrium to the reactants, thus producing more aromatics in the products. The effect of pressure on aromatics conversion is further illustrated in the two-dimensional plot of Figure 4.1b. This is an interaction plot of the effect of temperature and pressure (at the two extreme levels) on the conversion profile of aromatics at a constant LHSV of $1.25h^{-1}$. Conversion of aromatics is observed to pass through a maximum with increasing temperature and pressure. At lower pressure levels (6.9 MPa) less aromatic compounds are hydrogenated but when the reactor pressure is increased to 12.4 MPa, the hydrogenation activity increases significantly with higher conversions. This is because when the reactor pressure is increased, equilibrium is essentially forced towards the products, thus making hydrogenation virtually irreversible with a resulting increase in conversion (Gray, 1994). It can be inferred from Figure 4.1b that although higher pressures increase the overall conversion of aromatics, the reaction is still dominated by equilibrium effects at higher reaction temperatures.

The predicted model gives numerical values of the effects of the input variables on the response. However, it is difficult to see right away the dependence of the response surface on the design factors and to be able to achieve this, contour plots are usually used.

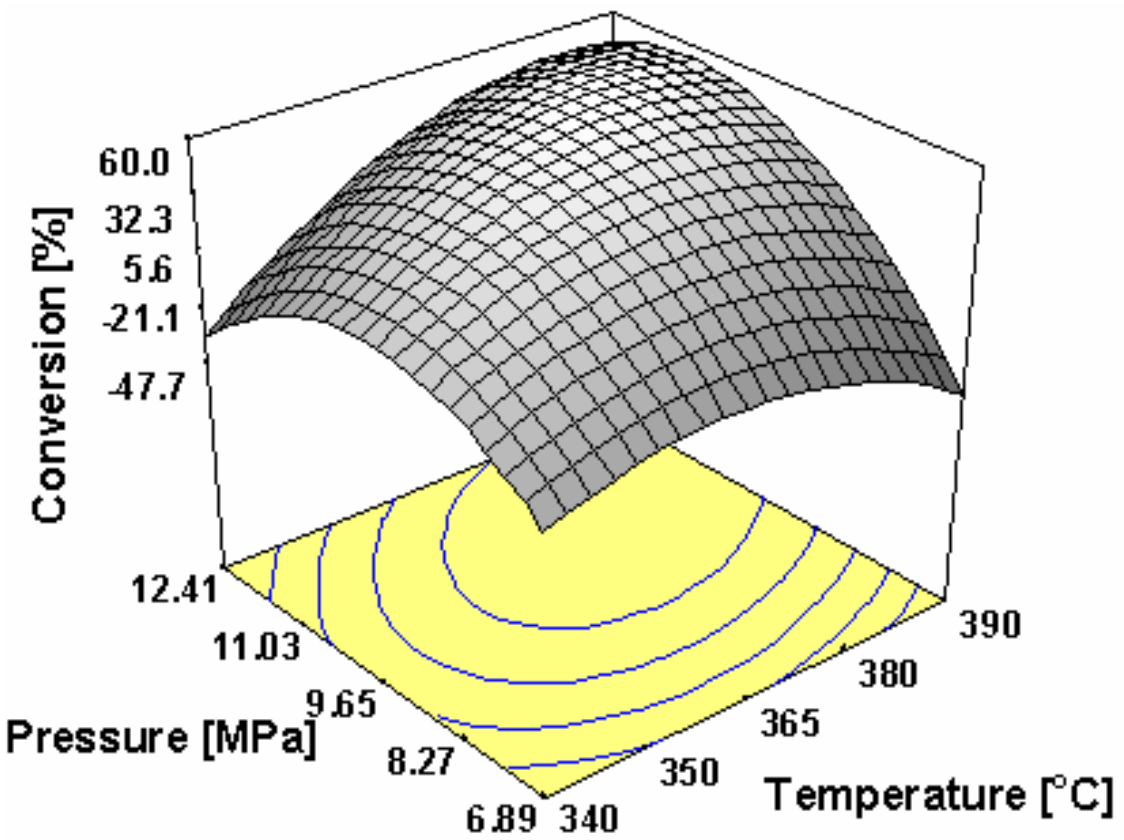

Figure 4.1a: Surface response plot for the effect of temperature and pressure on aromatics conversion (LHSV=1.25 h^{-1}, H2/oil ratio =550 ml/ml)

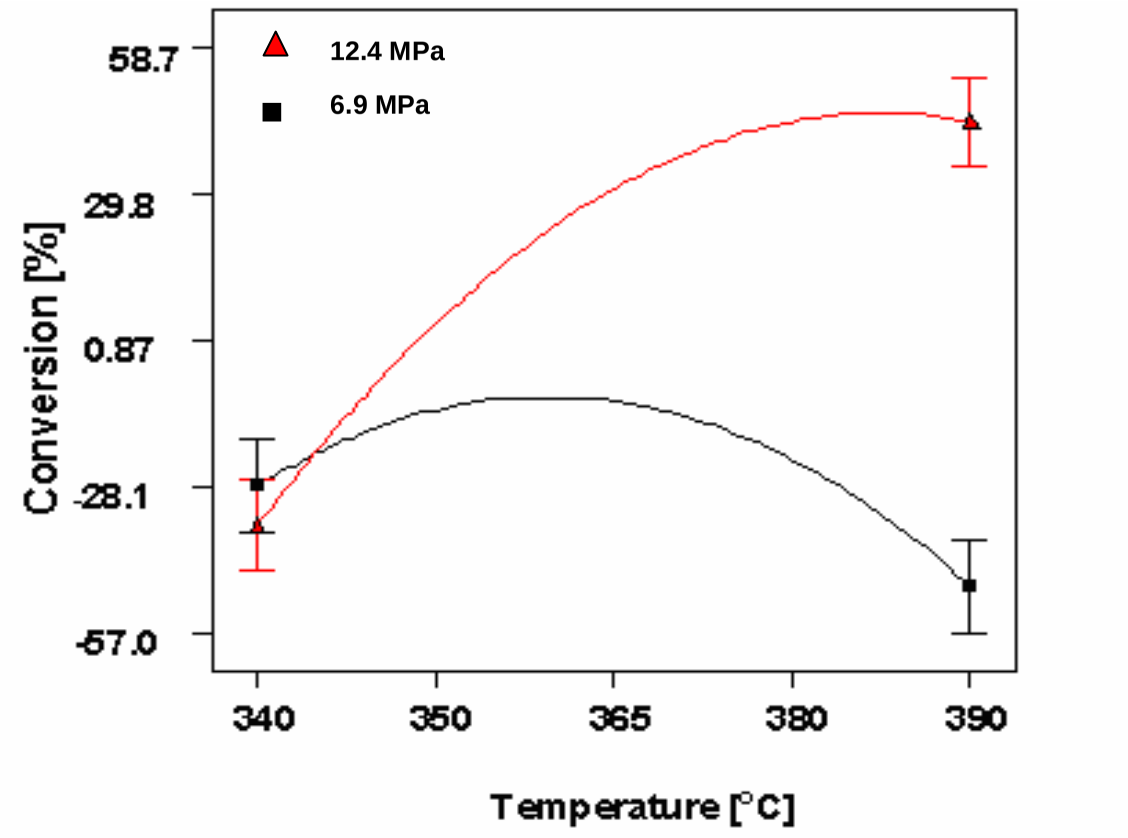

Figure 4.1b: Effect of interaction of temperature and pressure on HDA activity (LHSV=1.25 h^{-1}, H2/oil ratio =550 ml/ml)

Contours are 2-dimensional plots which give a geometric representation of the underlying response function over the experimental region. Figure 4.1c is a contour plot where each contour line represents the predicted value of response at a constant LHSV slice of 1.25 h^{-1}. As predicted by the model, it can be observed from Figure 4.1c, that the conversion of aromatics covers the range of -12.0 to 57.8 % when both temperature and pressure change from 340 to 390 ^{o}C and 6.9 to 12.4 MPa respectively. The negative conversion values observed at the extreme levels of temperature and pressure in the contour plot are due to the low temperature hydrogenation effects and equilibrium limitations at higher temperatures: at these conditions more aromatics are collected in the hydrotreated products compared to the feed thus, leading to negative conversion values.

Optimization of the aromatics hydrogenation shows that at the following operating conditions; temperature of 379 ^{o}C, pressure of 11.0 MPa and LHSV of 0.6 h^{-1}, conversion of aromatics can be maximized to 63 %. At these same conditions, sulfur and nitrogen conversions are 98.5 and 99.7 %, respectively. This result suggests that in order to maximize hydrogenation of aromatics in light gas oil feedstock from Athabasca bitumen, severe hydrotreating conditions are necessary.

4.1.3 Significant interacting parameters affecting HDS and HDN

The final models for HDS and HDN activities are also shown in Table 4.1. It can be inferred from both models that the interaction between temperature and LHSV was the most significant term affecting conversion. Thus, a simultaneous increase in temperature and space velocity at any constant pressure level would increase conversion of sulfur and nitrogen during hydrotreating.

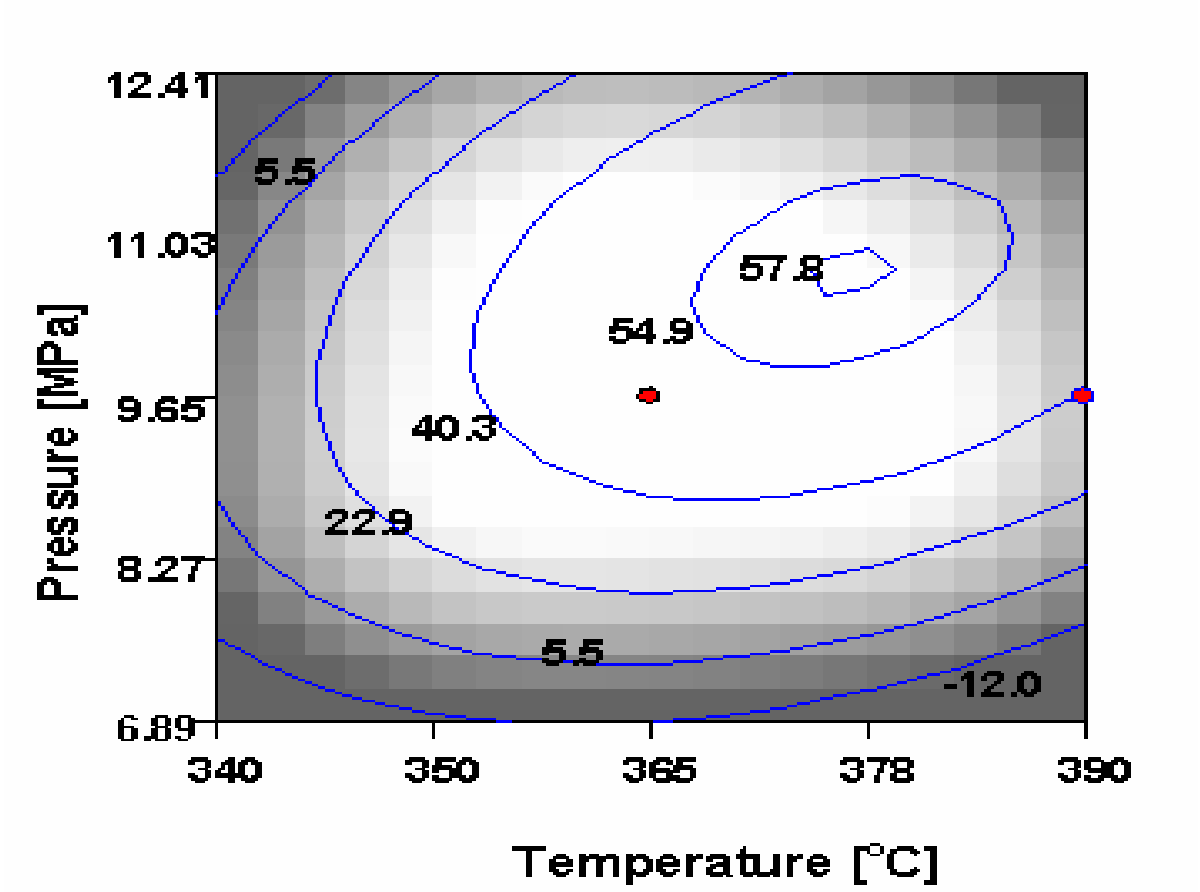

Figure 4.1c: Contour plots for the effects of temperature and pressure on aromatics conversion (LHSV=1.25 h^{-1}, H2/oil ratio =550 ml/ml)

Unlike HDN, increasing pressure for HDS with all other parameters remaining constant will have a negative impact on the sulfur conversion. This may be due to the fact that the reaction is already taking place in excess hydrogen therefore any further increase in pressure will have little or no effect on the system. Yui et.al., 1988 studied hydrogenation of coker naphtha with NiMo catalyst with the following reaction conditions; temperature (140-280 ^{o}C), pressure (3.0-5.0 MPa) and LHSV of (1.0-2.0 h^{-1}). Although their conditions are lower than the conditions used in this study, they also observed that during hydrotreating, temperature and LHSV are the only factors exhibiting remarkable effect on HDS- pressure had negligible influence on the HDS activity.

The response surfaces for HDS and HDN in Figures 4.2a and 4.2b, respectively, show high conversions of sulfur and nitrogen during hydrotreating. Sulfur conversion varied from ~88 to 99 wt % while nitrogen conversion approached 100 wt %. However, in both cases sulfur and nitrogen conversions passed through maximum with increasing temperature and pressure. This is due to equilibrium limitations affecting the reactions which mean that for sulfur and nitrogen species present in the feed, heteroatoms preferably react by hydrogenation followed by C-S and C-N bond cleavage due to the high hydrogenation activity of NiMo catalyst (Massoth et.al., 1990; Knudsen et.al., 1999).

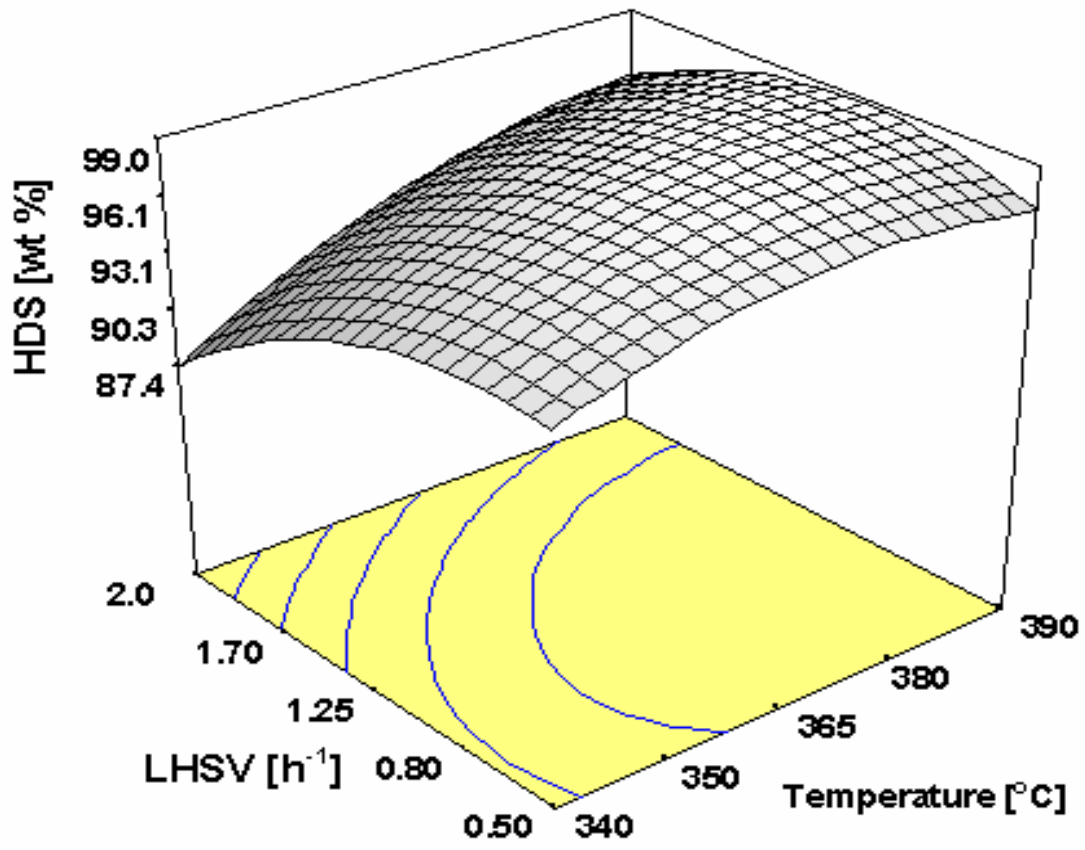

Figure 4.2a: Surface response plots showing the effect of interaction of temperature and LHSV on sulfur conversion (HDS activity) (LHSV=1.25 h-1; H_2/oil ratio = 550 ml/ml)

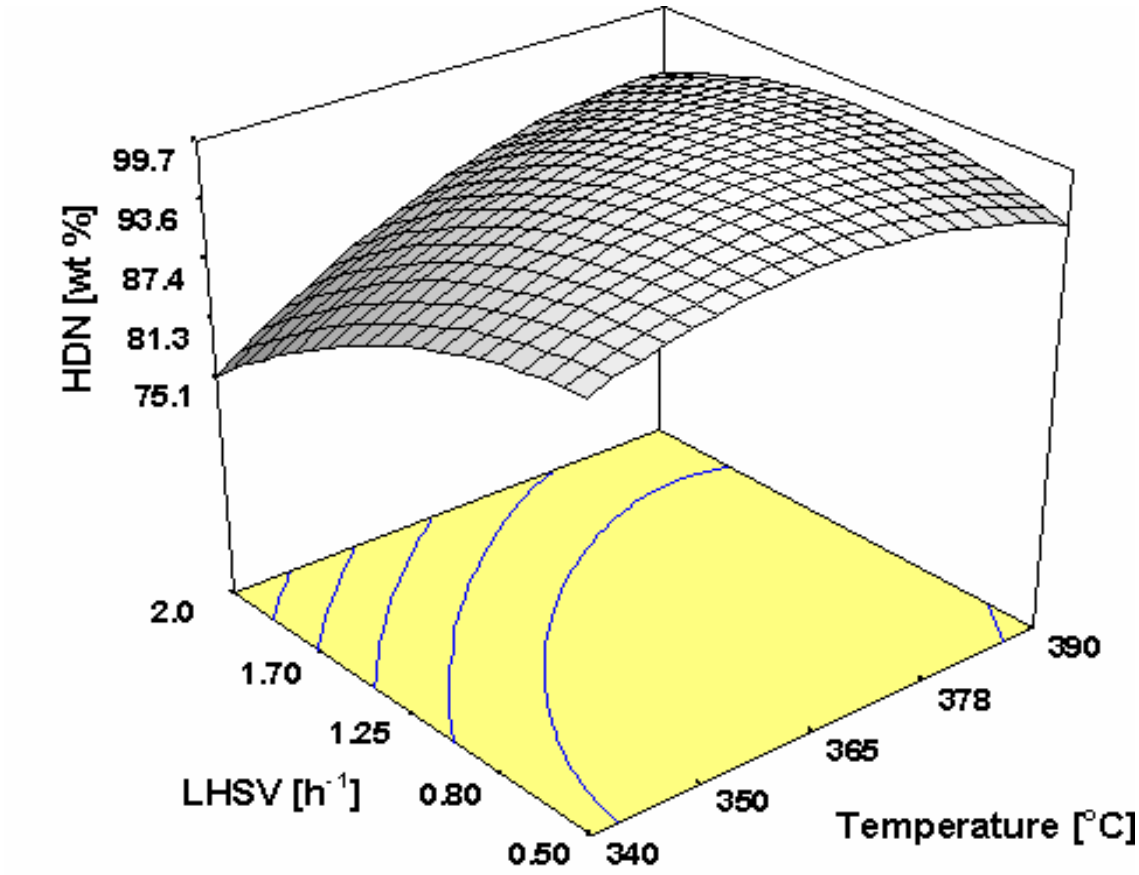

Figure 4.2b: Surface response plots showing the effect of interaction of temperature and LHSV on nitrogen conversion (HDN activity) (LHSV: 1.25 h^{-1}; H_2/oil ratio: 550 ml/ml)

4.1.4 Impact of temperature and pressure on cetane index (CI)

The effect of temperature and pressure on the CI was studied by varying temperature and pressure between 340-390 ^{o}C and 6.9-12.4 MPa respectively, at a constant LHSV of 1.25 h^{-1}. The cetane index of the feed and hydrotreated samples was calculated from the ASTM D976 correlation:

$$CI = 454.74 - 1641.416\rho + 774.74\rho^2 - 0.554M + 97.803(\log M)^2 \qquad (4.3)$$

where M = mid boiling point temperature (^{o}C) and ρ = specific gravity.

Table 4.2 shows the effect of temperature and pressure on the cetane index.

Table 4.2: Effect of temperature and pressure on cetane index

Impact of temperature on the cetane index at a constant pressure of 9.6 MPa			
Feed		36	
Temperature [^{o}C]	340	365	390
Cetane index,CI	42 ± 0.6	45 ± 0.7	34 ± 0.5
Impact of pressure on cetane index at a constant temperature of 365 ^{o}C			
Pressure [MPa]	6.9	9.6	12.4
Cetane index,CI	41 ± 0.6	45 ± 0.7	47 ±0.7

It is observed that increasing temperature from 340 to 365 ^{o}C leads to a marginal increase in cetane index from 42 to 45 after which further rise in temperature results in a progressive decrease in CI to about 34 at 390 ^{o}C. Hence, the cetane index of the diesel fraction also passes through a maximum and this is because of the direct relationship of the cetane with changes in the aromatics contents during hydrotreating. No equilibrium effects were however observed when the reaction pressure was varied from 6.9 to 12.4 MPa at a constant temperature of 365 ^{o}C and space velocity of 1.25 h^{-1}. The cetane index

rather increased from 41 to 47, well above the minimum specification of 40 (US EPA, 1999).

4.2 PHASE II- Single-stage hydrotreating with NiW/Al_2O_3

4.2.1 Hydrogenation of aromatics (HDA) in LGO blend

Following the Phase I study, another set of experiments was conducted to determine the activity of NiW/Al_2O_3 for hydrogenation of the total aromatics in different LGO feedstock. Prior to this study, hydrogenation of the mono, di and polyaromatics contained in a blend of light gas oils from Athabasca bitumen was investigated by varying the reaction temperature from 340-390 ^oC at the optimum pressure and LHSV conditions of 11.0 MPa and 0.6 h^{-1}, respectively.

Figure 4.3 shows the effect of temperature on the rate constants of mono-, di- and polyaromatic hydrogenation. The reaction rate constants were used as a measure of the speed of disappearance of poly, di or monoaromatics species during hydrogenation. The rate constants were derived from the pseudo-first order power law relation:

$$k_i = -LHSV\left(\ln\left(\frac{C_i}{C_{io}}\right)\right) \tag{4.4}$$

where k is the rate constant, LHSV is the liquid hourly space velocity, C_i is the concentration of aromatics in the products, and C_{io} is the concentration of aromatics in the feed. The subscript 'i' refers to the mono-, di- or polyaromatics species.

The rate of disappearance of the aromatic groups ranged from 0.63×10^{-4} s^{-1} for monoaromatics to 2.4×10^{-4} s^{-1} for polyaromatics. In terms of kinetics, the ease of hydrogenation followed the general order: polyaromatics > diaromatics >> monoaromatics with the fastest step (hydrogenation of polyaromatics) being about 6

orders of magnitude greater than the slowest step (hydrogenation of monoaromatics). Although the reactivity of a compound decreases with increasing molecular weight, the ease of hydrogenation of the higher order aromatic compounds (poly- and diaromatics) compared to the monoaromatics is because hydrogenation of the higher order aromatic species are thermodynamically favored even under mild hydrotreating conditions (Stanislaus and Cooper, 1996). The lower hydrogenation rate of the monoaromatics is because of the species' extra stability provided by its resonance structure.

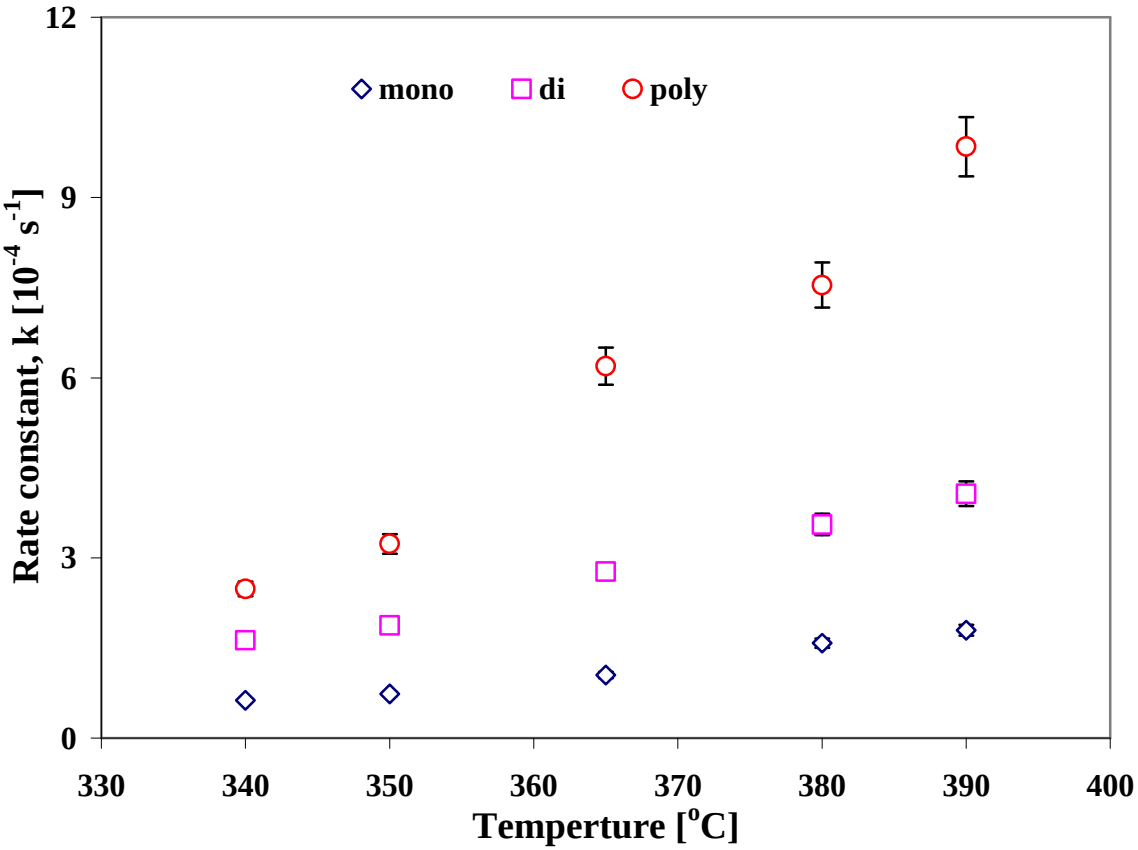

Figure 4.3: Effect of temperature on the rate of hydrogenation of mono, di and polyaromatics over NiW/Al_2O_3

It can be inferred from this result that hydrogenation of the monoaromatics is the most difficult and the rate-limiting step and this is consistent with other reports by Stanislaus and Cooper, 1996 and McCulloch, 1975. Hence, severe hydrotreating conditions are required to produce high quality diesel fuel since a significant increase in cetane number is observed when monoaromatics are fully hydrogenated (Hill, et.al., 2002).

4.2.2 Hydrodesulfurization (HDS) and Hydrodenitrogenation (HDN)

The effect of temperature on the rate of HDN and HDS over the NiW catalyst is shown in Figure 4.4. The rate constant values for the two processes were similar at lower temperatures, i.e. 340-350 ^{o}C. However, between 365-390 ^{o}C, the HDN activity was faster than that of the HDS but both reactions approached equilibrium with the former being about 1.5 orders of magnitude higher. Evaluation of the conversion data also showed that at equilibrium, nitrogen and sulfur conversions were approximately 99 and 96 %, respectively. The high HDN activity is due to the high hydrogenation propensity of the NiW/Al_2O_3 catalyst since most of the nitrogen species found in LGO have aromatic structures and removal of nitrogen proceeds by hydrogenation before hydrogenolysis. Another explanation to the higher HDN activity is the presence of less refractory nitrogen compounds in the feedstock (451 wppm) compared to the more refractory sulfur-containing compounds (18,451 wppm). Similar results have been reported by Botchwey et.al., 2003, when they also studied the effect of temperature on HDS and HDN activities in bitumen-derived heavy gas oil over $NiMo/Al_2O_3$ at the following operating conditions: temperature of 340-420 ^{o}C; pressure of 6.5-11.0 MPa; LHSV of 0.5-2.0 h^{-1} and H_2/oil ratio of 600ml/ml.

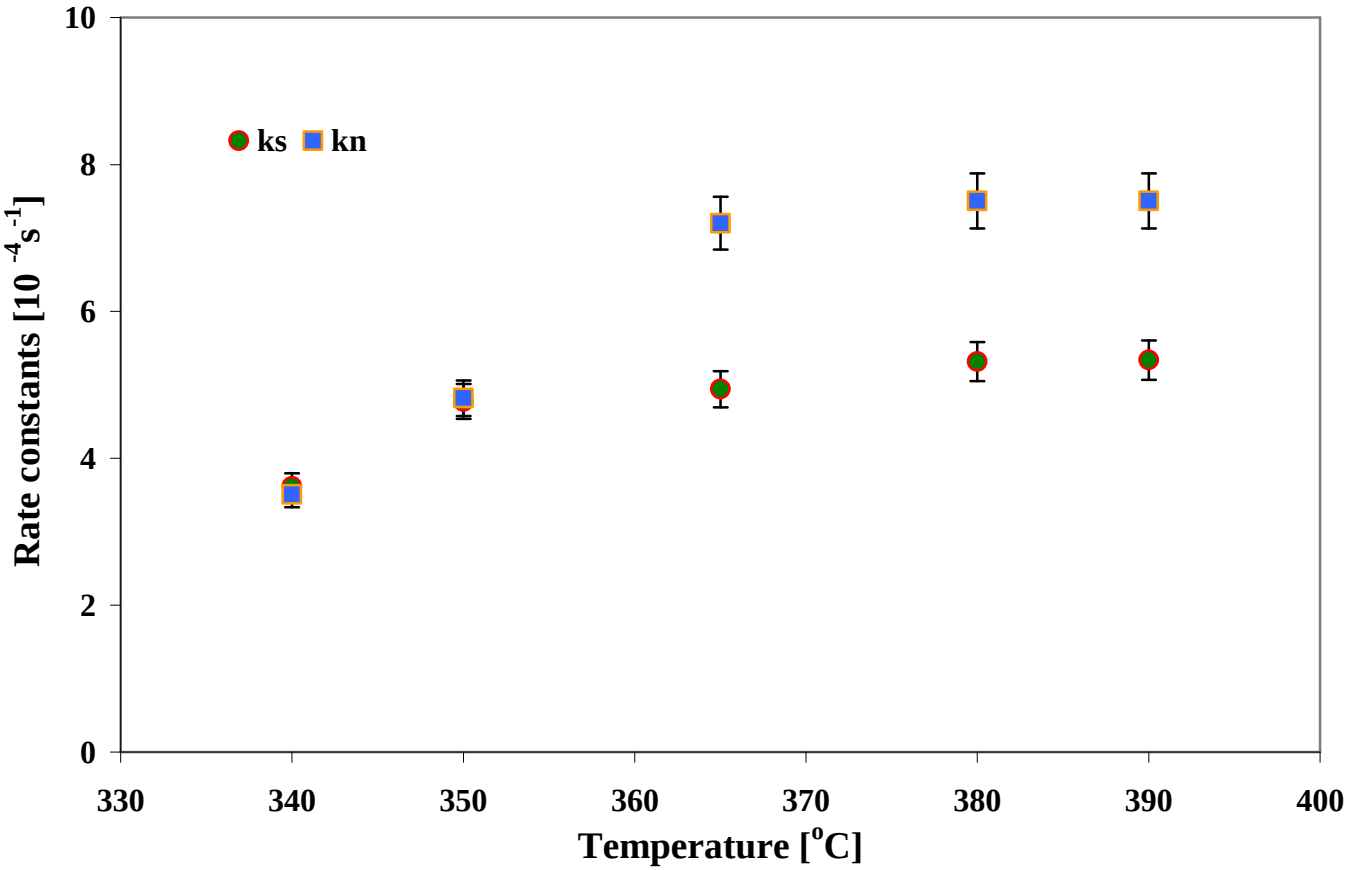

Figure 4.4: Effect of temperature on the NiW/Al_2O_3 activity for HDN and HDS (Pressure of 11.0 MPa, LHSV of 0.6 $h^{-1;}$ H_2/oil ratio of 550 ml/ml)

4.2.3 HDA of ALGO, HLGO and VLGO feedstock

The NiW/Al_2O_3 catalyst was also used to hydrotreat three other light gas oil feedstock types to determine their difference in hydrogenation reactivity and product yield. The feedstock used were atmospheric light gas oil, ALGO (160-393 ^oC); hydrocrack light gas oil, HLGO (163-404 ^oC) and vacuum light gas oil, VLGO (271-482 ^oC). The feedstocks have different compositions due to the varying processing conditions; ALGO is produced under atmospheric pressure conditions in a distillation unit. Bottoms from the atmospheric distillation unit are then sent to a vacuum distillation plant where VLGO is produced. Vacuum is needed for the production of the VLGO so as to lower the boiling temperature of the material, thereby allowing distillation without excessive decomposition. HLGO is produced under high pressure conditions via catalytic hydrogenation with a very high hydrogen/carbon (H/C) ratio.

The feedstock were first characterized to determine the distributions of boiling temperatures as a function of the amount and type of aromatics, sulfur and nitrogen contents. Simulated distillation curves of the LGO feedstock are shown in Figure 4.5. It is obvious that VLGO contains the highest boiling, possibly more complex and less reactive species followed by the ALGO and HLGO. Differences in the distribution of the boiling temperatures are mainly due to the sulfur contents in the feed (Ancheyta et.al., 2004 and Botchwey et.al., 2003). Above the 50 wt % fraction distilled, the distillation curves for both the ALGO and HLGO are the same, indicating the presence of similar sulfur species in both feeds. The dominant aromatic group in the ALGO feedstock may be diaromatics while the HLGO may also be dominated by monoaromatics due to the pretreatment of the feed.

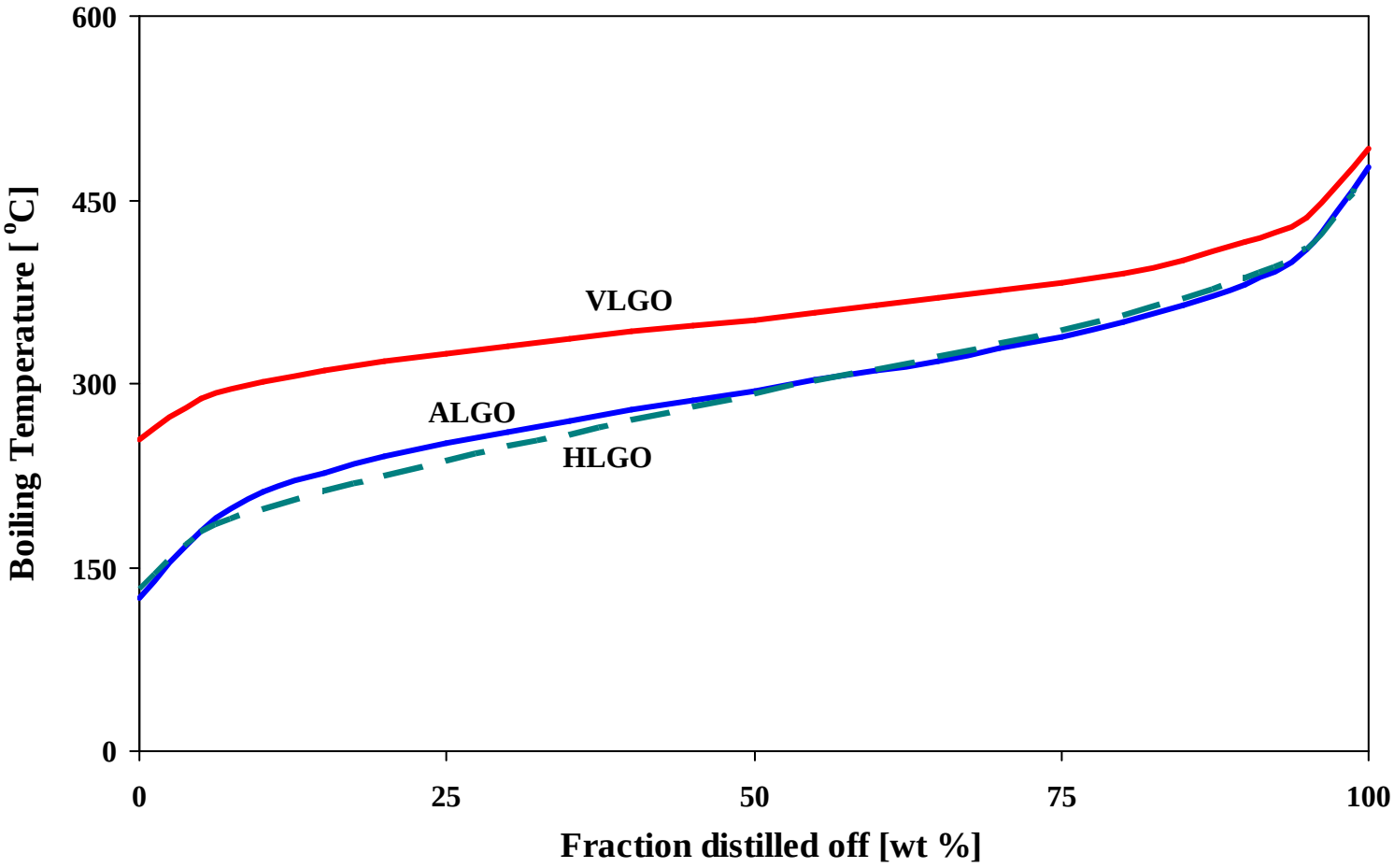

Figure 4.5: Simulated distillation curves of the VLGO, ALGO and HLGO

Figure 4.6 shows the plot of percent saturation of total aromatics in the LGO feedstock as a function of temperature. The order of ease of hydrogenation was VLGO >ALGO > HLGO. Since hydrogenation of higher order aromatic compounds is more thermodynamically favored than the lower group aromatics (Stanislaus and Cooper, 1996), the observed trend suggests that the dominant aromatic groups in the VLGO are polyaromatics whereas the ALGO and HLGO are dominated by di- and monoaromatics, respectively. Therefore, for every mole of polyaromatics that is saturated, a mole is added to the diaromatics group and for each mole of diaromatics reacted; a mole of monoaromatics is added to the existing monoaromatics content (McCulloch, 1975). It can be concluded that polyaromatics react more easily than the diaromatics, which in turn undergoes faster hydrogenation than the monoaromatics.

4.2.4 Product yield

The feed and products of the LGO feedstock were grouped into three main cuts based on their boiling point distributions: gasoline, (40–205 ºC); diesel (205-345 ºC) and the heavy gas oil (345+ ºC). Although the simulated distillation data shows that the feedstock are predominantly light gas oil, some tail-end cuts including heavy and vacuum gas oil fractions are also present. In this study all fractions above the 345+ ^{o}C were grouped as heavy gas oil. Product yield, in terms of gasoline and diesel production, was defined as:

$$\text{Yield} = \frac{\text{Products (desired)}}{\text{Reactants}} \times 100\ \% \qquad (4.5)$$

Product yield in the various LGO feestocks as a function of temperature is illustrated in Figure 4.7. When the feedstock were subjected to the same hydrotreating conditions,

there was a net increase in gasoline yield with a corresponding net decrease in diesel for all feed types except VLGO. The Hydrocrack light gas oil feedstock gave the highest gasoline yield at 365 ^{o}C. Maximum gasoline yield in the ALGO was 27 % at 390 ^{o}C. In the case of the VLGO there was a net steady increase in both the gasoline and the diesel fractions with increasing temperature. However, the diesel production was higher compared to the gasoline production.

4.3 Two-stage hydrotreating and H_2S inhibition studies

Several classes of reactions occur simultaneously in hydrotreating–HDA, HDS and HDN -and the presence of some of the reactants and products are known to markedly affect the reactivity (Girgis and Gates, 1991). In particular, H_2S produced from HDS reactions have been reported to be responsible for the hindrance of HDA as well as HDS and HDN reactions (Ishihara et.al., 2003; Kabe et.al., 1999; Nagai et.al., 1998).

In this part of the research the effect of hydrogen sulfide on hydrogenation, cetane index improvement, hydrodesulfurization and hydrodenitrogenation was studied at different space velocity ratios (ratio of the LHSV between stage I and stage II reactors) and temperatures using a two-stage hydrotreating unit with $NiMo/Al_2O_3$ in stage I and NiW/Al_2O_3 in stage II. The three LHSV ratio distributions between stages I and II are 1.5: 1, 1:1 and 1:1.5. At each set of LHSV ratio, temperature was varied from 350-390 ^{o}C. The combined reaction time of hydrotreating was, however, the same for all sets of experiments. The results from two-stage unit were then compared to those from the single-stage process where hydrotreating was carried out over commercial $NiMo/Al_2O_3$ catalyst.

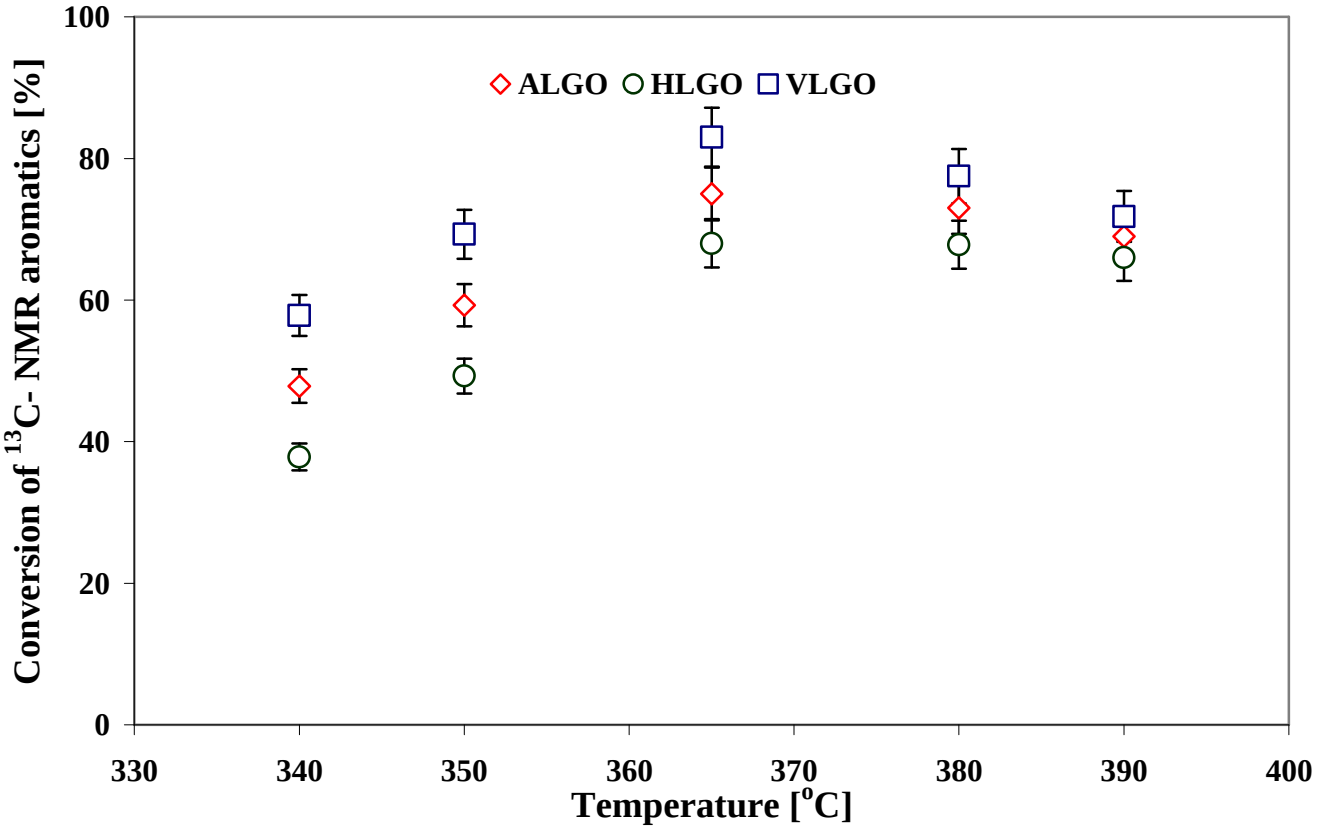

Figure 4.6: Conversion profiles for hydrogenation of total aromatics in ALGO, HLGO and VLGO over NiW/Al_2O_3 (Pressure: 11.0 MPa; LHSV: 0.6 h^{-1})

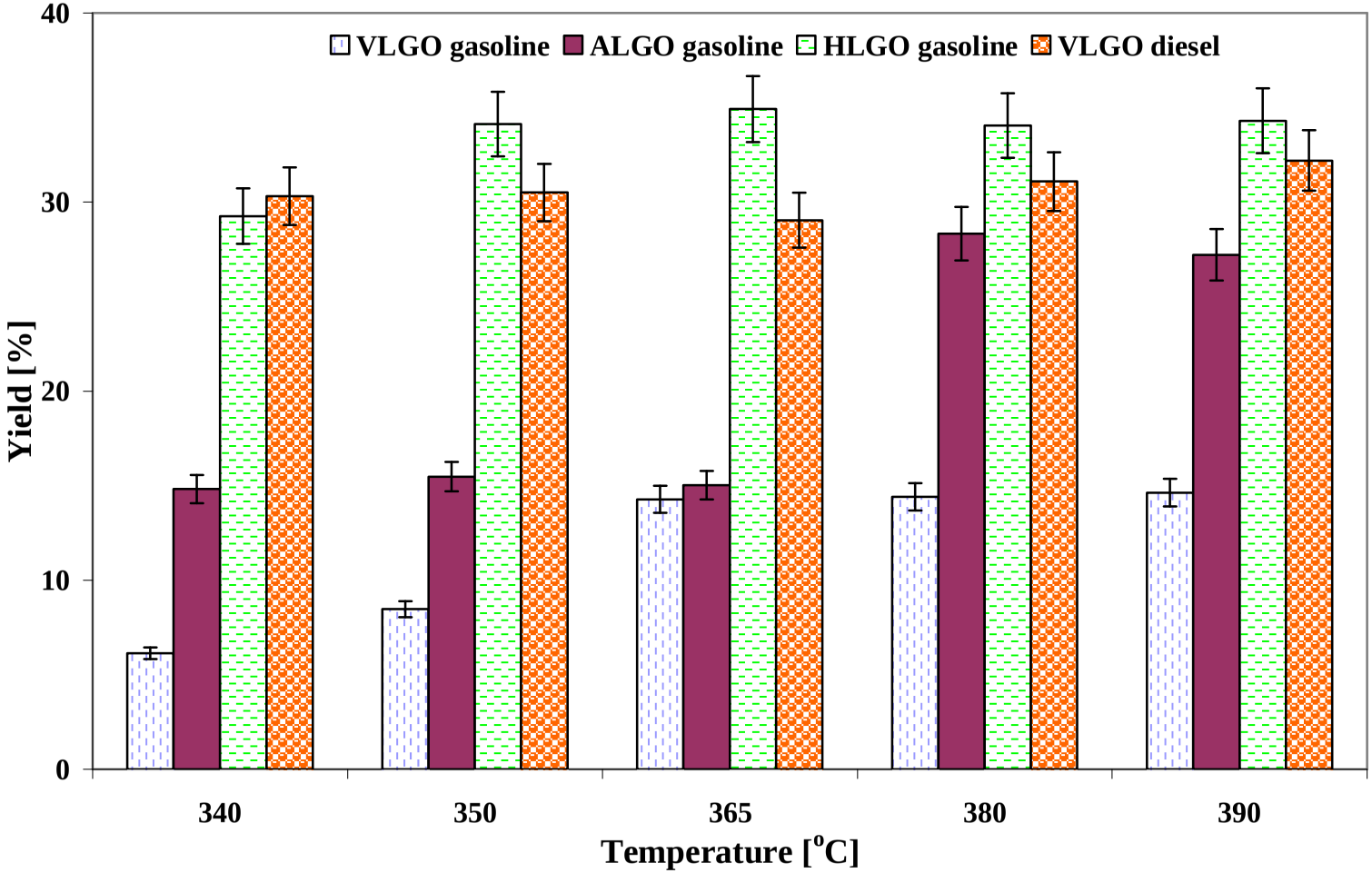

Figure 4.7: Effect of temperature and feed type on product yield (Pressure: 11.0 MPa and LHSV: 0.6 h^{-1})

4.3.1 Impact of H_2S removal and LHSV ratio on HDA

Figure 4.8 illustrates the relative gain in HDA rate constants at the different LHSV ratios in the two-stage process compared to the single- stage process. Relative gain is defined as:

$$\text{Relative gain, ki} = \frac{k_{\text{two-stage}} - k_{\text{single-stage}}}{k_{\text{single-stage}}} \quad (4.6)$$

where k_i is the reaction rate constant for HDA. The rate constants were derived from the Langmuir-Hinshelwood rate equations. Discussion of the determination of the kinetic parameters is presented in Section 4.4.

A general decrease in rate constants, k_A was observed with increasing temperature and this is because of the enhancement in the hydrogenation activity with increasing temperature and inter-stage removal of hydrogen sulfide. The negative gain in the reaction rate constants at higher temperatures is an indication that removal of H_2S at higher temperatures is not significant to the HDA activity since any hydrogen sulfide produced at these temperatures are quickly desorbed from the surface of the catalyst. The best activity for HDA in the two-stage was observed for the reaction with LHSV ratio of 1.5:1.0 between stage I and stage II. This is because of the higher hydrogenation activity and the longer reaction time on the NiW/Al_2O_3 catalyst in the stage II reactor. Hence, more NiW/Al_2O_3 catalysts may be loaded into the stage II reactor to maximize HDA activity.

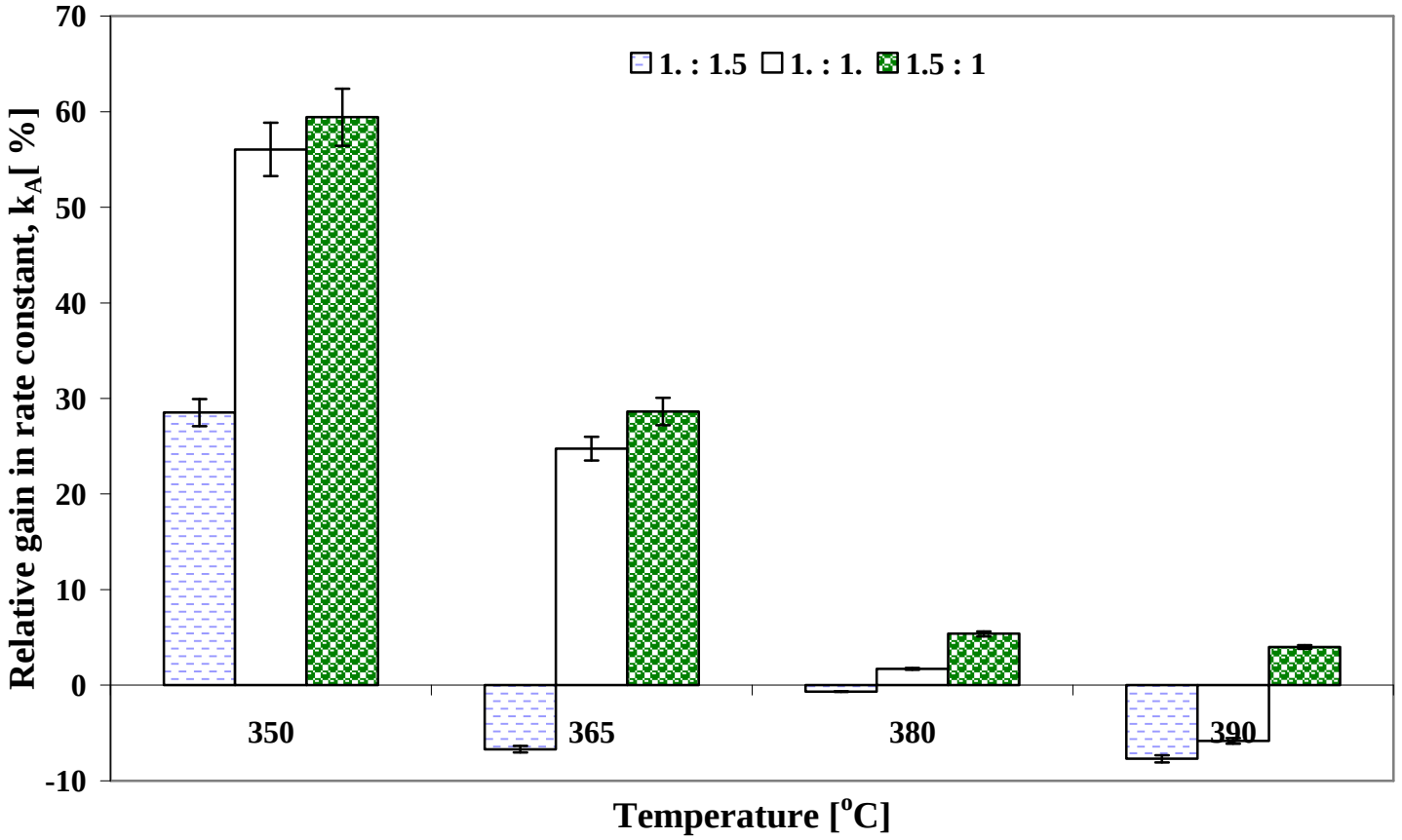

Figure 4.8: Effect of H_2S removal on the reaction rate constants of HDA in the two-stage process (Pressure: 11.0MPa, H_2/oil ratio: 550ml/ml)

4.3.2 Impact of H_2S removal and LHSV ratio on cetane index

Results for cetane index (CI) improvements in the single and the two-stage hydrogenation processes are shown in Table 4.3. Cetane index was calculated from the ASTM D976 correlation in equation 4.3. Significant differences in the cetane indices from the single and two-stage processes were observed at higher reaction temperatures (i.e.380 -390 ^{o}C), where about 7-10 % increments were observed for the two-stage process. At the lower temperatures (340-350 ^{o}C), only 2-3 % increase in the CI occurred in the two-stage unit. The highest cetane index in the single-stage process was 44 at 365 ^{o}C whereas for the two-stage process, a higher temperature of 380 ^{o}C was required to obtain the best cetane value of 46.

It is also observed from Table 4.3 that further increase in reactor temperature above 380 ^{o}C (in the two-stage) and 365 ^{o}C (in the single-stage) had limitations for additional increase in CI and this is because these temperatures are close to the equilibrium temperature for hydrogenation of aromatics and consequently, the cetane improvement. Figure 4.9 shows the impact of the H_2S removal on the overall cetane index improvement in the two-stage process at the different reaction temperatures and LHSV ratios. Just like hydrogenation of aromatics the best CI occurred at 380 ^{o}C at the LHSV ratio of 1.5:1.0.

4.3.3 Impact of H_2S on HDS and HDN

The impact of removal of hydrogen sulfide on HDS in the two-stage compared to the single-stage is shown in Figure 4.10. Similar to the HDA activity, the relative gain in rate constants decreased with increasing reaction temperature. This is because majority of hydrogen sulfide is produced in the stage I of the two-stage unit and adsorption of

Table 4.3: Cetane index improvement in single and two-stage processes at a pressure of 11.0 MPa

	Cetane index, CI	
Temperature [^{o}C]	**Single -stage**	**Two-stage**
350	42 ± 0.8	43 ± 0.8
365	44 ± 0.9	44 ± 0.9
380	43 ± 0.9	46± 0.9
390	41 ± 0.8	45 ± 0.9

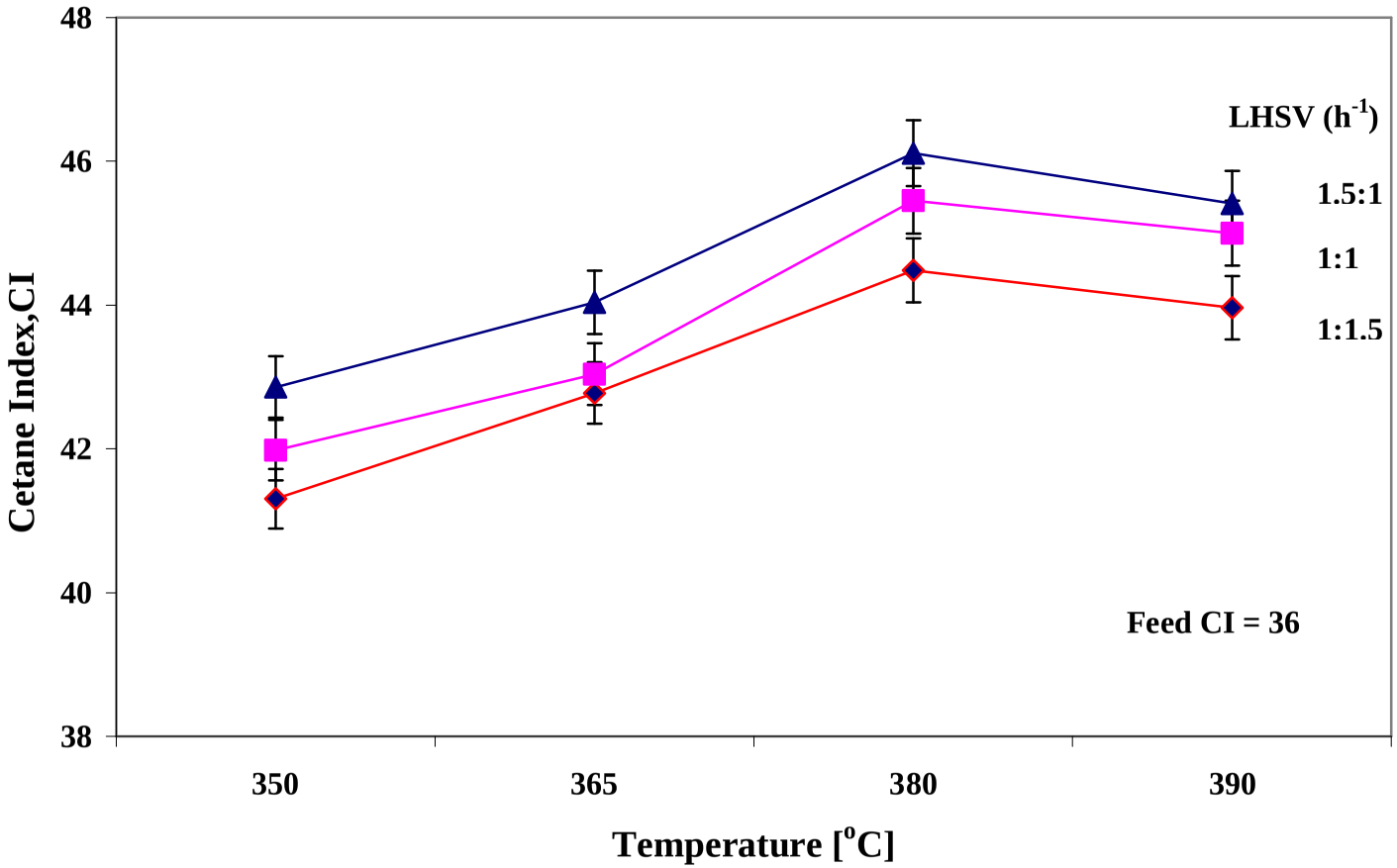

Figure 4.9: Effect of H_2S removal and LHSV ratio on the overall cetane index in the two-stage process (Pressure: 11.0MPa, H_2/oil ratio: 550ml/ml)

hydrogen sulfide on the active sites of the catalysts decreases with increasing temperature. Consequently, the rate of sulfur removal increases with further increase in temperature in both stages leading to a net decrease in the overall gain. This observation is consistent with other studies in literature (Kabe et.al., 1999; Botchwey et.al., 2003). The positive gain in the rate constants implies higher HDS activity in the two-stage than the single- stage. HDS activity at LHSV ratios of 1:1 and 1.5:1 were similar, however, at lower temperatures (350-365 ^{o}C), higher HDS activity were observed at the reaction conditions where the LHSV ratio was 1:1. From this results, it can be inferred that equal catalyst loadings or a higher amount of NiMo catalyst loading in stage I will maximize HDS activity in the two-stage process so long as there is an inter-stage removal of H_2S. In contrast to the HDA activity, inter-stage removal of H_2S was significant to HDS at all temperatures.

Unlike HDA and HDS very high HDN activities (95-100 % conversion) were observed for both the single and two-stage processes within the temperature range studied (350-390 ^{o}C). This implies negligible hydrogen sulfide inhibition for HDN. Satterfield et.al., 1981 and Landau et.al., 1996 have also reported negligible hydrogen sulfide inhibition on HDN reactions.

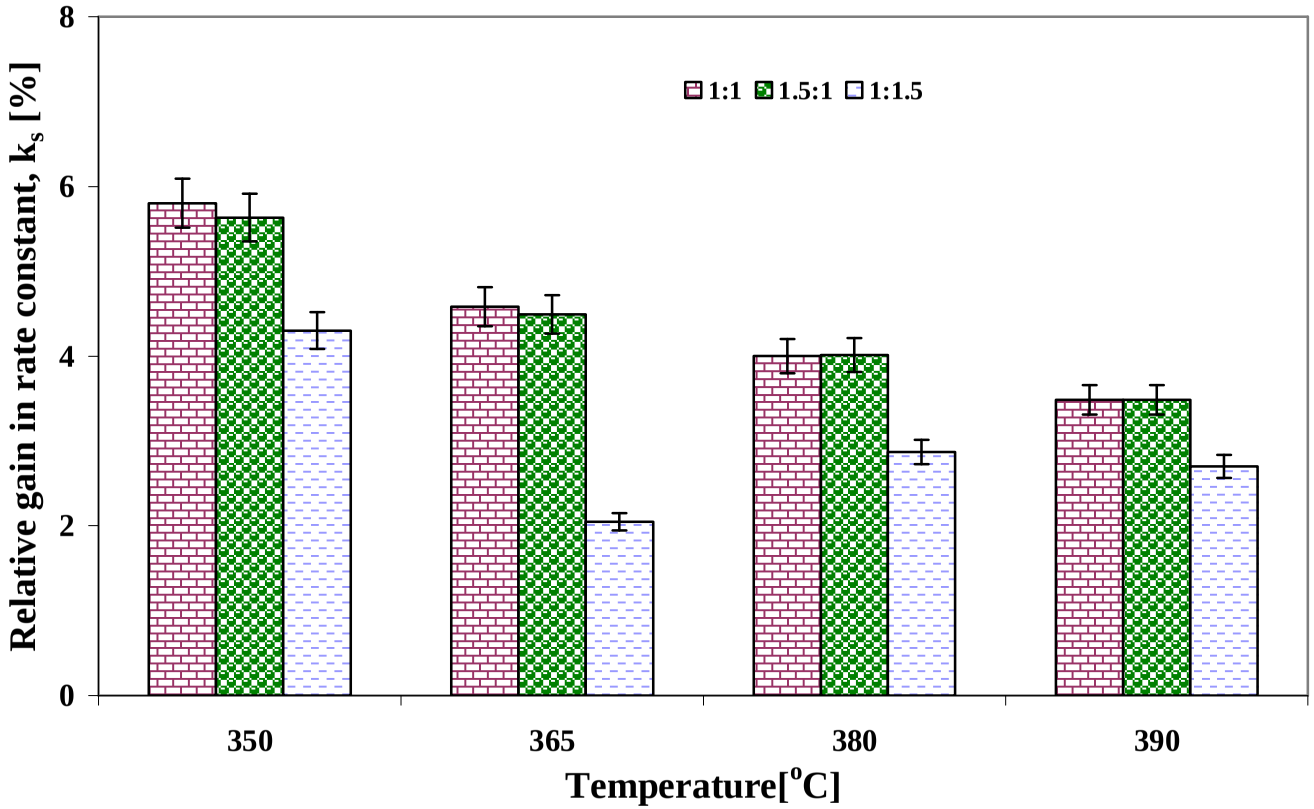

Figure 4.10: Impact of H_2S inhibition on HDS in the two-stage process. (Pressure: 11.0MPa; H_2/oil ratio: 550ml/ml)

4.4. Kinetic studies

The purpose of this section of the research was to derive mathematical models describing the rate of hydrotreating and mild hydrocracking (MHC) during light gas oil upgrading, as a function of the active components of the system such as the concentration and temperature. The Langmuir-Hinshelwood (L-H) rate of reaction equation was used to kinetically model the hydrogenation and hydrodesulfurization data. The L-H model was selected over that of the power law so as to account for any hydrogen sulfide inhibition. However, the pseudo-first order power law was used to model the MHC kinetics.

The experiments for the kinetic studies were performed by varying temperature from 350-390 ^{o}C at the optimum pressure of 11.0 MPa. The LGO blend from Athabasca bitumen was used as feedstock for the experiments. Simulated distillation data from of ALGO, HLGO and VLGO hydrotreating were used to develop the MHC kinetics. It may be noted that the catalyst packing and the experimental conditions were chosen such a way to eliminate mass transfer resistances (see Section 3.4.1 and Bej et.al., 2001)

4.4.1 Single-stage kinetics with $NiMo/Al_2O_3$

Kinetic analysis of the single-stage hydrotreating process is divided into three main sections: Kinetics of HAD; Kinetics of HDS and MHC kinetics.

4.4.1.1 Kinetics of HDA

It has been well established that hydrogenation of aromatics is an equilibrium reaction which is shifted in favor of aromatics with increasing temperature:

$$\text{Aromatics} + n\text{H}_2 \rightleftharpoons \text{Saturates} \qquad (4.7)$$

Using the Langmuir-Hinshelwood rate of reaction equation to model the HDA kinetics:

$$-r_A = -\frac{dC_A}{dt} = \left(\frac{k_F K_A K_{H2} P_{H2} C_A - k_R C_{AH}}{1 + K_A C_A + K_{H2S} P_{H2S}} \right) \tag{4.8}$$

where $-r_A$, k_F and k_R are the rate of reaction, forward and reverse rate constants, respectively, K_H, K_A and K_{H2S} are the equilibrium adsorption constants of hydrogen, aromatics and hydrogen sulfide, respectively. C_A and C_{AH} are the product concentration of aromatics and the saturated species, respectively. P_{H2S} and P_{H2} are partial pressures of hydrogen sulfide and hydrogen gas, respectively and t is the residence time.

Analysis of the hydrotreating data showed negligible equilibrium effects leading to the following assumptions for developing the final kinetic model:

- The surface reaction was rate limiting
- Reaction is pseudo first order in the forward reaction.
- The reaction occurred in a plug flow regime with negligible diffusion and mass transfer effects (HDA is reaction- controlled)
- Reaction occurred in excess amounts of hydrogen at constant partial pressure
- Hydrogenation is inhibited by hydrogen sulfide which is produced from the HDS process and H_2S is an ideal gas. The partial pressure of hydrogen sulfide is calculated from the ideal gas law equation:

$$P_{H2S} = \frac{n_{H2S}}{V} RT = C_{H2S} RT = b(C_{so} - C_{sp}) \tag{4.9}$$

where P_{H2S} is the partial pressure of H_2S, n_{H2S} is the number of moles, R is the universal gas constant, T is temperature, C_{so} and C_{sp} are the sulfur concentrations in the feed and products, b is a constant and V is the volume of the solution.

The final equation is given by:

$$-r_{AI} = -\frac{dC_{AI}}{dt} = \left(\frac{k_{AI} K_{AI} K_{HI} P_{H2} C_{AI}}{1 + K_{AI} C_{AI} + K_{H2SI} P_{H2SI}} \right) \qquad (4.10)$$

where k_{AI} is the apparent rate constant and all other terms are as defined. The subscript I, refers to the single-stage parameters.

The integral form of equation 4.10 was solved using MAPLE 6.0 software. Full details of the calculation are given in Appendix D. The apparent kinetic parameters were determined using non-linear least squares approach. Apparent activation energy and heats of adsorption were also determined from the slopes of the curve fitting by plotting the inverse of temperature against the logarithm of apparent kinetic and adsorption equilibrium constants [ln (k, K) vs. 1/T] in Figure 4.11. The high correlation coefficients obtained from the regression analysis indicated a good fit of the model to the experimental data.

4.4.1.2 Kinetics of HDS

Unlike the reaction mechanism of hydrogenation of aromatics, HDS is known to follow an irreversible pathway where:

Heteroatom sulfur species + Hydrogen $\longrightarrow$ Hydrocarbon + H_2S (4.11)

The final rate expression for HDS is:

$$-r_{S_I} = \frac{dC_{SI}}{dt} = \left(\frac{k_{sI} K_{SI} K_{HI} P_{H2} C_{SI}}{1 + K_{SI} C_{SI} + K_{HI} P_{H2} + K_{H2SI} P_{H2SI}} \right) \qquad (4.12)$$

where r_{SI} and k_{SI} are the rate equation and apparent rate constant of HDS, respectively, K_S, K_{H2}, K_{H2S} are the adsorption equilibrium constants of sulfur, hydrogen and hydrogen sulfide, respectively.

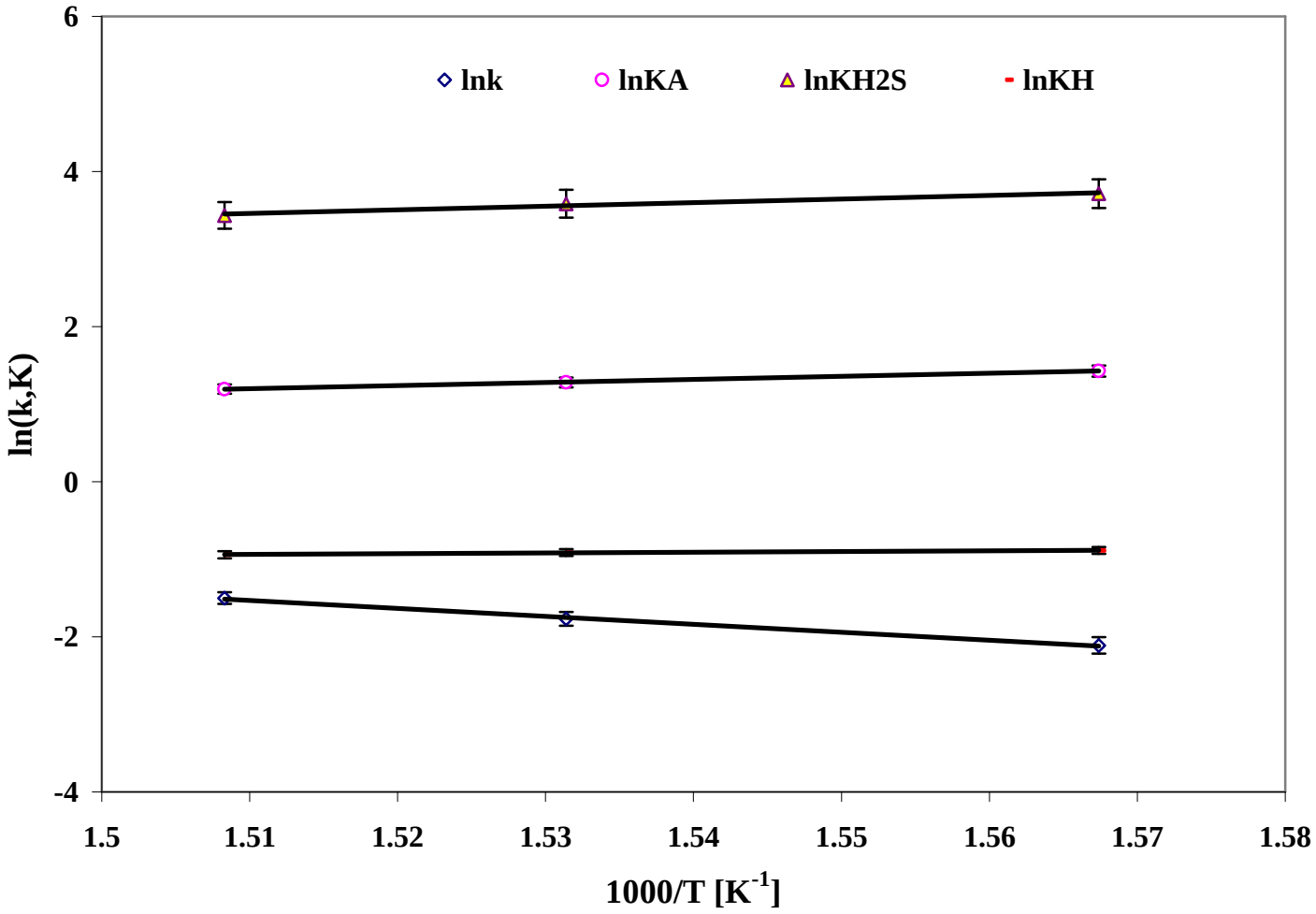

Figure 4.11: Arrhenius and Van't Hoff plot for single-stage HDA

The integral form of the rate expression in equation 4.12 is:

$$C_{SI} = \frac{\left[(1 + K_{HI}P_{H2} + K_{H2SI}P_{H2SI}) \times LambertW(\chi)\right]}{K_{sI}} \tag{4.13}$$

where

$$(\chi) = \frac{K_{sI} \exp\left(-\frac{k_{sI}K_{HI}K_{SI}P_{H2}\left(t - \frac{C_{SO}K_{SI} + \ln(C_{SO}) + \ln(C_{SO})K_{HI}P_{H2} + \ln(C_{SO})K_{H2SI}P_{H2SI}}{k_{SI}K_{HI}K_{SI}P_{H2}} \right)}{1 + K_{HI}P_{H2} + K_{H2SI}P_{H2SI}} \right)}{(1 + K_{HI}P_{H2} + K_{H2SI}P_{H2SI})} \tag{4.14}$$

And

$$LambertW(x) = x - x^2 + \frac{3}{2}x^3 - \frac{8}{3}x^4 + \frac{125}{4}x^5 - \frac{54}{5}x^6 + (o)^7 \tag{4.15}$$

The apparent kinetic parameters for HDS were also determined using nonlinear least squares method. The activation energy and heats of adsorption were calculated directly from the slopes of the Arrhenius and Van't Hoff plots in Figure 4.12. High correlation coefficients greater than 0.985, were obtained from the regression analysis. This indicated a good fit of the model to the experimental data.

4.4.1.3 MHC kinetics in ALGO, HLGO and VLGO

Hydrotreating and mild hydrocracking (MHC) are important catalytic processes for producing high quality diesel fuels from petroleum feedstock. Compared to hydrotreating however, the MHC mode of operation requires higher reactor temperatures (Yui et.al., 1989). It also improves hydrogen consumption economy and minimizes formation of undesirable lighter products (Satterfield, 1981). MHC has an advantage over conventional hydrocracking in improving the cetane rating of diesel by ring

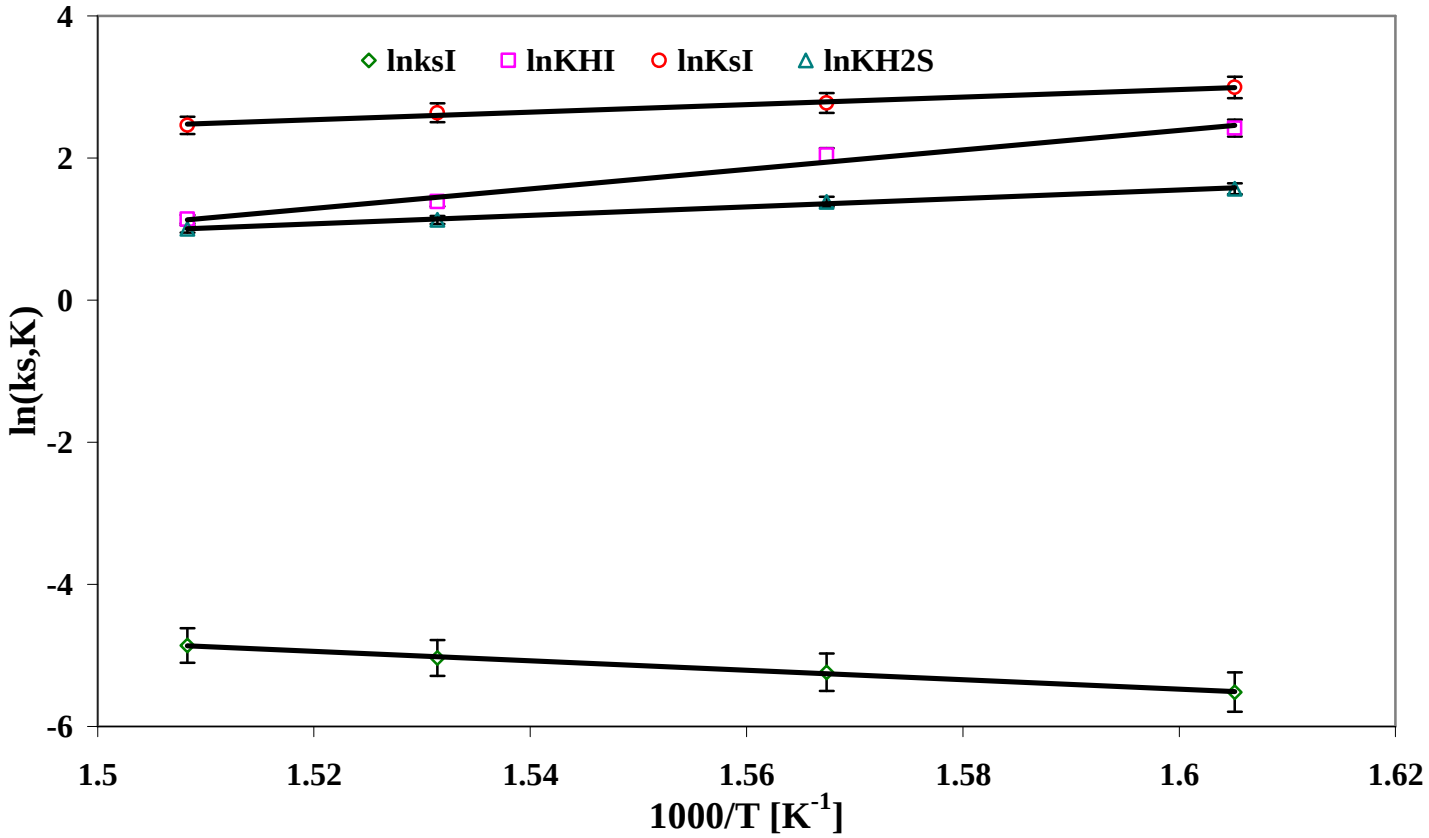

Figure 4.12: Arrhenius and Van't Hoff plots for single-stage HDS

opening of saturated rings thus converting naphthalene and branched-alkanes to lighter, gasoline-range products.

The projection of the long term middle distillate shortage in the mid 1980s spurred researchers and petroleum refiners to investigate mild hydrocracking of heavy gas oil with the view to shifting the product slate toward increased middle distillate production (Yui et.al., 1989). Middles distillates serve as a feed source for diesel fuel production. However, most of the literatures on MHC by workers including Desai et.al 1985; Wilson et.al., 1987; Hill et.al., 2002, have focused mainly on the product yields, properties and optimum conditions to produce a maximum distillate yield. Reports on the kinetics of MHC are limited.

The main objective of this part of the research was to investigate the MHC kinetics describing the results of the product yield in the three light gas oil feedstock (ALGO, VLGO and HLGO). MHC was measured by the extent of heavy gas oil (345+ ^{o}C) conversion:

$$Conversion(345+^{o}C) = \frac{345+^{o}C(feed) - 345+^{o}C(products)}{345+^{o}C(feed)} \qquad (4.16)$$

The feed and product samples were divided into three main fractions: Gasoline (G) (40–205ºC), Diesel (D) (205-345 ºC) and the heavy gas oil fractions (H) (345 + ºC). Conversion of the heavy gas oil fractions (H) was assumed to follow the parallel reaction mechanism in scheme 1:

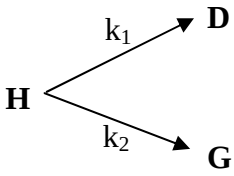

Scheme 1: Reaction pathway for conversion between 340-390 ^{o}C (H: 345+ ^{o}C; D: 205-345+^{o}C; G: 40-205 ^{o}C)

Cracking of diesel to gasoline was assumed to be negligible and cracking of the heavy gas oil fractions into gasoline and diesel was also assumed to obey pseudo first-order kinetic and given by:

$$\frac{dC_H}{dt} = -(k_1 + k_2)C_H \tag{4.17}$$

$$C_H = C_{HO}e^{-(k_1+k_2)t} \tag{4.18}$$

where C_H and C_{HO} are the product and feed mass fractions of the heavy has oil fraction, respectively, k_1 and k_2 are the rate constants for cracking into diesel and gasoline, respectively, and t is the reaction time.

Analysis of the MHC kinetic data in Table 4.4 shows that the activation energies of gasoline production (k_2) are much higher than those for diesel production (k_1) which is an indication that cracking to gasoline increases strongly as the temperature increases. Similar results have also been reported by Yui et.al., 1989 when they investigated MHC kinetics on bitumen-derived heavy gas oils. In terms of the activation energies of the combined rate constants ($k^*=k_1+k_2$), the ease of mild hydrocracking in the LGO feedstock followed the order: HLGO > VLGO > ALGO. Thus, more cracking products are obtained from the HLGO, followed by the VLGO and finally the ALGO.

Table 4.4: Kinetic parameters of MHC in ALGO, HLGO and VLGO

	E [kJ/mol]	ko	R^2
ALGO			
k_1	52	2.9×10^3	0.9906
k_2	102	2.3×10^7	0.9972
$k^* = k_1 + k_2$	88	4.8×10^6	0.9869
HLGO			
k_1	41	2.6×10^2	0.9913
k_2	62	9.4×10^3	0.9923
$k^* = k_1 + k_2$	49	2.0×10^3	0.9915
VLGO			
k_1	55	3.7×10^3	0.9937
k_2	85	7.5×10^5	0.9942
$k^* = k_1 + k_2$	67	5.8×10^4	0.9946

4.4.2 Two-stage kinetic studies

This section of the study, discusses the development of the overall kinetics of HDA and HDS in the two-stage process. Results from the kinetics studies are compared to those from the single-stage process to determine the effect of H_2S inhibition on the hydrotreating activities.

4.4.2.1 Overall HDA and HDS kinetics

The two-stage process was performed to study the effect of H_2S removal on HDA and HDS in light gas oil from Athabasca bitumen. Prior to the stage II reactions, H_2S present in the products from stage I were completely removed by bubbling nitrogen gas through the samples for at least two hours. The H_2S produced in the stage II reactions is due to the unreacted sulfur species from the stage I reaction effluents. The rate equations describing the overall HDA and HDS kinetics were similar to those developed in the single-stage process (see Appendix D for the HDA kinetic equations):

For HDA, the overall rate of reaction equation is:

$$-r_{AII} = -\frac{dC_{AII}}{dt} = \left(\frac{k_{AII} K_{AII} K_{HII} P_{H2} C_{AII}}{1 + K_{AII} C_{AI} I + K_{HII} P_{H2} + K_{H2SII} P_{H2SII}} \right) \tag{4.19}$$

Overall HDS rate of reaction equation is also defined by:

$$-r_{sII} = -\frac{dC_{SII}}{dt} = \left(\frac{k_{sII} K_{SII} K_{HII} P_H C_{SII}}{1 + K_{SII} C_{SII} + K_{HII} P_{H2} + K_{H2SII} P_{H2SII}} \right) \tag{4.20}$$

where P_{H2SII} = b (C_{SI}-C_{SII}) and all parameters are as defined earlier. The subscripts I and II refer to stage I and stage II, respectively.

The overall kinetic parameters were also determined using the non-linear least square regression approach. The activation energies and heats of adsorption were

obtained directly from the slopes of the Arrhenius and Van't Hoff plots. High correlations coefficients were also derived for the regression analyses which indicated accurate predictions of the experimental data by the models. A summary of the single-stage and the two-stage (overall) kinetic parameters for both HDA and HDS are shown in Table 4.5.

4.4.2.2 Effect of H_2S removal on HDA kinetics

The following observations were made from the kinetic parameters when hydrogen sulfide was removed from the two-stage process:

The rate constants, k_A derived from the single-stage hydrogenation activity were lower ($1.8\text{-}6.2\times10^{-5}s^{-1}$) than those from the two-stage hydrogenation data. Thus a faster rate of reaction favored the two-stage process.

For the single-stage process, the equilibrium adsorption constants of aromatics were lower than those for hydrogen sulfide whereas for the two-stage process, the opposite was observed. Hence, the aromatic compounds in the single-stage process were weakly adsorbed (low conversion) due to H_2S inhibition while for the two-stage process, the aromatic species were strongly adsorbed, leading to a higher HDA activity and consequently, higher conversions.

The activation energy of hydrogenation in the single-stage process was 85 kJ/mol but upon removal of hydrogen sulfide for the two-stage process, the activation energy dropped to 67 kJ/mol. This implies that when HDA in the bitumen-derived light gas oil is retarded by H_2S, more energy will have to be provided to the system in order to overcome the energy barrier and reduce the aromatics contents to lower levels below 10 vol % in compliance with the current diesel fuel specifications (US EPA, 1999).

Table 4.5: Summary of the apparent kinetic parameters of the overall kinetics studies in the single and two-stage processes (Temperature-340 -390 ^{o}C; Pressure-11.0 MPa; Total residence time-1.67 h)

Kinetic Parameters	lnk_{AI}	lnk_{AII}	lnK_{AI}	lnK_{AII}	lnK_{H2SI}	lnK_{H2SII}	lnK_{HI}	lnK_{HII}
Aromatics Hydrogenation(HDA)								
E_A and ΔH [kJ/mol]	85 ± 4.2	67 ± 3.3	33 ± 1.7	59 ± 3.0	39 ± 2.0	24 ± 1.2	7.6 ± 0.38	7 ± 0.36
ln (k_{Ao},K_o)	14 ± 0.70	10.6 ± 0.53	-4.8 ± 0.24	-8.2 ± 0.41	-3.5 ± 0.20	-5.4 ± 0.27	-2.3 ± 0.14	-4.8 ± 0.24
R^2	0.9967	0.9854	0.9995	0.9963	0.9729	0.9999	0.9833	0.9988
Hydrodesulfurization (HDS)								
	lnk_{sI}	lnk_{sII}	lnK_{SI}	lnK_{SII}	lnK_{H2SI}	lnK_{H2SII}	lnK_{HI}	lnK_{HII}
E_S and ΔH [kJ/mol]	55 ± 2.8	22 ± 1.1	44 ± 2.2	67 ± 3.4	50 ± 2.5	24 ± 1.2	114 ± 5.7	-33 ± 1.6
ln (k_{so},K_o)	5.2 ± 0.26	0.78 ± 0.04	-5.5 ± 0.28	-9.0 ± 0.45	-8.0 ± 0.40	-2.4 ± 0.12	-19 ± 0.98	4.4 ± 0.22
R^2	0.9963	0.9972	0.9868	0.9973	0.9941	0.9943	0.9863	0.9984

4.4.2.3 Effect of H_2S removal HDS kinetics

For the analysis of the single-stage overall kinetics, the activation energy of HDS was 55 kJ/mol. The heats of adsorption for sulfur and hydrogen sulfide were 44 and 50 kJ/mol, respectively. Therefore, H_2S was strongly adsorbed on to the active sites of the catalyst as compared to adsorption of the sulfur species. Furthermore, the adsorption equilibrium constants for H_2S were higher than those for total sulfur.The results suggest that in the HDS of light gas oil, the reaction was retarded by the H_2S produced in the reaction. This result is consistent with the studies by Kabe et.al., 1999 who reported a high adsorption constant of H_2S than those of dibenzothiophene compounds.

In the case of the two-stage kinetic analysis, the activation energy was 23 kJ/mol while the heats of adsorption were 67 and 24 kJ/mol for the total sulfur and hydrogen sulfide, respectively. Unlike the single-stage, the adsorption equilibrium constants of total sulfur were significantly higher than H_2S indicating that H_2S was weakly adsorbed. The inter-stage removal of H_2S from the two-stage process greatly enhanced the HDS activity as activation energy decreased from 55 kJ/mol in the single-stage to 23 kJ/mol in the two-stage.

4.4.3 Experimental versus model predictions

The best kinetic parameters for predicting the experimental results for HDA, HDS and MHC were selected based on the sum of square errors (SSE) approach.

$$SSE = \sum (y_i^{\,p} - y_i^{\,\exp})^2 \tag{4.21}$$

where SSE is the divergence, y_i^p is the model prediction and y^{exp} is the experimental results.

The criterion for this method was to minimize the differences between the experimental and the predicted results. Figures 4.13 and 4.14 compare the experimental and correlated product concentrations of aromatics and sulfur, respectively for three sets of hydrotreating data (same operating conditions). Figure 4.15 also compares the calculated and experimental concentrations of the heavy gas oil fraction, (H) ($345+^{o}C$) in the three LGO feedstock. As can be seen, the kinetic models predicted with reasonable accuracy the experimental results (with $R2 \geq 0.99$) over the entire temperature range.

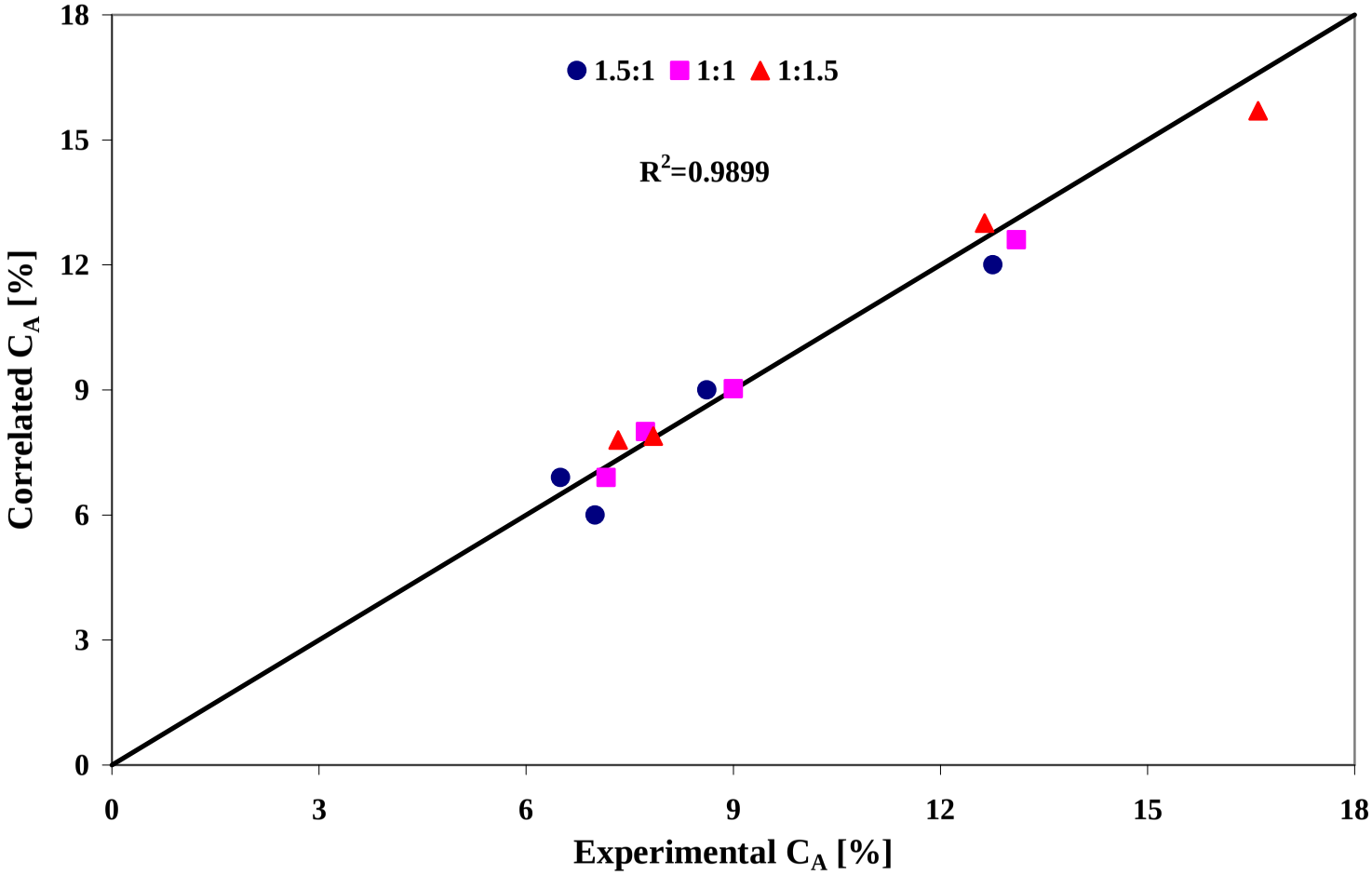

Figure 4.13: Correlated versus experimental concentrations of total aromatics, C_A at the different LHSV ratios

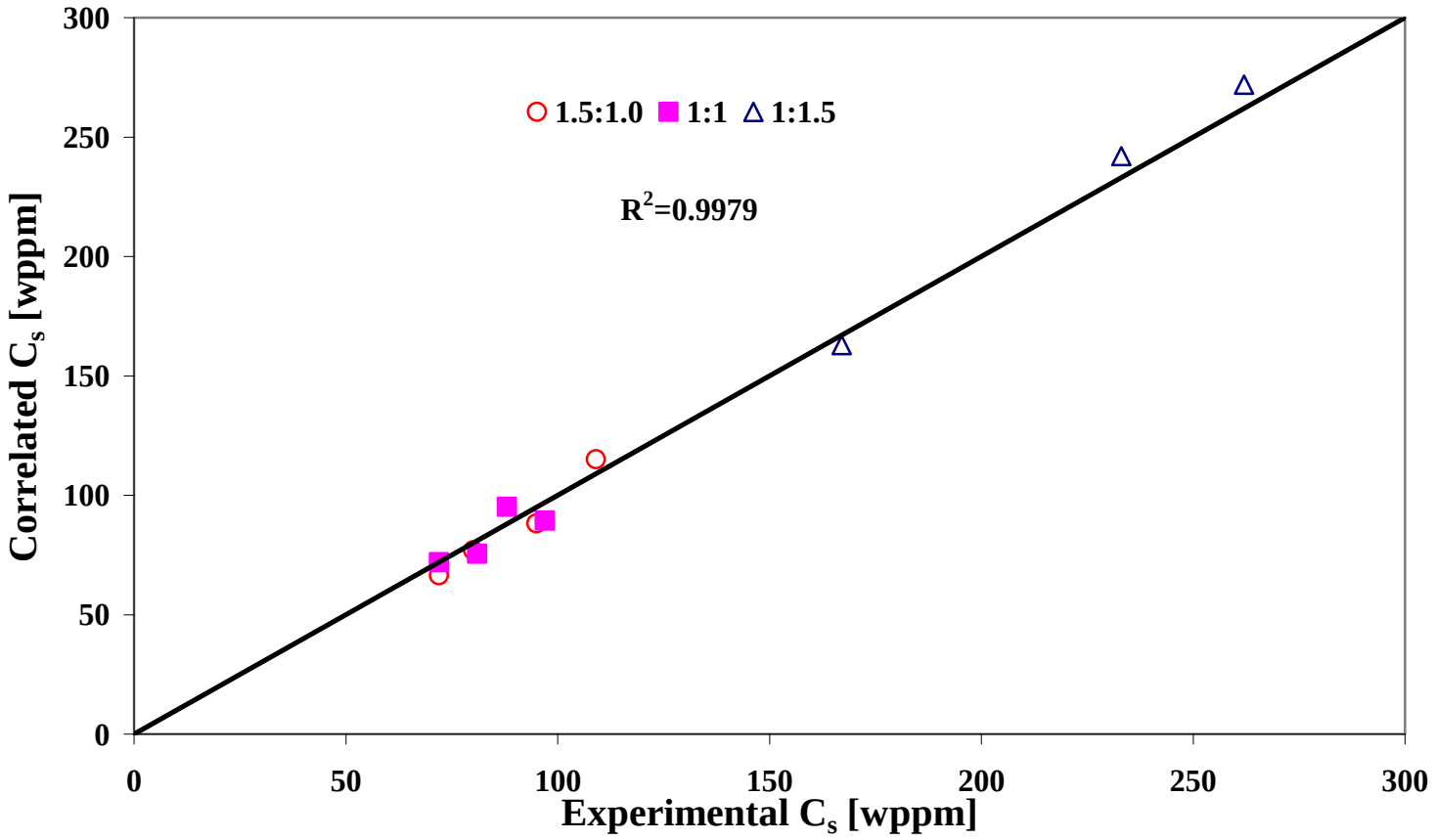

Figure 4.14: Correlated vs. experimental concentrations of product sulfur concentrations (Cs) at the different LHSV ratios

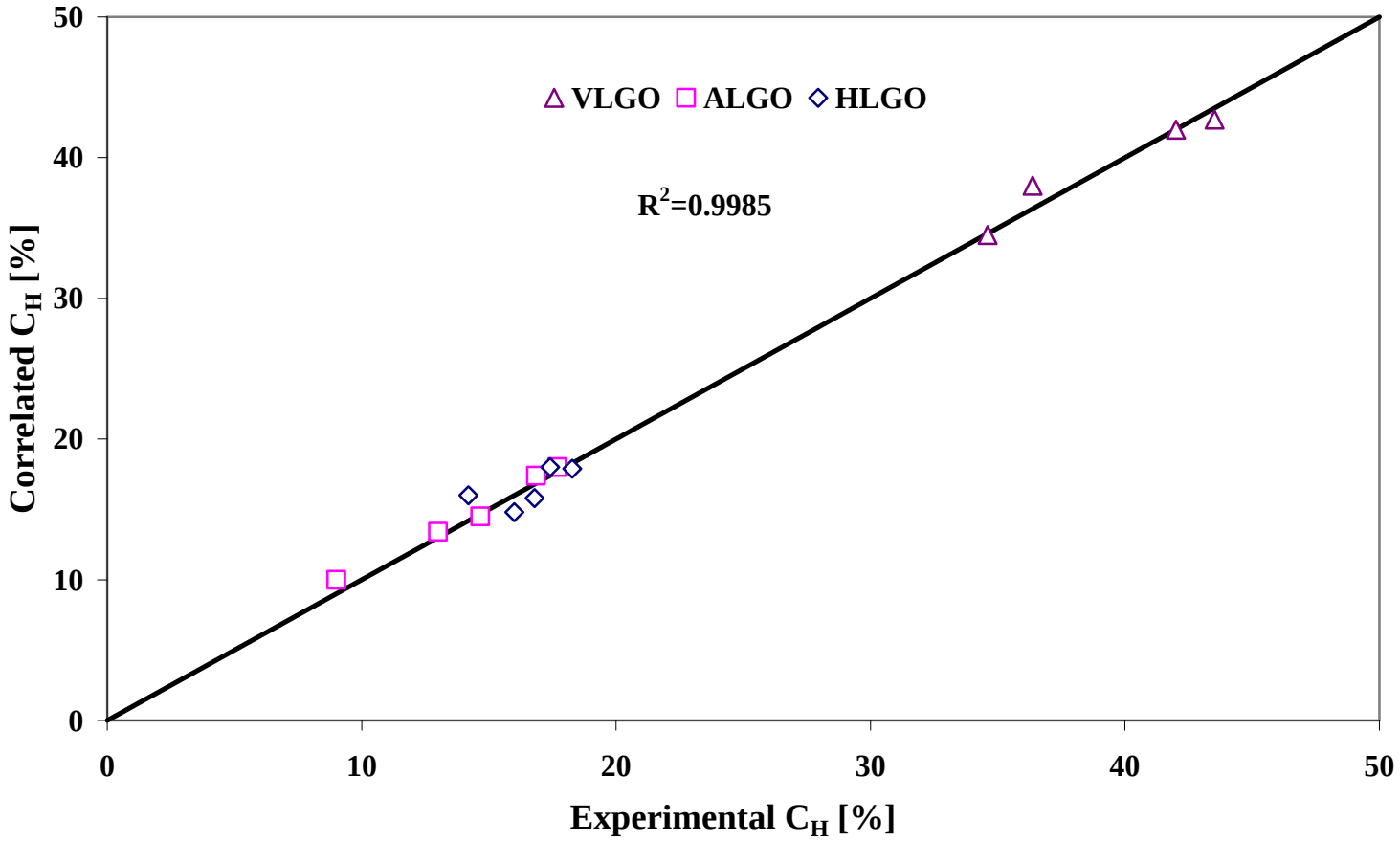

Figure 4.15: Correlated vs. experimental concentrations of the heavy gas oil (345+^{o}C) fractions from the mild hydrocracking data (simulated distillation) in VLGO, ALGO and HLGO

5.0 CONCLUSIONS

Interaction between temperature and pressure is the most significant factor affecting HDA while HDS and HDN are highly influenced by interaction between temperature and space velocity. The optimal conditions of HDA for maximum conversion of aromatics were found at a temperature, pressure and LHSV combination of 379 ^{o}C, 11.0 MPa and 0.6 h^{-1} respectively. At these conditions, the highest conversion of 63 % could be attained. HDS and HDN conversions at these conditions were 98.5 and 99.7 %, respectively.

Hydrogenation of monoaromatics is the key step for reducing the total aromatics content of light gas oils. The ease of hydrogenation of total aromatics in the LGO feedstock was observed to follow the general order: VLGO > ALGO > HLGO. Studies on MHC indicated a net increase in gasoline with a corresponding decrease in diesel during cracking. More cracking products were produced from the HLGO feed.

HDA, cetane rating and HDS processes were inhibited by hydrogen sulfide during hydrotreating in the single-stage reactor. However, with the two-stage process where hydrogen sulfide was removed inter-stage, significant improvement in hydrogenation, cetane and sulfur removal were observed.

HDA and HDS in LGO feedstock from Athabasca bitumen can be described by the Langmuir-Hinshelwood kinetic models. Mild hydrocracking was best described by a pseudo first-order parallel model.

6.0 RECOMMENDATIONS

From the experimental results obtained in this research, the following recommendations can be made:

1. Further studies could be carried out to determine the inhibition effects of ammonia (NH_3) on aromatics hydrogenation.
2. Future experiments could be also be carried out to study the hydrogenation activity of ring-opening catalysts such as the noble-metal catalysts for improving the diesel quality of light gas oil fractions from Athabasca oil sands.
3. For scaling up of the process, the design and development of two-fixed reactors arranged in series with inter-stage hydrogen-sulfide removal should be examined.

REFERENCES

Albertazzi, S., E. Rodríguez-Castellón, M. Livi, A. Jiménez-López, and A.Vaccari, "Hydrogenation and Hydrogenolysis/Ring-Opening of Naphthalene on Pd/Pt Supported on Zirconium-doped Mesoporous Silica Catalysts" Journal of Catalysis, **228**, 218-224 (2004).

Ali, S.A., "Influence of Heteroatom Removal on Aromatic Hydrogenation", Fuel Processing Technology, **55**, 93-98 (1998)

Ali, S.A and M.A.B Siddiiqui, "Dearomatization, Cetane Improvement and Deep Desulfurization of Diesel Feedstock in a Single-Stage Reactor", Reaction Kinetics and Catalysis Letters, **61**, 363-368 (1997).

Ancheyta, J., M.J.Angeles, M.J. Macías, G. Marroquín, and R. Morales "Changes in Apparent Reaction Order and Activation Energy in the Hydrodesulfurization of Real Feedstocks" Energy and Fuels, **16**,198-193 (2002).

Ancheyta, J., P. Morales, G. Betancourt, G. Centeno, G. Marroquín, and J. A. D. Muñoz, "Individual Hydrotreating of FCC Feed Components" **16**, 1001-1004 (2004).

Arribas, M. A. and A. Martinez, "The Influence of Zeolite Acidity for the Coupled Hydrogenation and Ring Opening of 1-methylnaphthalene on Pt/USY Catalysts" Applied Catalysis, A: General, **230**, 203-217 (2002).

Bej, S.K., A.K. Dalai, and J. Adjaye, **"**Comparison of Hydrodenitrogenation of Basic and Nonbasic Nitrogen Compounds Present in Oil Sands Derived Heavy Gas Oil", Energy and Fuels, **15**, 377-383 (2001).

Berger, D., M.V.Landau, M. Herskowitz, and Z. Boger, "Deep Hydrodesulfurization of Atmospheric Gas Oil. Effects of Operating Conditions and Modeling by Artificial Neural Network Techniques" Fuel, **75**, 907-911 (1996).

Botchwey, C., A.K. Dalai, and J. Adjaye, "Product Selectivity during Hydrotreating and Mild Hydrocracking of Bitumen-Derived Gas Oil", Energy & Fuels, **17**, 1372-1381 (2003).

Bouwens S. M. A. M., F.B.M. Vanzon, M.P. Vandijk, A.M. Vanderkraan, V.H.J. Debeer, J.A.R. Vanveen and D.C. Koningsberger,"On the Structural Differences Between Alumina-Supported Comos Type I and Alumina-, Silica-and Carbon-Supported Comos Type II Phases Studied by XAFS, MES, and XPS" Journal of Catalysis, **146**, 375-393 (1994).

Box, G., W. Hunter and W., J. Hunter, "Statistics for Experimenters", Wiley, New York, (1978), pp 23-50.

Box, G.E.P and N.R. Draper, "Empirical and Model Building and Response Surfaces", (1987), 515.

Canadian Crude Oil Production and Supply Forecast (2004-2015), (2004), pp.1-16.

Chasey, K.L. and T. Aczel, "Polycyclic Aromatic Structure Distributions by High-Resolution Mass Spectrometry" Energy and Fuels, **5**, 386–394 (1991).

Chianelli, R. R., "Fundamental Studies of Transition Metal Sulfide Hydrodesulfurization Catalysts", Catalysis Reviews - Science and Engineering, **26**,361-393 (1984).

Chmielowiec, J. "Impact of Nitrogen Compounds on the Processing of Synthetic Gas Oil". Final report to CANMET, Supply and Services Canada, Contract Serial No. OSQ84-00095, Ottawa, Ont., Canada (1986).

Chowdhury, R., E.Pedernera, and R. Reimert, **"**Trickle-Bed Reactor Model for Desulfurization and Dearomatization of Diesel", AIChE Journal, **48**,126-135 (2002).

Clausen, B. S., H.Topsoe, R. Candia, J.Villadsen, B.Lengeler, J.Als-Nielsen, and F. Christensen, "An EXAFS Study of the Structure of Cobalt-Molybdenum Hydrodesulfurization Catalysts", Report (DESY-SR-81/02) (1981), 17.

Cooper, B.H., and B. L. Donnis "Aromatic Saturation of Distillates: An Overview" Applied Catalysis A. General **137**, 203-223 (1996).

D. Eliche-Quesada, J. Mérida-Robles, P. Maireles-Torres, E. Rodríguez-Castellón, G. Busca, E. Finocchio and A. Jiménez-López "Effects of Preparation Method and Sulfur Poisoning on the Hydrogenation and Ring Opening of Tetralin on NiW/Zirconium-Doped Mesoporous Silica Catalysts" Journal of Catalysis, **220**, 457-467 (2003).

Daage, M. and R.R. Chianelli, "Structure-Function Relations in Molybdenum Sulfide Catalysts: The "Rim-Edge", Journal of Catalysis, **149**, 414-427 (1994).

Davis, G. "Energy Security and Sustainability, UNECE Sustainable Energy Committee", (2002).

Delmon, B "Proc. 3rd Int. Conf. on Chemisty and Uses of Molybdenum, Climax Molybdenum Compounds", (1979), 73.

Design Expert Software-Version 6.0, "User's Guide, Stat-Ease Inc'" (2003) pp. 1-10

Duchet, J. C., E.M.Van Oers, V.H.J. De Beer, and R. Prins, "Carbon-Supported Sulfide Catalysts" Journal of Catalysis, **80**, 386-402 (1983).

Dufresne, P., P.H.Bigeard, and A. Billon, "New Developments in Hydrocracking: Low Pressure High-Conversion Hydrocracking", Catalysis Today, **1**, 367-384 (1987).

Farragher, A. L., and P. Cossee, "Catalytic Chemistry of Molybdenum and Tungsten Sulfides and Related Ternary Compounds" Catal., Proc. Int. Congr., (1973), pp 1301-1318.

Ferdous, D., A.K.Dalai, and J. Adjaye, "A series of $NiMo/Al_2O_3$ Catalysts Containing Boron and Phosphorus: Part I. Synthesis and Characterization" Applied Catalysis A. General, **260**, 137-151 (2004).

Fisher, I. P.and M.F.Wilson, "Kinetics and Thermodynamics of Hydrotreating Synthetic Middle Distillates", Preprints-American Chemical Society, Division of Petroleum Chemistry, **32**, 310-314 (1987).

Fogler, H.S., "Elements of Chemical Reaction Engineering", 3rd Editon, Prentice Hall PTR, New Jersey (1999).

Frank, J.P and J. F. LePage, "Proceedings on the 7th International Congress on Catalysis" (1981), 792.

Fujikawa, T., K. Idei, T. Ebihara, H. Mizuguchi, and K. Usui, "Aromatic Hydrogenation of Distillates over SiO_2-Al_2O_3-Supported Noble Metal Catalysts" Applied Catalysis A. General, **192**, 253-261 (2000).

Gary, G.H. and G. E. Handwerk, "Petroleum Refining-Technology and Economics" Marcel Dekker (2001), 465.

Gazellot, P., and G. Bergeret, "Catalyst Deactivation" Dekker, New York, (1987), 263.

Geneste, P, J. Joffre, A. Guida, G. Szabo, C. Moreau, "Kinetic modeling of Heterogeneously Catalyzed Reactions with the ANACIN Software. Application to The Hydrodenitrogenation of Phenanthridine", Studies in Physical and Theoretical Chemistry, **71**, 409-415 (1990).

Geneste, P., P. Amblard, M. Bonnet, P. Graffin, "Hydrodesulfurization of Oxidized Sulfur Compounds in Benzothiophene, Methylbenzothiophene, and Dibenzothiophene Series over Cobalt (II) Oxide-Molybdenum (VI) Oxide-Alumina Catalyst", Journal of Catalysis, **61**, 115-127 (1980).

Gevert, B. S., Otterstedt, J. E., F.E. Massoth, “Kinetics of the Hydrodeoxygenation of Methyl-Substituted Phenols” Applied Catalysis, **31**, 119-131 (1987).

Girgis, M.G., and B.C. Gates, “Reactivities, Reaction Networks and Kinetics in High-Pressure Catalytic Hydroprocessing”. Industrial and Engineering Chemistry Research, **30**, 2021-2058 (1991).

Gray, M., “Upgrading of Petroleum Residues and Heavy oils”, (1994), pp10-25.

Gulder, O. M., B.Glavineevski, B G.F. Burton, “Ignition quality rating methods for diesel fuels- a critical appraisal”, SAE 852080 (1985).

Gully, A. J., and W.P. Balard, “Advances in Petroleum Chemistry and Refining”, Vol 7, Interscience Publishers, London, (1963), 241.

Ho, C. T. “Hydrogenation Catalysis” Catalysis Review Science and Engineering, **30**,117-160 (1988).

Ho, T.C., A.A.Montagna, and J.J. Steger, “Proceeding on 8th International Congress on Catalysis”, Verlag Chemie, **2** (1984).

Ignatiadis, I., J.M.Schmitter, M.Dorbon, H.P.Toulhoat, and P. Arpino, “Effect of Catalytic Hydrotreatments on the Distribution of Nitrogen Compounds in a Coker Gas Oil and in a Deasphalted Heavy Oil”, **40**, 423-427 (1984).

Ijam, M. J., S.Y.Al-Qatami, and S.F. Arif, “Bicyclic Aromatic Hydrocarbons of Kuwait Gas Oil”, Preprints - American Chemical Society, Division of Petroleum Chemistry, **35**, 821-826 (1990).

Isaacs, E., “Canadian Oil Sands: Development and Future Outlook” Alberta Energy Research Institute, http://www.aeri.ab.ca (2004).

Ishihara, A., J. Lee, F. Dumeignil, M. Takashi, E.W. Qian, and T. Kabe, “Elucidation of Retarding Effects of Sulfur and Nitrogen Compounds on Aromatic Compounds Hydrogenation” Energy and Fuels, **17**, 1338 – 1345 (2003).

Jaffe, S. B., “Hot Spot Simulation in Commercial Hydrogenation Processes”, Industrial and Engineering Chemistry Process Design and Development, **15**, 410-416 (1976).

Kabe, T., K., Akamatsu, A., Ishihara, S. ,Otsuki, M., Godo, Q. Zhang, W.Qian, and S. Yamada, “Deep Hydrodesulfurization of Light Gas Oil. Effect of Hydrogen Sulfide on Hydrodesulfurization of Dibenzothiophenes included in Hydrotreated Light Gas Oil”, Sekiyu Gakkaishi, **42**, 150-156 (1999).

Kabe, T., A.Ishihara, and W. Qian, “Hydrodesulfurization and Hydrodenitrogenation: Chemistry and Engineering” Wiley-VCH, New York (1999), page 374.

Kasztelan. S., and D. Guillaume, **"**Inhibiting Effect of Hydrogen Sulfide on Toluene Hydrogenation over a Molybdenum Disulfide/Alumina Catalyst" Industrial and Engineering Chemistry Research, **33**, 203-210 (1994).

Kataria, K.L., R.P. Kulkarni, A.B. Pandit, J.B.Joshi, and M. Kumar "Kinetic Studies of Low Severity Visbreaking" Industrial and Engineering Chemistry Research, **43**, 1373- 1387 (2004).

Katzer, J. R. and R. Sivasubramanian, "Process and Catalyst needs for Hydrodenitrogenation", Catalysis Reviews-Science and Engineering, **20**,155-208 (1979).

Kim, J.-W and F.V.Hanson, "Catalytic Hydrotreatment of PR Spring Bitumen over an HDM Catalyst", Energy (Oxford). **23**,221-229 (1998).

Kiperman,S. L. "Some Problems of Chemical Kinetics in Heterogeneous Hydrogenation Catalysis", Studies in Surface Science and Catalysis, **27**, 1-52 (1986).

Knudsen, K. G., B.H.Cooper and H.Topsoe, "Catalyst and Process Technologies for Ultra- Low Sulfur Diesel Fuel" Applied Catalysis, A: General **189**, 205-215 (1999).

Koseoglu, R.O. and C. R. Phillips, "Kinetics and Product Yield Distributions in the Cobalt Monoxide-Molybdenum Trioxide/Alumina-Catalyzed Hydrocracking of Athabasca Bitumen", Fuel, **67**, 1411-1416 (1988).

Laherrere, J. "Forecast of oil and Gas Supply to 2050, Petrotech 2003", New Delhi (2003).

Lapinas, A.T., M.T. Klein, B.C. Gates, A. Macris, and J.E. Lyons, "Catalytic Hydrogenation and Hydrocracking of Fluorene: Reaction Pathways, Kinetics, and Mechanisms". Industrial & Engineering Chemistry Research, **30**, 42-50 (1991).

Lee, S. L., M. De Wind, P.H.Desai, C.C. Johnson, and Y. M. Asim, "Aromatics Reduction and Cetane Improvement of Diesel Fuels", Fuel Reformulation **5**, 26-31 (1993).

Leglise, J. and J.V.Gestel, "Duchet Symposium on Advances in Hydrotreating Catalysis", 208th ACS National Meeting, Washington DC, (1994).

Mahay, A., J. Chmielowiec, I.P.Fisher and J. Monnier, "Two-Stage Hydroprocessing of Synthetic Crude Gas Oil", Fuel Processing Technology, **30**, 33-45 (1992).

Martin, B., P. Aakko, D.Beckman, N.F.Giacomo and F. Giavazzi, "Influence of Future Fuel Formulations on Diesel Engine Emissions - A Joint European Study". Society of Automotive Engineers, [Special Publication] (1997), pp 97-109.

Massoth, F. E. “Molybdena-Alumina Catalysts.IV. Rates and Stoichiometry of Sulfidation”, Journal of Catalysis, **36**, 164-184 (1975).

Massoth, F. E., K.Balusami and J. Shabtai, “Catalytic Functionalities of Supported Sulfides VI. The effect of Hydrogen Sulfide promotion on the Kinetics of Indole Hydrogenolysis” Journal of Catalysis, **122**, 256-270 (1990).

McCulloch, D. C., “Feed Hydrotreating Improves FCCU Performance”, Oil & Gas Journal, **73**, 53-58 (1975).

McCulloch, D.C., M. D. Edgar and J.T. Pistorius, “Higher Severity HDT needed for Low-Sulfur Diesel”,Oil & Gas Journal, **85**, 33-38 (1987).

McVicker, G. B., M.Daage, M.S.Touvelle, C.W.Hudson, D.P.Klein, W.C. Baird, B.R. Cook, J.G. Chen, S. Hantzer, D.E.W.Vaughan, E.S. Ellis, and O.C. Feeley, “Selective Ring Opening of Naphthenic Molecules” Journal of Catalysis, **210**, 137-148, (2002).

Moreau, C. and P.Geneste, “Factors Affecting the Reactivity of Organic Material Compounds in Hydrotreating Reactions” in Theoretical Aspects of Heterogeneous Catalysis, New York (1990), page 256.

Naber, J.E. and W.H.J. Stork, “Proceedings of First Japan-C Joint Workshop on the Frontiers of Catalytic Science and Technology for Alternative Energy and Global Environmental Protection”, Tokyo (1991).

Nagai, M., T. Masunaga, and N. Hanaoka, “Hydrodenitrogenation of Carbazole on a Molybdenum/Alumina Catalyst. Effects of Sulfiding and Sulfur Compounds” Energy and Fuels, **2**, 645-651 (1988).

Nishijima, A., T. Kameoka, T. Sato, H. Shimada, Y. Nishimura, Y.Yoshimura, N. Matsubayashi and M. Imamura, “Catalyst Design and Development for Upgrading Hydrocarbon Fuels”, Catalysis Today, **29**,179-184 (1996).

Nishijima, A., T. Sato, Y. Yoshimura, H. Shimada, N. Matsubayashi, M. Imamura, Y. Sugimoto, T. Kameoka and Y. Nishimura, “Two Stage Upgrading of Middle and Heavy Distillates over Newly Prepared Catalysts” Catalysis Today, **27,129**-135 (1996).

Nishijima, A., H. Shimada, Y. Yoshimura, T. Sato and N. Matsubayashi, “Deactivation of Molybdenum Catalysts by Metal and Carbonaceous Deposits during the Hydrotreating of Coal-Derived Liquids and Heavy Petroleum” Studies in Surface Science and Catalysis, **34**, 39-58 (1987).

Pauls, R.E. and G.J. Weight, “Methods for Determining Aromatics and Benzene in Reformulated Gasolines” Prepr. ACS Div. Fuel Chem. **37**, 9 (1992).

Peries, J.P., A. Billon, A. Hennico, and S. Kressmann, "Paper presented at the NPRA 89th Annual Meeting", San Antonnio, TX, March 17-19 (1991).

Perot, G., "Reactions Involved in Hydrodenitrogenation", Catalysis Today, **10**, 447-4772 (1991).

Perot, G., S. Brunet and N. Hamze, "Proceedings on the 9th International Congress on Catalysis" Philips and M. Terna, Editions, **1**, 19 (1988).

Rautanen, P. A., Aittamaa, J. R., A.O.I. Krause, "Liquid Phase Hydrogenation of Tetralin on Ni/Al_2O_3"**,** Chemical Engineering Science, **56**, 1247-1254 (2001).

Reid, C.R., J.M. Pruasnitz, and T.K. Sherwood, "The Properties of Gases and Liquids" McGraw-Hill, New York (1977).

Rigas,F, P. Panteleos and C. Laoudis, "Central Composite Design in a Refinery's Waste Water Treatment by Air Floatation" Global Nest. International, **2**, 245-253 (2002).

Sanford, E. C. and S.M., Yui, "Hydrotreating Characteristics of Coked and of Hydrocracked Gas Oils from Alberta Heavy Bituminous Oils with Commercial Nickel-Molybdenum Catalysts, and Prediction of Some Product Properties", Studies in Surface Science and Catalysis, **19**, 585-592 (1984).

Sapre, A. V. and B.C. Gates, "Hydrogenation of Aromatic Hydrocarbons Catalyzed by Sulfided Cobalt Monoxide-Molybdenum Trioxide/γ-Aluminum Oxide: Reactivities, Reaction Networks, and Kinetics", Preprints of Papers - American Chemical Society, Division of Fuel Chemistry, **25,** 66-77 (1979).

Sapre, A.V and B. C. Gates, "Hydrogenation of Aromatic Hydrocarbons Catalyzed by Sulfided Cobalt Oxide-Molybdenum Oxide/ Aluminum Oxide. Reactivities and Reaction Networks" Industrial and Engineering Chemistry Process Design and Development" **20**, 68-73 (1981).

Sapre, A.V and B.C. Gates, "Hydrogenation of Biphenyl Catalyzed by Sulfided Cobalt Monoxide-Molybdenum Trioxide-Aluminum Trioxide. The reaction kinetics" Industrial and Engineering Chemistry Process Design and Development" **21**, 86-94 (1981).

Sato, T., T. Kameoka, S. Yoshitomi, Y. Yoshimura, H. Shimada, N.Matsubayashi, M. Imamura and A. Nishijima, "Two-Stage Upgrading of Coprocessing Oil over Newly Prepared Catalysts", Conference Proceedings. – 7th International Conference on Coal Sciences, **1**, 242-245 (1993).

Satterfield, C. N and S.Gultekin, "Effect of Hydrogen Sulfide on the Catalytic Hydrodenitrogenation of Quinoline" Industrial and Engineering Chemistry Process Design and Development, **20**, 62-68 (1981).

Satterfield, C.N. “Heterogeneous Catalysis in Practice”. McGraw Hill, (1980), pp 235.

Schuit, G. C. A. and B.C. Gates, “Chemistry and Engineering of Catalytic Hydrodesulfurization”, AIChE Journal **19**, 417-438 (1973).

Shimada, H., T. Kameoka, H. Yanase, M. Watanabe, A. Kinoshita, T. Sato, Y. Yoshimura, N. Mastubayashi, and A. Nishijima, “Highly Active Nickel-Tungsten/ Alumina Catalyst for Upgrading Unconventional Feedstocks”, Studies in Surface Science and Catalysis, **75**, 1915-1918 (1993).

Song, C. and Ma, X. “New Design Approaches to Ultra-Clean Diesel Fuels by Deep Desulfurization and Deep Dearomatization” Applied Catalysis B: Environmental, **41**, 207-238 (2003).

Speight, J.G., “The Desulfurization of Heavy Oils and Residua”, Marcel Dekker Inc., New York (2000)

Stanislaus, A.and B.H. Cooper, “Aromatic Hydrogenation Catalysis: A Review. Catalysis Reviews - Science and Engineering, **38**, 76-123 (1996).

Suchanek, A. J. and A.S. Moore, “Efficient carbon rejection upgrades Mexico's Maya Crude oil”, Oil and Gas Journal, **84**, 36-40 (1986).

Sundaram, K.M., J.R. Katzer and K.B. Bischoff, “Modeling of Hydroprocessing Reactions” Chemical Engineering Communications, **71**, 53 (1988).

Topsoe, H, ‘News-HDS/HDA, “Hydrodearomatization, Hydrocarbon Process”. **79**, 118 (2001).

Topsoe, H, B.S. Clausen, W. Niemann, P. Zeuthen, “XANES and EXAFS Studies of the Nickel-Molybdenum-Sulfur (Cobalt-Molybdenum-Sulfur) Structures in Hydrotreating Catalysts”, Preprints - American Chemical Society, Division of Petroleum Chemistry, **35**, 208-210 (1990).

US EPA, Diesel Fuel Quality- “Advance Notice of Proposed Rulemaking”, EPA420-F-99-01, Office of Mobile Sources (1999).

Van Gestel, J., J. Leglise, and J.C. Duchet, “Effect of Hydrogen Sulfide on the Reaction of 2,6- Dimethylaniline over Sulfided Hydrotreating Catalysts” Applied Catalysis, A: General, **92**, 43-154 (1992).

Vivier, L., S. Kasztelan, G. Perot, “Kinetic Study of the Decomposition of 2, 6-Diethylaniline in the Dresence of 1,2,3,4-Tetrahydroquinoline over a Sulfided NiMo-Al_2O_3 Catalyst. I. Effect of the Partial Pressure of Nitrogen Compounds”, Bulletin des Societes Chimiques Belges **100**, 801-805 (1991).

Voorheeve,R.J.H., “Electron Spin Resonance Study of Active Centres in Nickel-Tungsten Sulfide Hydrogenation Catalysts”, Journal of Catalysis, **23**, 236-242 (1971).

Vradman, L., M.V.Landau and M. Herskowitz, “Hydrodearomatization of Petroleum Fuel Fractions on Silica Supported Ni-W Sulfide with Increased Stacking Number of the WS_2 Phase”, Fuel, **82**,633-639 (2003).

Weiseer, O. and S. Landa, “Sulfide Catalyst, Their Properties and Applications”, Pergamon Press; Oxford (1973).

Whitehurst, D.D., I. Takaaki and I. Mochida, “Present State of the Art and Future Challenges in the Hydrodesulfurization of Polyaromatic Sulfur Compounds”, Advances in Catalysis, **42**, 344-368 (1998).

Wilson, M. F. and J.F., Kriz, “Upgrading of Middle Distillate Fractions of Syncrude’s from Athabasca Oil Sands” Preprints - American Chemical Society, Division of Petroleum Chemistry, **28**,640-649 (1983).

Wilson, M. F., I.P. Fisher, and J.F. Kriz, “Hydrogenation and Extraction of Aromatics from Oil Sands Distillates and Effects on Cetane Improvement” Energy and Fuels, **1**, 540-544 (1987).

Wilson, M. F., I.P. Fisher and J.F. Kriz, “Hydrogenation of Aromatic Compounds in Synthetic Crude Distillates Catalyzed by Sulfided Nickel-Tungsten/γ-Alumina”, Journal of Catalysis, **95**,155-166 (1985).

Wilson, M. F., J.F.Kriz, and I.P. Fisher, “Selected Aspects of Catalytic Refining of Middle Distillates from Athabasca Syncrudes” Preprints of Papers-American Chemical Society, Division of Fuel Chemistry, **29**,284-291 (1984).

Wilson, M. F., J.F.Kriz and I.P., Fisher, “Cetane Improvement of Middle Distillates from Oil Sands by Catalytic Hydroprocessing”, Preprints-American Chemical Society, Division of Petroleum Chemistry, **30**,303-308 (1985).

Yang, H., H. Wilson, C. Fairbridge, Z. Ring, Z. and J. M. Hill. **“**Mild Hydrocracking of Synthetic Crude Gas Oil Over Pt Supported on Pillared and Delaminated Clays”, Energy and Fuels, **16**, 855-863 (2002).

Yang, S. H. and C.N. Satterfield, “Some Effects of Sulfiding of a Nickel-Molybdenum (NiMo)/Alumina Catalyst on its Activity for Hydrodenitrogenation of Quinoline” Journal of Catalysis, **81**, 168-178 (1983).

Yoes, J.R. and Y.M. Asim, “Diesel Aromatics Difficult to Reduce” Oil & Gas Journal **85**, 54-58 (1987).

Yui, S. M. and E.C. Sanford, “Diesel and Jet Fuel Production from Athabasca Bitumen,

and Cetane Number Correlation. Energy Processing / Canada, **82**, 22-26 (1989).

Yui, S. M. and E.C. Sanford, "Kinetics of Aromatics Hydrogenation and Prediction of Cetane Number of Synthetic Distillates", Proceedings - Refining Department, American Petroleum Institute, **64**, 290-297 (1985).

Yui, S. M. and E.C. Sanford, "Kinetics of Hydrogenation of Aromatics Determined by Carbon-13 NMR for Athabasca Bitumen-Derived Middle Distillates", Preprints-American Chemical Society, Division of Petroleum Chemistry, **32**, 315-320 (1987).

Yui, S.M., "Two-Stage Hydrotreating of Bitumen-Derived Middle Distillate to Produce Diesel and Jet Fuel", Chemical Industries, **58,** 235-252 (1994).

Zaman, A. A., F. Demir and E. Finch**,** "Effects of Process Variables and their Interactions on Solubility of Metal Ions from Crude Kaolin Particles: Results of a Statistical Design of Experiments" Applied Clay Science, **22**, 237-250 (2003).

Zdrazil, M. "Recent Advances in Catalysis Over Sulfides" Catalysis Today, **3**, 269-361 (1988).

APPENDIX

Appendix A: Experimental calibration

A.1 Calibration of mass flow meter

The mass flow controller was calibrated for hydrogen flow at the experimental operating conditions using a bubble flow meter connected to the exit of the backpressure regulator. The flow rates measured at atmospheric conditions were standardized using equation A.1.

$$V^o = \left(\frac{P^a}{P^o}\right)\left(\frac{T^a}{T^o}\right)V^a \qquad \textbf{(A.1)}$$

Where V is the flow rate in ml/hr, T is temperature, P is pressure, the superscripts 'o' and a represent standard conditions normal operating conditions, respectively.

Figure A.1 shows the calibration curve of the mass flow controller.

A.2 Reactor temperature calibration

The reactor was temperature calibrated at the same conditions as used in the actual experimental runs. Temperature was varied from 150 to 420 ^oC while maintaining the reaction pressure and hydrogen-to-oil ratio constant at of 9.6 MPa and 550 ml/ml, respectively. The corresponding reactor temperature was measured using a single thermocouple inserted just below the catalyst bed. The thermocouple was then moved every 1 cm up the catalyst bed to measure the temperature along the reactor bed. Profile for the variation of the temperature along the reactor bed is shown in Figure A.2 and Figure A.3 shows the calibration curve for the temperature controller.

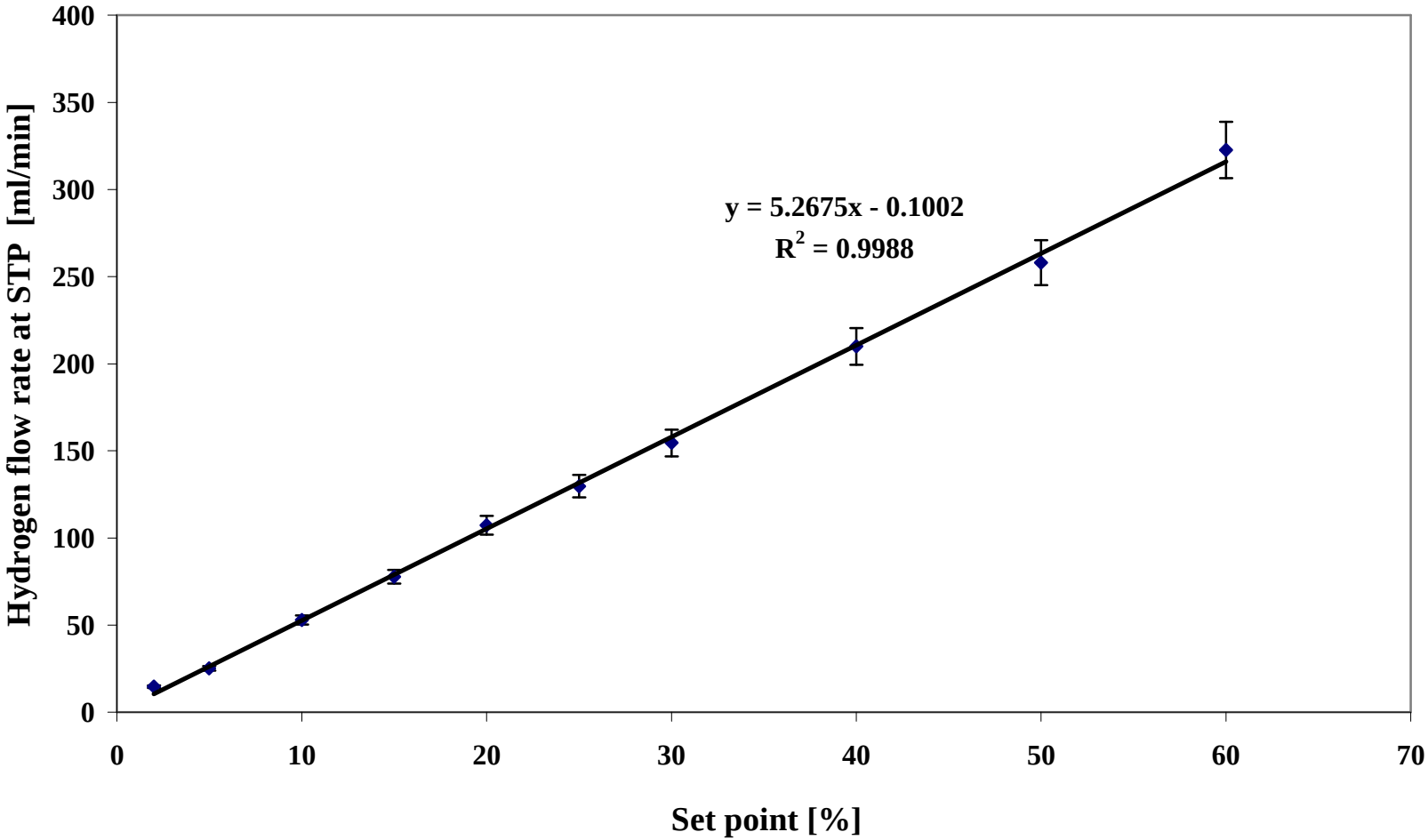

Figure A.1: Calibration curve for mass flow meter

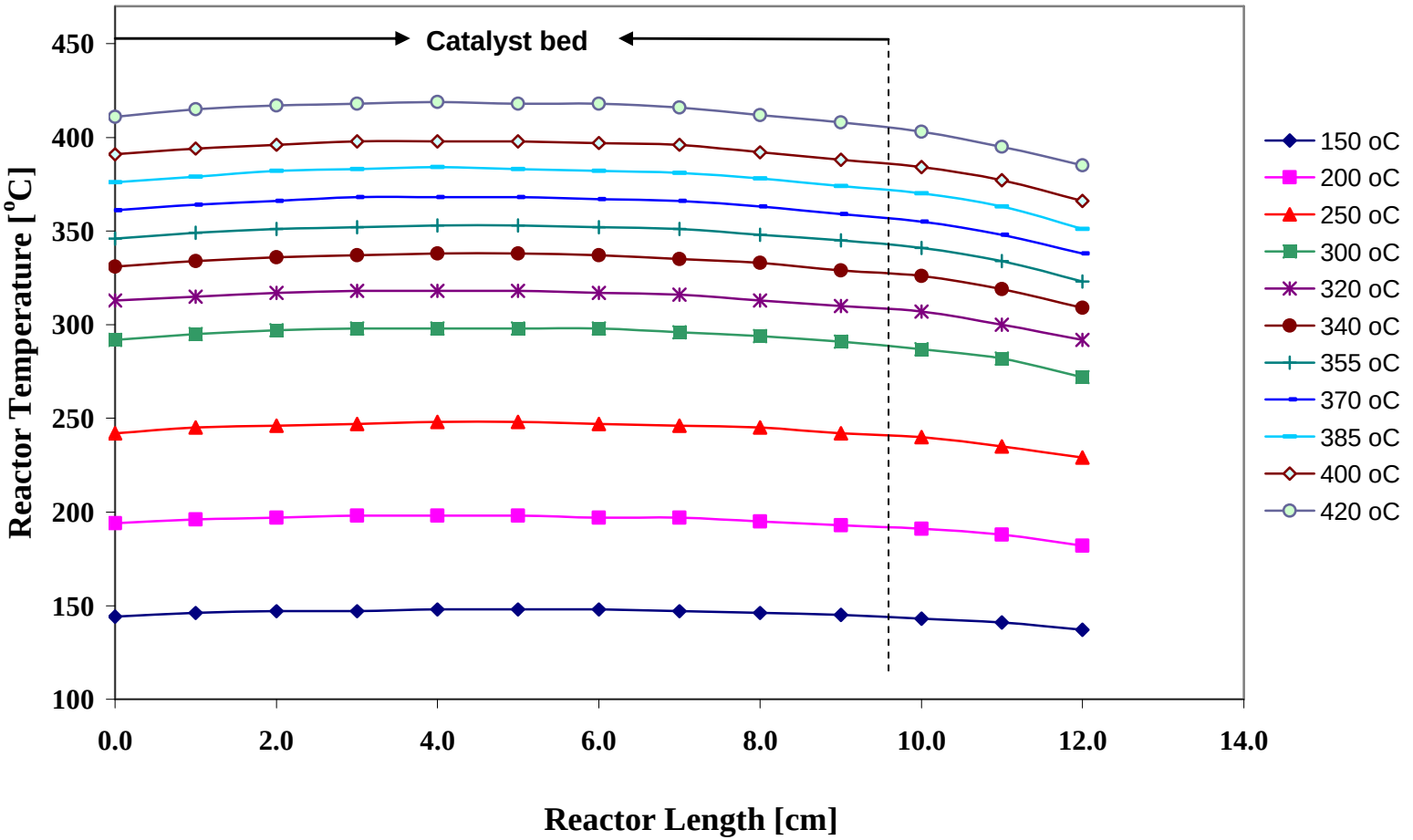

Figure A.2: Temperature distribution along the axial length of the reactor

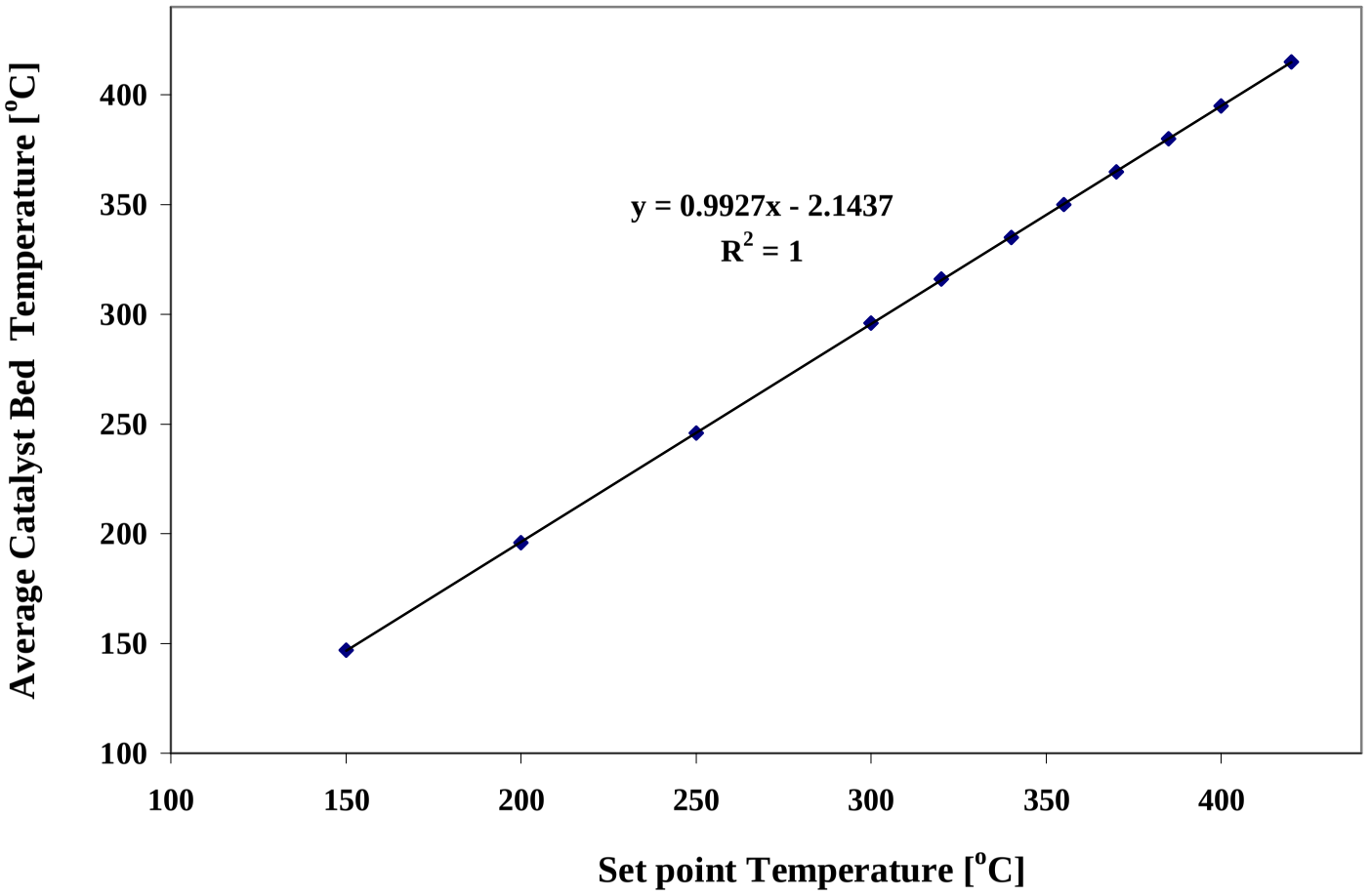

Figure A.3: Temperature calibration curve of reactor

Appendix B: Feed and product analyses

B.1 Analysis for aromatics contents

The aromatics contents of the feed and products were determined using ^{13}C-NMR spectrometry and Supercritical fluid chromatography. The former was used to determine the total aromatics content (aromaticity) while the latter was used to determine the individual concentrations of the mono-, di- and polyaromatics.

B.1.1 ^{13}C-NMR spectrometry

Aromaticity is the mole per cent of carbon (%C_A) in a sample that is present as part of an aromatic ring structure. Feed and product aromaticity were measured directly from the carbon-13 nuclear magnetic resonance (^{13}C –NMR) spectroscopy. The spectra were obtained in the Fourier Transform (FT) mode operating at a frequency of 500 MHz. The instrumental conditions were: pulse delay of 4 s, sweep width of 27.7 kHz and inverse gated proton coupling. Overall time for each sample was one hour, 30 minutes for 2000 scans. Deuterated chloroform, $CDCl_3$ was used to dilute the samples.

Figure B.1 shows a typical spectrum for ^{13}C-NMR with two distinct zones separated by the solvent bar. These are the total aromatics found between 120-150 ppm and total saturated hydrocarbons between 0-50 ppm. The total aromaticity of each sample is measured directly from the spectra by finding the percentage of total aromatics from the equation:

$$Car = \frac{I_{ar}}{I_{ar} + I_{sat}} \times 100 \quad \% \qquad \textbf{(B.1)}$$

Where I_{ar} is the integral of total aromatics; I_{sat} = integral of total saturates; C_{ar} is the aromatics content.

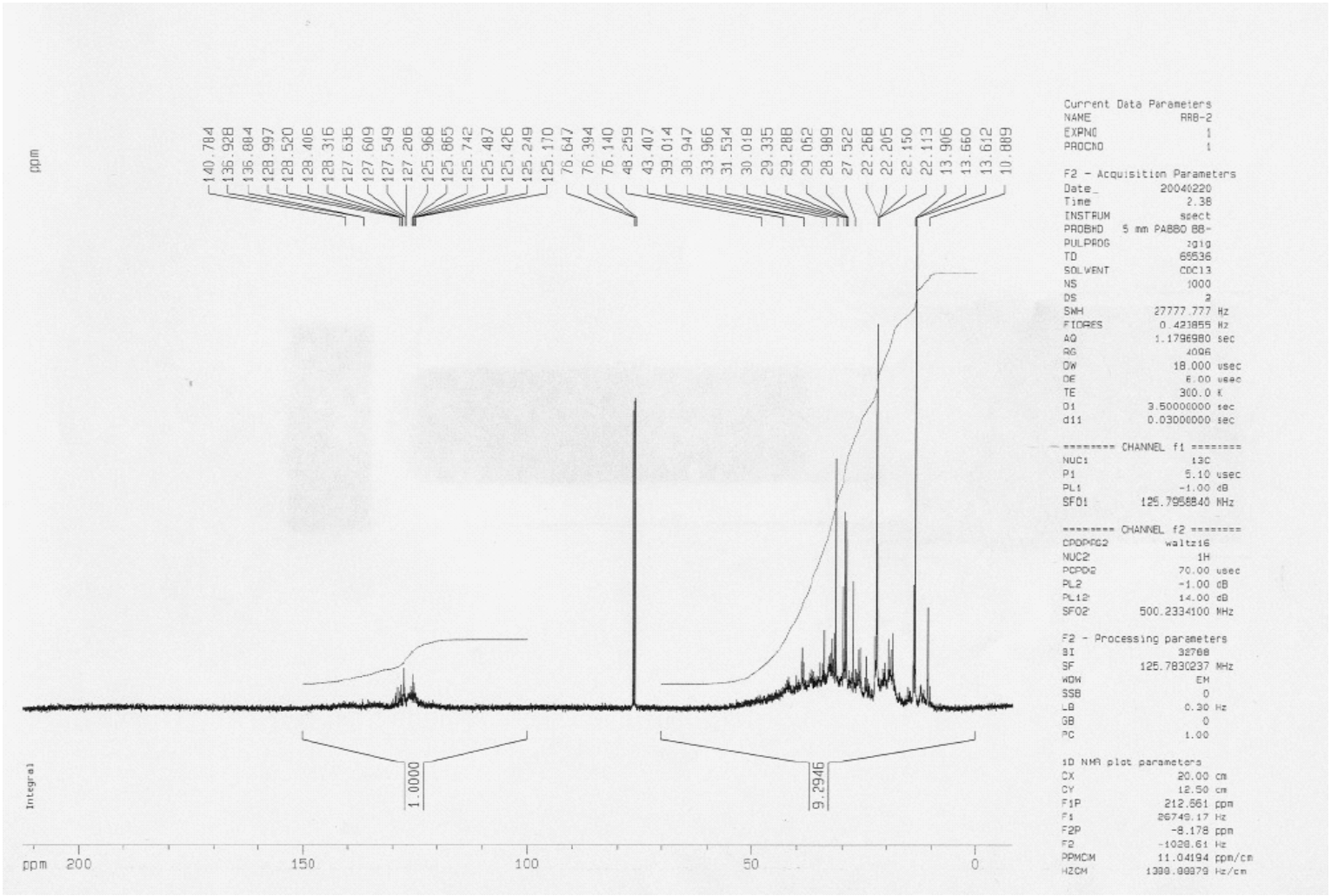

Figure B.1: Sample ^{13}C-NMR spectra for a hydrotreated sample

B.1.2 Supercritical fluid chromatography (SFC)

The individual concentrations of the mono, di and polyaromatics contents were determined using the supercritical fluid chromatography technique. This is a relatively recent chromatographic technique which is an adaptation of the high performance liquid chromatography (HPLC). The major modification is the replacement of the liquid mobile phase with a supercritical fluid mobile phase (carbon dioxide, CO_2). A supercritical fluid chromatograph consists of a liquid supply, usually CO_2, a pump, the column in a thermostat-controlled oven, a restrictor to maintain the high pressure in the column and a detector.

The mobile phase is initially pumped as liquid and brought into the supercritical region by heating it above its critical temperature before it enters the analytical column. It then passes through an injection valve where the sample is introduced into the supercritical stream and then into the analytical column. The mixture of the sample and the mobile phase is maintained supercritical as it passes through the column and into the detector by a pressure restrictor placed either after the detector or at the end of the column. The column contains a highly viscous liquid (stationary phase) into which the analytes can be temporarily adsorbed and then released based on their chemical structure; the monoaromatics are eluted first followed by the di- and the polyaromatics.

Part of the theory of separation in SFC is based on the density of the supercritical fluid which corresponds to solvating power. As pressure in the system is increased, the supercritical fluid density increases with a corresponding increase in the solvating power. Therefore as the density of the mobile phase is increased, components retained in the column can be made to elute.

B.2 Total sulfur analysis

Total sulfur in the feed and sample products was analyzed by combustion/fluorescence technique as provided by the ASTM D5453 method. The hydrocarbon sample is injected into a sample boat and then inserted into a high-temperature combustion tube where sulfur is oxidized to sulfur dioxide in an oxygen rich atmosphere. Any water produced during sample combustion is removed and the sample combustion gases are next exposed to Ultraviolet (UV) light. The SO_2 absorbs the energy from the UV light and is converted to excited SO_2*. The fluorescence emitted from the excited SO_2* as it returns to its stable state SO_2 is detected by a photomultiplier tube and the resulting signal is a measure of the sulfur contained in the sample. The sulfur content of the test specimen in parts per million (ppm) is calculated as:

$$C_S\,(ppm) = \frac{(I - Y)}{S \times M^* \times Kg} \qquad \textbf{(B.2)}$$

Where C_s is the concentration of sulfur, I is the average integrated detector response for test specimen solution, counts; Y is the y-intercept of standard curve, counts; S is the slope of standard curve, counts/mg, M* is the mass of test specimen solution injected and K_g of the gravimetric dilution factor, mass of test specimen/mass of test specimen and solvent, g/g.

B.3 Total nitrogen analysis

The feed and sample products are injected into a sample boat. A helium or argon carrier gas then sweeps the sample into a pyrolysis tube. The nitrogen in the sample is then oxidized to nitric oxide (NO) in an oxygen chamber. The oxides of nitrogen are contacted with ozone (O_3) which converts NO to NO_2. As the metastable species decays

a photon of light is emitted and detected by the photomultiplier. The chemiluminescence's emission is specific for nitrogen and is proportional to the amount of nitrogen on the original sample. The nitrogen content, C_N in parts per million is evaluated as:

$$C_N(ppm) = \frac{(I - Y)}{S \times M^* \times Kg} \qquad \textbf{(B.3)}$$

Where C_N is the concentration of nitrogen, I is the average integrated detector response for test specimen solution, counts; Y is the y-intercept of standard curve, counts; S is the slope of standard curve, counts/mg, M^* is the mass of test specimen solution injected and K_g of the gravimetric dilution factor, mass of test specimen/mass of test specimen and solvent, g/g.

B.4 Simulated distillation

The simulated distillation chromatography analysis method is a substitute for conventional distillation methods to estimate parameters (boiling temperature distribution) for large scale petroleum refining process. A Varian Model CP 3800 Gas Chromatography (especially configured for simulated distillation) coupled to a Varian CP 8400 auto sampler was used for the boiling point distribution analysis. The simulated distillation chromatography is used to determine the boiling range distribution of crude petroleum and various petroleum fractions and products by assigning the boiling temperatures as a function of retention time. The temperatures at which specific percentages of total sample elutes from the column is then measured.

B.5 Catalyst (NiW/Al_2O_3) characterization

BET surface area, pore volume and size of the fresh and spent catalysts were determined using an automated gas (N_2) adsorption analyzer ASAP 2000 (Micrometrics) with pure nitrogen gas (99.9 % pure). About 0.05 g of sample was used and before each analysis, the catalyst sample was evacuated at 200 ^oC for 4h in a vacuum to remove all adsorbed moisture from the catalyst surface. Prior to surface area/porosity determinations, all spent catalysts were thoroughly washed with hexane solution to remove volatiles as well as gas oil present on the surface and in the pores of the catalysts. Cleaned catalysts were then dried in an oven at 120 °C for 12 hours.

BET surface area, pore volume and pore diameter of lab-prepared NiW/Al_2O_3 catalyst were 174 m^2/g, 0.495 cc/g and 114 Å, respectively. In the case of the commercial $NiMo/Al_2O_3$ catalyst, the BET surface area, pore volume and pore diameter were reported to be 169 m^2/g, 0.412 cc/g and 97.8 Å, respectively.

High resolution transmission electron microscopy (TEM) analyses of sulfided NiW/Al_2O_3 catalysts was carried out with a Philips CM20 electron microscope with a LaB6 filament as a source of electron and operated at 200kV. The purpose of the TEM analysis was to determine the dispersion of the WS_2, which is the active phase of the hydrotreating catalysts in its working state. For the TEM analysis, the sample was cleaned sample was powdered and a small amount of the powdered sample was then sprinkled on a piece of parafilm with a droplet of water. A 400 mesh carbon coated grid was floated on the droplet of water and then picked. The retained droplet of material was allowed to air dry on the grid and then mounted on a specimen holder where the analysis was carried out.

Figure B.2 and Figure B.3 show the TEM micrographs of the $NiMo/Al_2O_3$ and NiW/Al_2O_3 catalysts, respectively. The lattice images of the MoS_2 and WS_2 slabs are indicated by the solid black lines in both figures. The sulfided $NiMo/Al_2O_3$ catalyst showed higher dispersion of MoS_2 slab compared to that of WS_2 in case of sulfided NiW/Al_2O_3 catalyst.

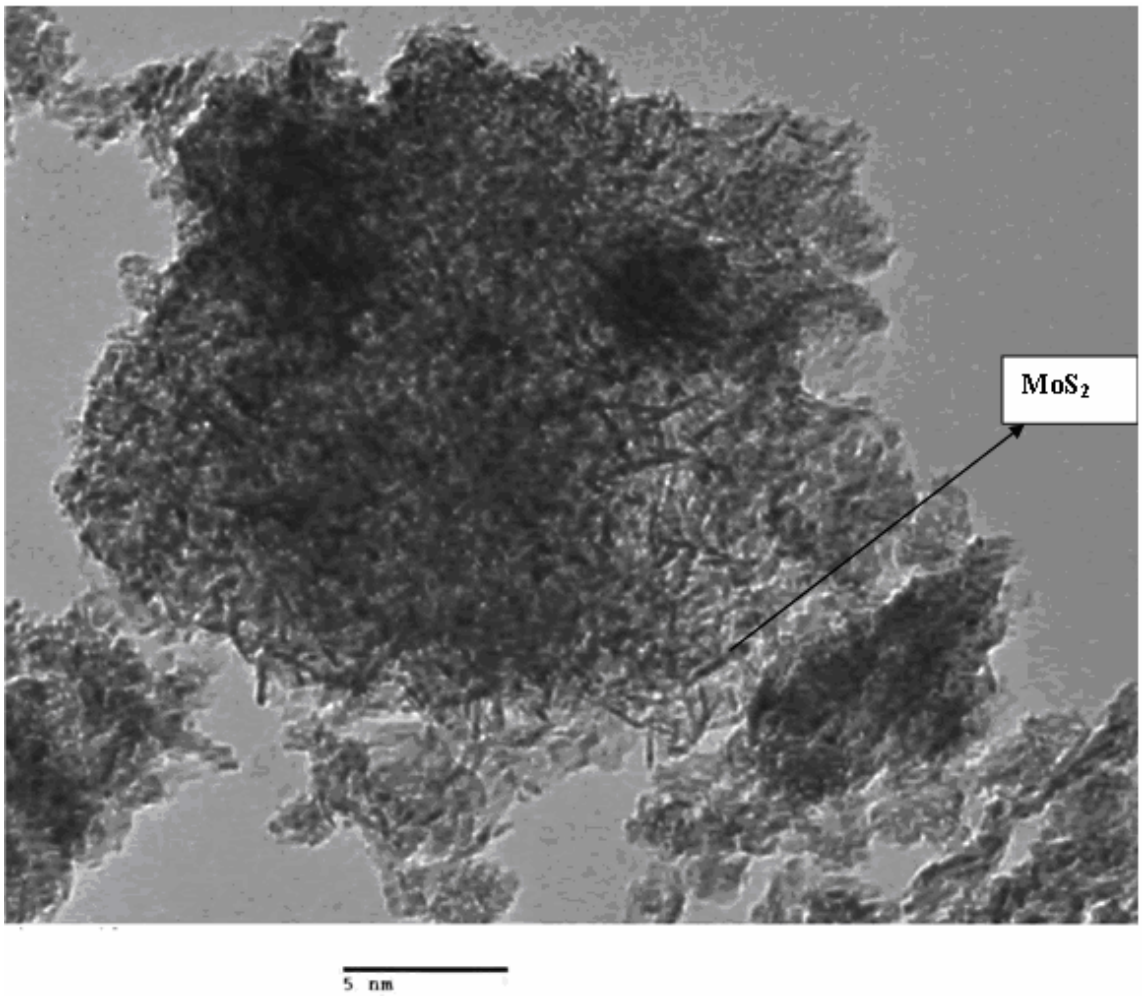

Figure B.2: TEM micrograph of the sulfided $NiMo/Al_2O_3$ catalyst

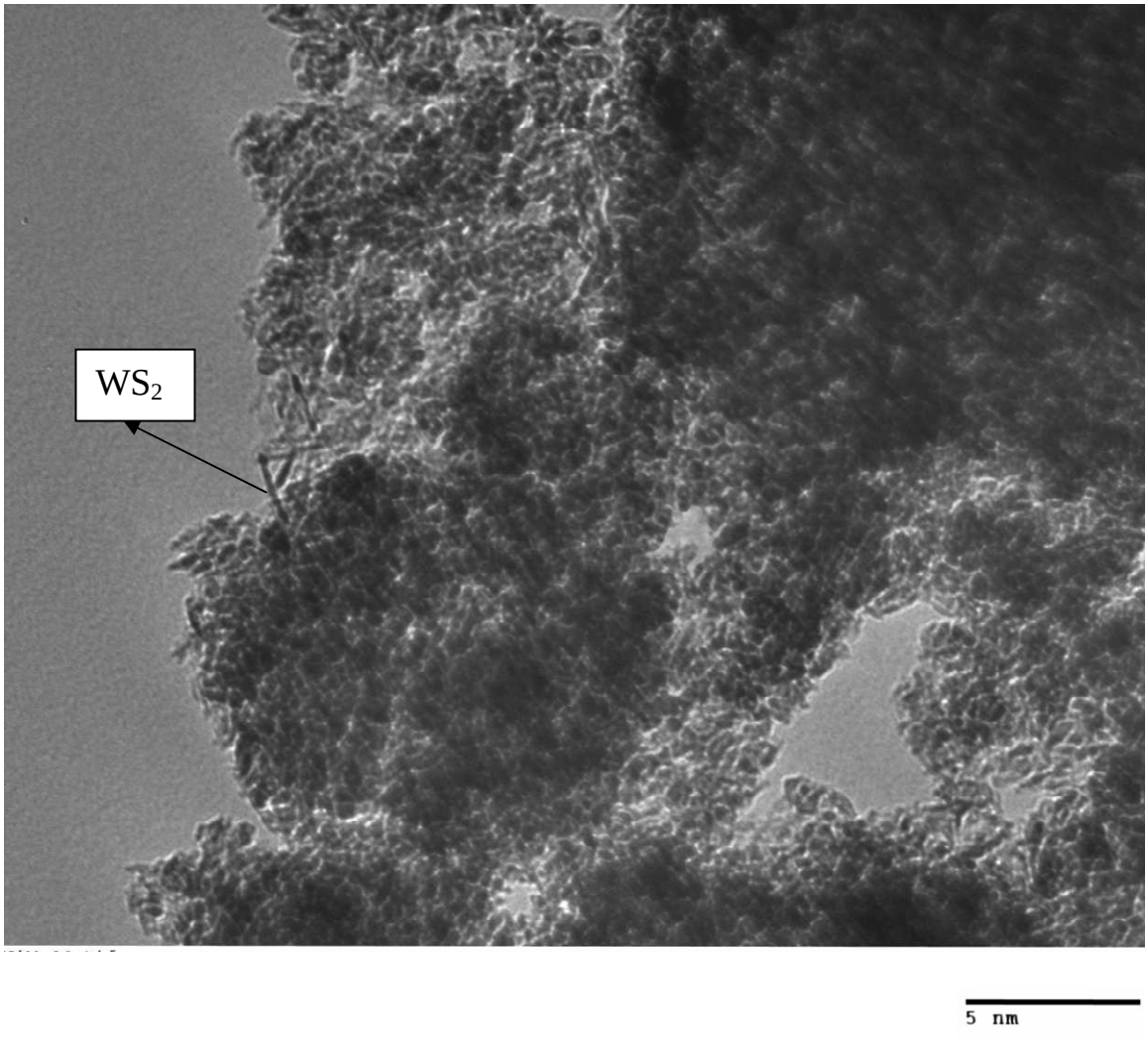

Figure B.3: TEM micrograph of the sulfided NiW/Al_2O_3 catalyst

Appendix C: Log sheets

C.1 Data recording

Table C.1 is an example of the log sheets used to record data and monitor experiments. The experiments were monitored for pump performance, temperature, pressure, space velocity, flow rates and hydrogen-to-oil ratio.

Table C.1: Sample of the data recording sheet

Reactor #: 5 **Date:** 2/05/2004 **Feed Type:** LGO Blend **Catalyst Type:** NiW/Al_2O_3

Date	Time	TOS	H_2 system pressure (psig)				Temperature (^oC)		Pump set point	Oil Weight	Flow rate	LHSV	H_2 MFM	Remarks
d.m:yr	(h)	(h)	Tank.	PGI	PG3	PG4	Furnace	Rxt	(%)	(g)	(g/h)	(h^{-1})	(ml/ml)	

Appendix D: Experimental calculations and mass balance closure.

D.1 Equations used for calculating the HDA kinetic parameters

The Langmuir-Hinshelwood rate equation model was used to describe the kinetics of hydrogenation of aromatics. This is given by:

$$-r_{Ai} = -\frac{dC_{Ai}}{dt} = \frac{k_{Ai}K_{Ai}K_{Hi}P_{H2}C_{Ai}}{1+K_{Ai}C_{Ai}+K_{H2Si}P_{H2Si}} \quad \textbf{(D.1)}$$

Where $-r_A$, k_A are the rate of reaction, and the forward rate constants, respectively, K_H, K_A and K_{H2S} are the equilibrium adsorption constants of hydrogen, aromatics and hydrogen sulfide, respectively. C_A is the product concentration of aromatics and the saturated species, respectively. P_{H2S} and P_H are partial pressures of hydrogen sulfide and hydrogen gas, respectively and t is the residence time. The subscript, i, refers to either the single-stage or two-stage kinetic parameters.

Partial pressure of hydrogen sulfide is assumed to be an ideal gas and calculated by:

$$P_{H2S} = \frac{n_{H2S}}{V}RT = C_{H2S}RT = b(C_{so}-C_{sp}) \quad \textbf{(D.2)}$$

$$C_A = \frac{(1+K_{H2S}P_{H2S})\,LambertW\left(\dfrac{K_A\exp\left(\dfrac{kK_AK_HP_H(t-\frac{C_{AO}K_A+\ln C_{Ao}+\ln C_{AO}K_{H2S}P_{H2S}}{kK_AK_HP_H})}{1+K_{H2S}P_{H2S}}\right)}{1+K_{H2S}P_{H2S}}\right)}{K_A} \quad \textbf{(D.3)}$$

Where

$$LambertW(x) = x - x^2 + \frac{3}{2}x^3 - \frac{8}{3}x^4 + \frac{125}{4}x^5 - \frac{54}{5}x^6 + (o)^7 \quad \textbf{(D.4)}$$

And

$$X = \left(\frac{K_A \exp\left(\frac{kK_A K_H P_H \left(t - \frac{C_{AO}K_A + \ln C_{Ao} + \ln C_{AO}K_{H2S}P_{H2S}}{kK_A K_H P_H}\right)}{1 + K_{H2S}P_{H2S}}\right)}{1 + K_{H2S}P_{H2S}} \right) \quad \textbf{(D.5)}$$

D.2 Mass Balance Calculations

The mass balance closure for aromatics, sulfur, and nitrogen and the hydrocrack materials were calculated using the following steady-state equations:

For HDA:

$$C_{so} + C_{mo} + C_{do} + C_{po} = C_s + C_m + C_d + C_p \quad \textbf{(D.6)}$$

Where C_{so}, C_{mo}, C_{do} and C_{po} represent the percentage of saturates, mono-, di-, and polyaromatic compounds in the feed, respectively C_s, C_m, C_d and C_p are the percentage saturates, mono, di- and polyaromatics in the hydrotreated products, respectively.

Overall material balance closure was 99.5 %.

For HDS:

$$C_{SF} = C_{SP} + C_{H2S} \quad \textbf{(D.7)}$$

Where C_{SF} and C_{SP} represent the concentrations of sulfur in the feed, and products, respectively and C_{H2S} is the concentration of hydrogen sulfide gas produced during reaction. The overall material balance closure was 97 %.

For HDN:

$$C_{NF} = C_{NP} + C_{NH3} \quad \textbf{(D.8)}$$

Where C_{NF} and C_{NP} represent the concentrations of nitrogen in the feed and products, respectively and C_{NH3} is the concentration of ammonia produced during HDN reactions.

For MHC:

$$C_{HO} + C_{DO} + C_{GO} = C_H + C_D + C_G \quad \textbf{(D.9)}$$

Where C_{HO}, C_{DO} and C_{GO} are the percentage amounts of heavy gas oil, diesel and gasoline in the feed, respectively. C_H, C_D and C_G are the percentages of heavy gas oil, diesel and gasoline in the products, respectively. The overall mass balance closure, ignoring gases mixed in the liquid products, ranged from 97-98.5 % for all the light gas oil feedstock.

Appendix E: Experimental results

Table E.1: Total aromatics, sulfur and nitrogen concentrations after the single-stage hydrotreating with commercial $NiMo/Al_2O_3$ catalyst

Temp [^oC]	Pressure [MPa]	LHSV [h^{-1}]	^{13}C-NMR [%]	Sulfur [wppm]	Nitrogen [wppm]
Feed	-	-	17.1	17420	461
365	6.9	1.25	5.2	305	20
390	9.6	1.25	4.0	201	10
365	9.6	1.25	5.4	1163	63
350	9.6	1.25	4.9	403	11
380	12.4	1.70	5.9	430	16
350	8.3	1.25	7.7	1310	96
380	8.3	1.70	7.5	286	21
365	11.0	1.70	6.9	1385	63
350	11.0	2.00	4.6	732	19
380	9.6	0.80	4.9	393	20
350	8.3	1.00	6.9	346	14
380	8.3	0.80	6.5	191	9
350	11.0	0.80	6.6	617	13
380	11.0	0.50	3.6	298	10
365	9.6	1.25	4.1	261	10
365	9.6	1.25	4.5	258	<10
365	9.6	1.25	4.4	262	<10
365	9.6	1.25	3.9	260	<10
365	9.6	1.25	4.0	263	<10

Table E.2: Aromatics, sulfur and nitrogen concentrations in the LGO blend after single-stage hydrotreating

Sample ID	Temp [^{o}C]	Pressure [MPa]	LHSV [h^{-1}]	Saturates [%]	SFC Aromatic contents [%]				Sulfur [wppm]	Nitrogen [wppm]
					Mono-	Di-	Poly-	Total		
Hydrotreating over $NiMo/Al_2O_3$										
	340	11.0	0.6	75.90	20.30	3.60	0.150	24.08	871	16
	350	11.0	0.6	81.70	16.10	2.20	0.030	18.32	576	<10
	365	11.0	0.6	87.90	10.70	1.30	0.004	12.05	297	<10
	380	11.0	0.6	91.40	7.70	0.87	0.004	8.55	222	<10
	390	11.0	0.6	95.60	4.60	0.40	0.001	4.98	271	<10
Hydrotreating over NiW/Al_2O_3										
	340	11.0	0.6	68.05	6.11	3.60	0.830	34.71	2105	55
	350	11.0	0.6	69.82	5.26	0.83	0.530	33.03	1049	25
	365	11.0	0.6	76.73	3.09	0.53	0.090	26.82	949	<10
	380	11.0	0.6	83.40	1.93	0.09	0.040	20.15	758	<10
	390	11.0	0.6	85.74	1.42	0.04	0.010	17.84	748	<10

Table E.3: Simulated distillation data obtained for the feed characterization study of the different light gas oil feedstock.

Fraction	ALGO	LGOB	HLGO	VLGO
Mass, wt %	**Boiling point [^{o}C]**			
IBP	125	130	133	254
5	180	191	179	288
10	212	219	197	301
15	228	236	211	311
20	240	250	224	318
25	252	262	236	325
30	261	273	248	331
35	269	283	258	337
40	278	292	269	342
45	287	302	280	347
50	295	310	291	353
55	303	319	301	358
60	311	327	311	364
65	319	336	321	370
70	329	345	332	376
75	339	355	343	383
80	350	366	356	391
85	364	378	369	401
90	381	395	386	415
95	409	420	410	436
100	476	484	472	492

Table E.4: Mild hydrocracking data of LGO types at a pressure of 11.0 MPa and LHSV of 0.6 h^{-1}

Feed type	Temp. [^{o}C]	Gasoline [wt %]	Diesel [wt %]	HGO [wt %]
ALGO	340	19	63	18
	350	20	63	17
	365	21	64	15
	380	22	65	13
	390	23	68	9
HLGO	340	27	55	18
	350	28	55	17
	365	26	57	17
	380	27	57	16
	390	27	60	14
VLGO	340	0.9	57	48
	350	0.7	51	42
	365	3	59	44
	380	4	59	36
	390	7	59	35

Table E.5: Overall aromatics, sulfur and nitrogen concentrations in the LGO blend after the two-stage hydrotreating process

Sample ID	Temp [^{o}C]	Pressure [MPa]	LHSV [h^{-1}]	Saturates [%]	SFC Aromatic contents [%]				Sulfur [wppm]	Nitrogen [wppm]
					Mono-	Di-	Poly-	Total		
Feed	-	-	-	63.3	20.7	12.2	3.6	36.5	17420	461
SS-350-1	350	11.0	1.5	83.2	14.6	2.2	0.03	16.8	262	<10
SS-365-1	365	11.0	1.5	87.4	10.9	1.7	0.03	12.6	690	<10
SS-380-1	380	11.0	1.5	92.7	6.3	1.0	0.02	7.3	233	<10
SS-390-1	390	11.0	1.5	92.2	6.7	1.1	0.05	7.8	167	<10
SS-350-2	350	11.0	1.2	86.7	11.9	1.4	0.02	13.3	78	<10
SS-365-2	365	11.0	1.2	91.2	8.0	0.9	0.00	8.9	97	<10
SS-380-2	380	11.0	1.2	92.9	6.4	0.7	0.00	7.1	88	<10
SS-390-2	390	11.0	1.2	92.3	7.0	0.7	0.00	7.7	79	<10
SS-350-3	350	11.0	1.0	87.2	11.5	1.3	0.00	12.8	109	<10
SS-365-3	365	11.0	1.0	91.4	7.7	0.9	0.00	8.6	95	<10
SS-380-3	380	11.0	1.0	93.0	6.2	0.8	0.00	7.0	80	<10
SS-390-3	390	11.0	1.0	93.9	5.8	0.3	0.00	6.4	68	<10